5-2013

The Calibration and Uncertainty Evaluation of Spatially Distributed Hydrological

JongKwan Kim

THE CALIBRATION AND UNCERTAINTY EVALUATION OF SPATIALLY

DISTRIBUTED HYDROLOGICAL MODELS

by

JongKwan Kim

A dissertation submitted in partial fulfillment

of the requirements for the degree

of

DOCTOR OF PHILOSOPHY

in

Civil and Environmental Engineering

Approved:

Dr. Mac McKee Major Professor	Dr. Jagath J. Kaluarachchi Committee Member
Dr. Christopher M. U. Neale Committee Member	Dr. Gilberto E. Urroz Committee Member
Dr. Richard Peralta Committee Member	Dr. Mark R. McLellan Vice President for Research and Dean of the School of Graduate Studies

UTAH STATE UNIVERSITY
Logan, Utah

2012

ABSTRACT

The Calibration and Uncertainty Evaluation of Spatially Distributed Hydrological Models

by

JongKwan Kim, Doctor of Philosophy

Utah State University, 2012

Major Professor : Dr. Mac McKee
Department : Civil and Environmental Engineering

The availability of spatially distributed information, from remote sensing and Geographic Information Systems (GIS), has allowed for the development and implementation of spatially distributed hydrologic models. In particular, remotely sensed distributed snow data sets and precipitation forcing from radar information have allowed us to conduct various studies about snow modeling, snow calibration, and snow effects on runoff. The snow information is very important as a water source, especially in the snowy mountainous regions of the western United States. In this study, we calibrate, evaluate and diagnose the National Weather Service Office of Hydrology HL-RDHM model, a spatially distributed hydrological model to investigate both snow and runoff information over the Durango river basin, which is a mountainous snow-dominated area. For the calibration and evaluation of the HL-RDHM model, we employ overall basin runoff discharge Q_1, upstream sub-basin runoff discharge Q_2, snow water equivalent and snow cover data in situ and remotely sensed from USGS, SNOTEL and NSIDC as observations, respectively. The snow cover extent is also used as an observation. Through the calibrations and evaluations of HL-RDHM, this study investigates the effect of the additional snow information on runoff simulations only; and on both runoff and snow simulation together; and contrasts the model performance attained when using single- or multi-criteria calibrations. We explore the advantages and disadvantages of using shape-matching error functions such as Hausdorff and Earth Movers' Distance (EMD) in the calibration procedures. Additionally, we seek to establish an appropriate level of model spatial distribution (model complexity) based on the quality of the calibrated model performances. Finally, through parameter estimations, we seek to decide the constrained parameter ranges and parameter uncertainty for the HL-RDHM.

We showed that snow simulations are improved with both single- and multi-criteria calibrations using either traditional or shape-matching error functions. The snow information is very useful to calibrate and evaluate the hydrologic model for snow and runoff information. The multi-criteria calibrations reveal better performances for simultaneously improving overall and sub-basin runoff discharges based on snow information only. The use of shape-matching error functions shows several advantages for model performances: the use of non-commensurate observations, and constrained parameter estimations. In general, after calibration, a distributed model (multi signatures) yields a better performance of snow and runoff than a single signature model, for the case study. Lastly, the shape-matching error functions are more effective in constraining the parameter estimations into physically plausible ranges for the HL-RDHM model.

(161 pages)

PUBLIC ABSTRACT

The Calibration and Uncertainty Evaluation of Spatially Distributed Hydrological Models

by

JongKwan Kim, Doctor of Philosophy

Utah State University, 2012

Major Professor : Dr. Mac McKee
Department : Civil and Environmental Engineering

In the last decade, spatially distributed hydrological models have rapidly advanced with the widespread availability of remotely sensed and geomatics information. Particularly, the areas of calibration and evaluation of spatially distributed hydrological models have been attempted in order to reduce the differences between models and improve realism through various techniques. Despite steady efforts, the study of calibrations and evaluations for spatially distributed hydrological models is still a largely unexplored field, in that there is no research in terms of the interactions of snow and water balance components with the traditional measurement methods as error functions. As one of the factors related to runoff, melting snow is important, especially in mountainous regions with heavy snowfall; however, no study considering both snow and water components simultaneously has investigated the procedures of calibration and evaluation for spatially distributed models. Additionally, novel approaches of error functions would be needed to reflect the characteristics of spatially distributed hydrological models in the comparison between simulated and observed values. Lastly,

the shift from lumped model calibration to distributed model calibration has raised the model complexity. The number of unknown parameters can rapidly increase, depending on the degree of distribution. Therefore, a strategy is required to determine the optimal degree of model distributions for a study basin. In this study, we will attempt to address the issues raised above. This study utilizes the Research Distributed Hydrological Model (HL-RDHM) developed by Hydrologic Development Office of the National Weather Service (OHD-NWS). This model simultaneously simulates both snow and water balance components. It consists largely of two different modules, i.e., the Snow 17 as a snow component and the Sacramento Soil Moisture Accounting (SAC-SMA) as a water component, and is applied over the Durango River basin in Colorado, which is an area driven primarily by snow. As its main contribution, this research develops and tests various methods to calibrate and evaluate spatially distributed hydrological models with different, non-commensurate, variables and measurements. Additionally, this research provides guidance on the way to decide an appropriate degree of model distribution (resolution) for a specific water catchment.

To my Grandfather …

This work is dedicated to all of my family and friends.

ACKNOWLEDGMENTS

Most of all, I deeply appreciate my major professor, Dr. Mac McKee, for his kind guidance and leading my dissertation. I would like to express my heartfelt thanks to Dr. Jagath J. Kaluarachchi and Dr. Gilberto E. Urroz, as well. Their friendly behavior and guidance made me finish my Ph.D work. Since spring 2007 they have supervised my research and have truly improved my academic life. I would like to thank Dr. Luis A. Bastidas for his professional guidance and advice about my research and dissertation. I am grateful to Dr. Christoper Neale and Dr. Richard Peralta for being my committee members and correcting my dissertation.

I would like to send my gratitude to all of my family. Especially, I truly thank my wife, SinAe Park, and two sons, YoonWon and JunWon Kim. Without their devotion and love, I could not accomplish anything for my academic life.

My sincere gratitude goes to all of my mentors and especially Dr. JaeSoo Lee, Dr. ChulSang Yoo, and Dr. TaeGyun Kim. Their dedicated teaching and assistance have led me to reach this point with their encouragement and best wishes.

I would like to thank the Korean communities at Utah State University and Logan. The president of Utah State University Korea Alumni, Hong Young-chul, supported my life and family in Logan, UT. As my family, Chang Lee’s family – Hye Lee, Tappy Lee, and Donna Lee, helped me and my family to live in Logan like my home town.

I would like to voice my gratitude to all of my friends and colleagues in South Korea and the Utah Water Resources Laboratory who have been supportive to my academic life.

The financial aid from the Utah Water Research Laboratory that has supported this research has helped me accomplish this work, and I am very grateful for this support.

With this research I would like to remember my late grandfather. His teaching, devotion, care and love will be carved on my mind forever....

JongKwan Kim

CONTENTS

LIST OF TABLES

LIST OF FIGURES

CHAPTER 1

INTRODUCTION

Model calibration and evaluation are fundamental techniques in the study of hydrological modeling. However, as the hydrological models are becoming more complex from lumped to distributed, the calibration and evaluation of distributed hydrological models have taken on a new aspect. The number of parameters to be optimized increases with model complexity, and large amounts of data are needed to secure inputs to run models and outputs to compare between models and observations. Many hydrologists have attempted to solve those issues in term of the calibration and evaluation of distributed hydrological models with runoff information. However, the research related to calibration and evaluation of spatially distributed hydrological models is one of the still an unexplored field, in that there is no research with respect to the interactions of snow and water balance components, although snow melt is one of the most important sources of runoff.

In this dissertation, we carry out the calibration and evaluation of a spatially distributed hydrological model with single- and multi-criteria methods in a snow dominated site. With this research we improve overall insights about calibration and evaluation for a spatially distributed hydrological model in snow driven areas. In particular, through calibrations using snow only, runoff only, and both types of information, it would be possible to quantitatively estimate snow component effects on runoff and the interaction of snow and runoff.

Also, unlike previous research with respect to the calibration and evaluation of spatially distributed hydrological models, this dissertation applies the novel approach of shape-matching error functions to compute the differences of observation and simulation in the procedures of model calibration and evaluation. In fact, the novel approaches of error functions would be needed to reflect the characteristics of spatially distributed hydrological models. In particular, the elevation factor is very crucial in mountainous regions; hence, shape-matching error functions can be considered for comparisons between simulated and observed values.

When dealing with spatially distributed models, it is important to decide the proper degree of distribution (complexity) because the running time rapidly increases depending on the model complexity. Therefore, a strategy is needed to decide the optimal degree of mode complexity for a study site. In this dissertation, we assess the model prediction uncertainty associated with the parameter estimates for different levels of model complexity; therefore, the study provides a way for hydrologists to identify an optimal degree of complexity for the spatially distributed hydrological models.

Finally, the model parameter estimations are very important for spatially distributed hydrological models in order to reduce the model uncertainty. Some parameters for hydrological models are easily measured from the real system; however, others cannot be obtained with direct measurements from the real world. Therefore, we need to estimate and select proper ranges for spatially distributed hydrological models. In this dissertation, we decide the appropriate parameter values with the calibrations of diverse variables such as runoff and snow information. We can confirm the effects of both traditional and shape-matching error functions on the parameter estimations.

This research focuses on the use of HL-RDHM as a spatially distributed hydrological model. This model is used by many hydrologists and meteorologists to simulate snow and runoff. Through this study, we will contribute to building the proper framework for model calibration and evaluation of this operational model. It is also expected that this research will contribute to greater realism of spatially distributed hydrological models in general.

This dissertation is organized as follows: Chapter 2 presents the research objectives along with the background study and literature reviews. In this chapter, the originality of this dissertation is mentioned based on previous literature in terms of calibration and evaluation of spatially distributed hydrological models with snow or runoff information. Also, we identify the differences between traditional and novel approaches of error functions. Chapter 3 presents the model used, the calibration methods, the study basin, and the available datasets employed for this study. In particular, chapter 3 includes the availability of a variety of variables with respect to runoff and snow information for calibration and evaluation. Chapter 4 presents the application of calibration and evaluation for HL-RDHM model to simulate both snow and runoff information on the study basin. In the application processes, a variety of variables are used with traditional as well as novel approaches of error functions. Particularly, chapter 4 includes the estimations for a priori parameters (starting points) as a benchmark and the process for parameter estimations of each calibration case. In Chapter 5, we present the analysis and evaluation of results for each calibration and parameter estimation. In this chapter, we compare each calibration case with different degree of distributions. Also, the model verification is carried out with different data set for single-signature, semi-distributed, and full-distributed models. Through the model calibrations we decide best model complexity for the HL-RDHM model in a specific site.

Chapter 6 includes model parameter estimations with model uncertainty. The parameters are calculated with various model calibrations for different degree of distributions. We analyze the parameter distributions for each calibration case and model complexity. The model uncertainty is estimated with model parameter uncertainty for single-signature, semi-distributed, and full-distributed models. Lastly, Chapter 7 summarizes the findings along with the scope for future works.

CHAPTER 2

BACKGROUND AND STUDY OBJECTIVES

In this dissertation, we calibrate, evaluate and diagnose a spatially distributed hydrological model by simultaneously using snow and runoff information over a mountainous snow-dominated area. The main objectives of the study are to investigate the effect of the additional snow information on runoff simulations only and on runoff and snow simulations together and to contrast the model performance attained when using single- or multi-criteria calibrations. Also, we explore the advantages and disadvantages of using shape-matching error functions in the calibration procedures. We seek to establish an appropriate level of model spatial distribution (model complexity) based on the quality of the calibrated model performance. Lastly, we estimate and select proper values for the parameters of a spatially distributed hydrological model.

2.1 Calibration of Spatially Distributed Hydrological Models

Many hydrologists have attempted to calibrate and evaluate spatially distributed hydrological models in order to reduce the differences between model performances and real system. First of all, uncertainty evaluation of spatially distributed hydrological models has been attempted using the Generalized Likelihood Uncertainty Estimation (GLUE) based on Monte Carlo sampling methods (Beven and Binley, 1992; Beven, 1993; Beven and Freer, 2001, Aronica et al., 2002; McMichael et al., 2006). These works investigated the uncertainty associated with parameters for various distributed hydrological models such as MIKE SHE, TOPMODEL and Soil and Water Assessment Tool (SWAT). However, despite several attempts to overcome the problems with the Latin Hypercube sampling (Muleta and Nicklow, 2005), Shuffled Complex Evolution

Metropolis (SCEM) algorithm (Blasone et al., 2008a, 2008b), fuzzy rule (Freer et al., 2004), multi-criteria concept (Choi and Beven, 2007), and the case studies to verify usefulness (Beven et al., 2007, 2008; Liu and Gupta, 2007), the GLUE technique has several known drawbacks with the two most important being (see comments by Thiemann et al., 2001; Kaheil et al., 2006):

i) Subjectivity in determining the likelihood function and the threshold for behavioral solutions;

ii) The large number of simulations that must be run for the application of the technique evaluation

In particular, many papers, in terms of the calibrations and evaluations for a spatially distributed hydrological model, have been published through the Distributed Model Inter-comparison Project (DMIP). In Phase-I of this project, they simulated and evaluated 12 different distributed models to compare the differences between lumped and distributed models in streamflow (Smith et al., 2004). Furthermore, while assessing the differences between calibrated and uncalibrated model performances, they have shown that some calibration efforts improved simulation results in distributed models in spite of the insufficient calibration strategies for distributed models (Reed et al., 2004). There are three different studies about calibrations and evaluations for distributed models in DMIP Phase-I. Using the radar information and GIS, they investigated the effects of calibration in distributed models for SAC-SMA (Ajami et al., 2004), TOPNET – networked version of TOPMODEL (Bandaragoda et al., 2004), and SWAT (Luzio and Arnold, 2004). In the research, they employed Shuffled Complex Evolution (SCE) algorithm (Duan et al., 1992, 1993) as a single-criterion calibration and traditional measurement methods such as Root Mean Square Error (RMSE) for high flow, LOG for low flow (Ajami et al., 2004), Nash-Sutcliffe Efficiency (NSE) (Bandaragoda et al., 2004), and the Sum of Squares of Residuals (SSQ) (Luzio and Arnold, 2004) in the procedures of model calibration and evaluation. This research has shown a significant improvement in runoff simulations with calibrated distributed models.

DMIP Phase-II deeply investigated the calibration and evaluation of spatially distributed hydrological models through comparing streamflow observations based on the results of Phase-I (Smith et al., 2012a). As a result, the differences between simulations and observations at the outlet and interior points in several study basins are reduced through parameter calibrations. However, the calibration using only an outlet point was not able to greatly improve the runoff compared to the calibration using a priori parameters (Smith et al., 2012b). During the progress of DMIP Phase-II, various approaches have been introduced for the calibration and evaluation of distributed models. In order to provide a benchmark for the calibration, an a priori parameter set for SAC-SMA was derived from the Soil Survey Geographic (SSURGO) Database and the National Land Cover Database (NLCD) on the Hydrologic Rainfall Analysis Project (HRAP) (Reed and Maidment, 1999) of $4\text{km} \times 4\text{km}$ grids (Zhang et al., 2011). This a priori parameter set has been used to provide default values to diagnose the degree of improvement with model calibrations. Also, Khakbaz et al. (2012) introduced some efficient calibration strategies for semi-distributed hydrological models. Basically, they attempted the calibrations using lumped or semi-distributed parameters and averaged or distributed forcing data to diminish the gaps between simulation and observation at outlet and interior points in a target catchment. They used a single-criterion calibration

(SCE) as an optimization algorithm and traditional error functions such as RMSE, percent Bias and modified correlation coefficient. In the distributed model calibration, the number of unknown parameters is very crucial; therefore, hydrologists have tried to decrease the number of unknown parameters using spatial regularization approaches to parameter estimation. For example, Pokhrel et al. (2008) develop a regularization relationship using the observable static characteristics of catchment such as soils, vegetation, topography, and so on. The relationship is based on a priori estimates of spatial parameters developed by Koren et al. (2003). They used a regression approach to derive empirical equations between a priori estimates and observable watershed characteristics. Therefore, the number of unknown parameters is diminished from 858 to 33 over the area of study. However, they found that the commonly used parameter field "multiplier" approach may not be proper for the parameter regularization of distributed models. Later on, Pokhrel and Gupta (2010) presented another strategy of spatial parameter regularization to improve the multiplier approach. In that study, they used a multi-criteria parameterization approach with adjustment of a mean (multiplier), variance (additive constant), and shape (power term) of the parameter distributions. In particular, they employed simple squashing functions to constrain the parameter boundaries. When a parameter passes outside of the feasible range, the parameter distribution is reformed with squashing functions. Therefore, a parameter is constrained to remain at its boundary. Based on this parameter regularization, Pokhrel et al. (2012) calibrated a spatially distributed model using multi-criteria calibration with the Multi-objective Shuffled Complex Evolution Metropolis (MOSCEM) (Vrugt et al., 2003a). Another study examined the effects of precipitation bias on the calibration and prediction of a distributed model (Looper et al., 2012). They have revealed the impacts of bias corrected precipitation usage in the procedures of distributed model calibration. Lastly, Safari et al. (2012) presented a study about calibration of a distributed model using WetSpa model. In the procedures of calibration and evaluation, they employed the traditional error functions such as Bias, modified correlation coefficient and NSCE, as well as Aggregated Measure (AM), to compare shape, size, and volume of the hydrograph.

The various insights and ideas related to the calibration of spatially distributed hydrological models presented through the DMIP Phase-I and II have had a great deal of influence on this proposed research. However, the DMIP has focused on catchments with no significant snow component in the runoff generation process. Also, this proposed study is distinct from the DMIP in that it will employ a novel approach of shape-matching error functions to consider time and location variables in the procedures of calibration and evaluation of a distributed model.

The results of DMIP aside, hydrologists have been continuously interested in the calibration and evaluation of distributed models. Some other studies have investigated the calibration of MIKE SHE as a spatially distributed model (Refsgaard, 1997; Madsen and Jacobsen, 2001; Madsen, 2003; Sahoo et al., 2006; Blasone et al., 2007). In this research, streamflow points and ground water levels were used to compare simulated and observed values (Refsgaard, 1997). Also, the concepts of single- and multi-criteria calibration have been applied to MIKE SHE (Madsen and Jacobsen, 2001; Madsen 2003; Blasone et al., 2007) in a mountainous Hawaii basin with error functions such as RMSE, correlation coefficient, and mean error (Sahoo et al., 2006).

Other hydrologists have tried to calibrate and evaluate the SWAT model as a distributed model. Eckhardt and Arnold (2001) attempted parameterization and automatic calibration of SWAT as an initial stage. After that, the SWAT model was calibrated using a multi-variable and multi-site approach with radar information (Cao et al., 2006; Schuol and Abbaspour, 2006; Immerzeel and Droogers, 2008).

Aside from the studies mentioned above, hydrologists have attempted to calibrate and evaluate various spatially distributed hydrological models using diverse approaches of spatially distributed forcing data, calibration methods, and error functions (Motovilov et al., 1999; Senarath et al., 2000; Jasper et al., 2002; Brath et al., 2004; Campo et al., 2006; Moussa et al., 2007; Frances et al., 2007; Marce et al., 2008; Shafii and Smedt, 2009; Segui et al., 2009). Although research with respect to the calibration and evaluation of spatially distributed hydrological models have been conducted, they have concentrated only on the water component. Therefore, it is hard to apply the studies to snow dominated areas such as the mountainous western United States. It is necessary to carry out the calibration and evaluation considering both snow and water balance components in a snow dominant area in order to investigate the effects of snow melting on runoff information.

2.2 Calibration of snow and water balance model components

Snow is very important as a water source, especially in the snowy mountainous regions of the western United States. In fact, about 40% to 70% of the total annual precipitation in the region falls in the form of snow (Serreze et al., 1999). The calibrations and evaluations of distributed snow models are relatively poor when compared to those of rainfall runoff models.

There are several studies in which model prediction verification, parameter sensitivity, and uncertainty analysis of the Snow 17 model have been carried out, but only with a few points for evaluation (Franz et al., 2008a, 2008b, 2010; He et al., 2011a, 20011b; Mizukami et al., 2011). Also, Carrera et al. (2010) investigated the snowpack simulations in the Canadian Rockies with an experimental hydrometeorological model. These studies have used point data for snow water equivalent from the SNOwpack TELemetry (SNOTEL) network of the Western United States and Canada for the evaluations. A few studies using other distributed snow models based on energy balance to investigate the snow information such as snow melting, snow water equivalent, and snow albedo using in situ or remotely sensed data sets have also been carried out (Marks et al., 1999; Wilson et al., 1999; Molotch et al., 2004). Although calibrations and simulations using snow information, such as snow water equivalent or snow cover, have been attempted, they do not link with water balance components or runoff. Unlike previous research, this dissertation carries out the calibrations and evaluations in both snow and water balance components for a distributed model.

In the last two decades, some scientists have been studying the effects of snow on runoff with various methods. Wigmosta et al. (1994) and Xue et al. (2003) have performed a sensitivity analysis and parameterization for the snow component using snow and runoff information. A few hydrologists have taken the snow component into consideration for calibration; however, their focus has been mainly on the water balance component (Dunn and Colohan, 1999; Hogue et al., 2000; Konz et al., 2010; Martinez and Gupta, 2010; Ragettli and Pellicciotti, 2012). Consequently, they do not provide the parameter behavior for snow and comparing snow information. In particular, Hogue et al. (2000) investigated the impacts of the snow component through the calibrations of snow and water balance simultaneously. However, they were based solely on a lumped model without considering distribution. Martinez and Gupta (2010) have a calibration with snow information consisting of snow or no snow, but they have concentrated only on water balance modeling over the conterminous United States. Also, Ragettli and Pellicciotti (2012) have investigated the interactions between glaciers and climate with a spatially distributed model. As they simulated and calibrated the glacier melt and runoff, they have assessed the model applicability and estimated snow and runoff model parameters. They have carried out a parameter sensitivity analysis as well; however, they do not analyze the parameter behavior and parameter interaction between the snow and water balance components because they have focused only on snow-melt and runoff.

This dissertation shows its originality by performing the calibrations and evaluations of snow and water balance components in a spatially distributed hydrological model. Also, diverse variables, in terms of snow and runoff in situ and remotely sensed information, will be employed in the procedures of calibration and evaluation.

2.3 Error Functions for Distributed Information

It is crucial to choose proper objective functions in model calibration and evaluation. The question of which error function is best for a selected model and hydrological variables has persisted since the 1980’s. Some hydrologists developed and applied the error functions related to maximum likelihood estimators: AMLE (maximum likelihood estimator for the auto-correlated error case) and HLME (maximum likelihood estimator for the heteroscedastic error case) (Soroosian and Dracup, 1980; Soroosian et al., 1983; Gan et al., 1997). Previous research revealed the importance of appropriate error function in procedures of model calibration and evaluation. The usage of proper error function has been emphasized in the shift from lumped to distributed models because of the utilization of diverse variables and distributed observations in distributed models. In particular, DMIP Phase-II, despite using traditional error measurement functions (Yilmaz et al., 2008; Pokhrel and Gupta, 2010; Pokhrel et al., 2012; Safari et al., 2012). Yilmaz et al. (2008) and Pokhrel et al. (2012) introduced the concept of signature measures, multiple relevant hydrological variables, and various measurement methods to evaluate model performance at the watershed outlet. Through the signature measures and error functions introduced in previous studies, it is possible to compare various error functions at a glance. Pokhrel and Gupta (2010) attempted to test the simple squashing functions to maintain reasonable parameter values in the spatial area, and Safari et al. (2012) introduced the Aggregated Measure (AM) to calculate the differences between simulated and observed hydrographs with shape, size and volume. As a simple combination of model bias, modified correlation coefficient, and NSE, the AM can compare the shape, size and volume of the hydrograph; however, it cannot reflect both temporal and spatial coordinates for distributed data. They used both methods in the procedures of calibration and evaluation to achieve improved model performances.

2.3.1 Traditional Error Function

One of the most important aspects of a spatially distributed hydrological model is the use of distributed input and output datasets. Most of the studies referred to in this dissertation have employed spatially distributed datasets from in situ and remotely sensed information. For model calibrations and evaluations, however, traditional error measures between observed and computed values, such as RMSE, bias, NSE, R-square and others, focused on runoff at the basin outlet despite the use of spatially distributed information (Hogue et al., 2000; Senarath et al., 2000; Madsen and Jacobsen, 2001; McMichael et al., 2006; Blasone et al., 2008a, 2008b; Franz et al., 2008a, 2008b, 2010; Immerzeel and Droogers, 2008; Martinez and Gupta, 2010; He et al., 2011a, 2011b; Khakbaz et al., 2012; Looper et al., 2012; Ragettli and Pellicciotti, 2012). In the DMIP Phase-II, spatially distributed hydrological models have been improved with traditional measurement methods. As mentioned in section 2.3, however, a few hydrologists have attempted to develop various error functions to reflect only the characteristics of hydrological variables. The classical approaches to error functions would not be appropriate for spatially distributed hydrological models, where it is possible to carry out a quantitative comparison of spatial fields.

2.3.2 Shape-Matching Error Functions

Shape-matching error functions are widely used in image processing (Huttenlocher et al., 1993; Yi et al., 1996; Belogay et al., 1997; Beauchemin et al., 1998; Rubner et al., 2000; Assent et al., 2008). An image yields a distribution in color space by mapping each pixel of the image to its color. This characteristic is very similar to the remotely sensed information in the spatially distributed models in that they have a pattern. Therefore, some scientists have employed the shape-matching error functions to compute the differences between simulated and observed values in the field of rainfall distribution (Dodov and F.-Georgiou, 2005; Venugopal et al., 2005; Li, 2006; Nan et al., 2010; Van den Berg et al., 2011). In the previous research, Dodov and F.-Georgiou

(2005) and Venugopal et al. (2005) have proved the availability of similarity functions (Hausdorff) to compare precipitation distributions and patterns. Bastidas (1998) used a similarity approach to compare a whole set of solutions to a single observation, and Nan et al. (2010) have analyzed the spatial similarities between two different precipitation data sets from radar information using Hausdorff. On the other hand, Van den Berg et al. (2011) have shown the analysis of rainfall distributions like an image using a new shape-matching function – Earth Mover's Distance (EMD).

Hausdorff Distance

The Hausdorff norm is well known in set theory as a measure of the distance between two sets. It has been largely applied for pattern recognition and comparison in the areas of image processing. The Hausdorff distance has great advantages when comparing spatial patterns in that it is relatively tolerant of small position errors that occur with edge detectors. Moreover, the Hausdorff can be calculated without the correspondence between the model and image, as well as naturally extended to the problem, for comparing a part of a model with an image. The original application of the Hausdorff distance was proposed for curve matching in a two-dimensional space (Marron and Tsybakov, 1995); however, it is very easy to extend to *n* dimensions. The computation of the norm according to (Marron and Tsybakov, 1995) follows.

A set *G* (a curve in two-dimensional spaces) is defined as:

$$G = \{(x, y) : x \in [a, b], y = f(x)\} \subset \Re^2 \tag{1}$$

The distance from any point *(x,y)* to a set *G* is defined as:

$$d\left(\left(x,y\right),G\right)=\inf_{\left(x',y'\right)\in G}\left\|\left(x,y\right)-\left(x',y'\right)\right\|_2 \tag{2}$$

That is, the shortest distance from the given point (x, y) to any point (x', y') in the closed set *G*, where $\|\cdot\|_2$ denotes the usual Euclidean distance (any other properly defined norm or distance can be used, e.g. the more general Minkowsky distance). Distances from a set G_1 as an observation to a set G_2 as a computation can then be combined into the set of distances:

$$d\left(G_1,G_2\right)=\left\{d\left(\left(x,y\right),G_2\right):\left(x,y\right)\in G_1\right\} \tag{3}$$

Given that the distances between sets G_1 and G_2 are not interchangeable, these distances are combined to give the Hausdorff distance as:

$$Hausdorff = \max\left\{\sup\left(d\left(G_1,G_2\right)\right),\sup\left(d\left(G_2,G_1\right)\right)\right\} \tag{4}$$

Basically, the Hausdorff measures the degree of mismatch between two sets of points, thus it is possible to verify whether a pattern matches a template image or not. The lower the distance value, the better the match. There have been two applications in which the Hausdorff distance was used to calibrate spatially distributed fields (Bastidas, 1998; Li, 2006). In previous research, they have compared modeled and observed values in time and space of several distributed fields such as ground temperature and soil moisture.

Based on the previous research, this study uses a multi-dimensional point set, $P(t, x, y, z, v_1, v_2, ..., v_n)$ to calculate the Hausdorff between observed and computed values for hydrological applications. Considering a point set with multi-dimensions such as time (*t*), location (*x*, *y*), elevation (*z*), and variables (e.g. snow information) it is possible to compare distributed observed and computed variable values in the cells over time and space.

The original Hausdorff requires large computation times, an important consideration in the procedures of calibration. For that reason, in this dissertation we have used a modified formulation of the Hausdorff (after Bastidas, 1998; Venugopal et al., 2005) to reduce the computational overburden and remove the dependence on outliers. In hydrology, temporal and spatial coordinates remain the same, i.e., for $\mathbf{x}(t, x, y, z)$, we define a vicinity (neighborhood) Ω of the point $\mathbf{x}$:

$$\Omega : |x - \varepsilon| < \delta \qquad \forall \varepsilon < \delta\ ,\ \delta > 0 \tag{5}$$

Therefore, the set to set distance is calculated with only the points within the vicinity instead of the entire sets. The running time for calibration and evaluation is significantly decreased as the vicinity (neighborhood) is pre-defined outside optimization algorithms. Also, a partial Hausdorff is utilized to avoid the effect of outliers using a probability of exceedance, P_H described as:

$$p\left(d(A, B) \geq d(\Omega_A, \Omega_B)\right) = P_H \tag{6}$$

Although the partial Hausdorff could not perfectly achieve the formal definition of a metric, it is possible to use it as an objective function. In order to verify the effects of the size of neighborhood on the value of Hausdorff, the Hausdorff values are computed with different δ values. Hence, computational overburden is reduced by determining an average 30 percent along each dimension for vicinal subsets from the entire sets.

To facilitate the comparison, before the computation of the distance, all the variables of the multi-dimensional point set (observed and computed) are normalized with respect to the observations and are computed using a new variable $x^{(new)}$:

$$x_i^{(new)} = \frac{x_i - \min\left(x_i^{(obs)}\right)}{\max\left(x_i^{(obs)}\right) - \min\left(x_i^{(obs)}\right)} \tag{7}$$

where x_i is any of the coordinates of the *n*-dimensional point *P*.

Earth Mover's Distance (EMD)

The EMD is a method to evaluate dissimilarity between two different signatures in some feature spaces (Rubner et al., 2000). Informally, the surfaces can be interpreted as a certain amount of dirt over a region *D*. The EMD is the minimum cost of turning one pile into the other, where the cost is assumed to be amount of dirt moved times the distance it is moved. If the domain *D* is discrete, the EMD can be computed by solving an instance transportation problem. In particular, if *D* is a one-dimensional array of "bins" the EMD can be efficiently computed by scanning the array and keeping track of how much dirt needs to be transported between consecutive bins. The bins will be considered as a signature in a case study. The signatures can describe the variable-size of distributions so that a signature $\{s_j = (m_j, w_j)\}$ represents a set of clusters. Each cluster is represented by its *d*-dimensional mean or mode m_j and by the number w_j of pixels that belong to that cluster.

Intuitively, given two distributions, one can be seen as a mass of earth properly spread in space, the other as a collection of holes in that same space. It can be always assumed that there is at least as much earth as needed to fill all the holes to capacity by switching what we call earth and what we call holes, if necessary. For instance, $P = \{(p_1, w_{p_1}),...,(p_m, w_{p_m})\}$ is the signature of fist distribution (observations) with m clusters, cluster representative (mean or mode), p_1 and the weight of the cluster, w_{p_1}. In the same way, $Q = \{(q_1, w_{q_1}),...,(q_m, w_{q_m})\}$ is the signature of the second distribution (simulations) with n clusters. If the ground distance matrix $D = \lfloor d_{ij} \rfloor$, d_{ij} is the ground distance between clusters of p_i and q_j. The flow between p_i and q_j is f_{ij}, such that we can find a flow $F = \lfloor f_{ij} \rfloor$, that minimizes the overall cost:

$$WORK\,(P,Q,F) = \sum_{i=1}^{m}\sum_{j=1}^{n} d_{ij}\, f_{ij} \tag{8}$$

Subject to the following constraints:

$$f_{ij} \geq 0 \qquad 1 \leq i \leq m,\ 1 \leq j \leq n \tag{9}$$

$$\sum_{j=1}^{n} f_{ij} \leq w_{p_i} \qquad 1 \leq i \leq m \tag{10}$$

$$\sum_{i=1}^{m} f_{ij} \leq w_{q_j} \qquad 1 \leq j \leq n \tag{11}$$

$$\sum_{i=1}^{m}\sum_{j=1}^{n} f_{ij} = \min\left(\sum_{i=1}^{m} w_{p_i}, \sum_{j=1}^{n} w_{q_j}\right) \tag{12}$$

where the constraint (9) allows shipping from *P* to *Q* and not vice versa. The constraint (10) forces the amount to fill up all of their capacities, and constraint (11) limits the cluster in *Q* to receive no more than their weights. Lastly, constraint (12) limits the maximum possible amount to move which called total flow. Once the problem is solved, the optimal flow *F* is found and the EMD is defined as:

$$EMD(P,Q) = \frac{\sum_{i=1}^{m}\sum_{j=1}^{n} d_{ij} f_{ij}}{\sum_{i=1}^{m}\sum_{j=1}^{n} f_{ij}} \tag{13}$$

where the denominator is a normalization factor that avoids favoring signatures with smaller total weights. Therefore, the EMD naturally extends the notion of a distance between single elements to that of a distance between sets, or distributions, of elements.

In hydrology, EMD can calculate overall errors between two different gridded data sets by considering them as different pattern images.

2.4 Research Objectives

In reviewing the previous studies and investigations, the classical approaches for the calibration and evaluation of spatially distributed hydrological models have been shown to face a number of issues. It is clear that surface water discharge has a close relationship with snow, especially in mountainous regions. However, the available calibration strategies to investigate the interaction of snow and water balance components are still an unexplored field in the calibration of spatially distributed hydrological models.

Furthermore, although spatially distributed data sets, from in situ or remotely sensed information, have been used in the procedures of calibration and evaluation of spatially distributed hydrological models, the characteristics of spatially distributed observations should be reflected, and the traditional error measurement methods are incapable of doing that.

Lastly, one of the most important aspects of the calibration and evaluation of spatially distributed hydrological models is the degree of distribution, or the model complexity. The number of model parameters increases with the number of grids and has a significant influence on the calibration efficiency; however, there are no appropriate ways to decide the optimal degree of distribution for a particular basin.

This research contributes to the solutions and addresses those problems, recognizing the need to attend to the following issues:

i) There is no generally recognized successful calibration framework for spatially distributed hydrological models with the parameters of both snow and water balance components.

ii) Novel approaches for error measurement, such as shape-matching functions, are needed to reflect the characteristics of spatially distributed in situ and satellite observations.

iii) There is a need for a criterion by which to judge an appropriate degree of distribution for effective calibration and evaluation of spatially distributed hydrological models.

The primary goal of this research is to devise ways for a proper calibration, performance evaluation, and diagnosis of a spatially distributed hydrological model in snow dominated areas. The following are major specific objectives:

i) Quantitatively evaluate the influence/contribution of snow information to the performance of model runoff simulations.

ii) Conduct an inter-comparison of model performance and parameter estimation when using snow only, runoff only, and both sources of information for the calibration of the model.

iii) Explore and evaluate the advantages/disadvantages of shape-matching error functions on the calibration of the model.

iv) Assess the model prediction uncertainty associated with the parameter estimation for the different situations.

v) Identify an appropriate degree of distribution (complexity) for the model.

CHAPTER 3

METHODS AND DATASETS

The main objective of this dissertation is to calibrate, evaluate, and estimate the appropriate complexity of a spatially distributed hydrological model, the HL-RDHM, based on the parameter estimations. Through these endeavors we investigate the influences of snow information on runoff simulations only and on runoff and snow simulations together and we compare the model performances of different single- and multi-criteria calibrations. Additionally, we explore the advantages and disadvantages of shape-matching functions in the procedures of calibration and evaluation for distributed models. For these purposes we simultaneously consider snow distribution information (snow water equivalent and snow presence) and water balance components (multi-gauge discharge). Due to its significance, as the new NWS operational forecast model, we use the HL-RDHM model. The evaluations and calibrations are carried out using both traditional and shape-matching error functions. The influence that spatially distributed snow information has on the overall performance of the model is exhaustively evaluated. A detailed analysis of the role that the snow information plays on the uncertainty due to parameter estimation is also performed.

3.1 Model Used: HL-RDHM

The HL-RDHM (Koren et al., 2004) is used in this research as the spatially distributed hydrological model. Because the HL-RDHM includes both snow and water balance components, it is suited for the main objectives of the study. The model is under continuous development and is currently in version 3.2; however, in this dissertation we have used version 2.4. We stopped updating the version because the objectives of the study are general and the changes in the versions are mostly in the computer code and are of a technical nature (related to the handling of data), not to the specific components of the model.

For the snow component, the HL-RDHM uses the Snow17 model developed by Anderson (1973). This is a conceptual model for snow accumulation and ablation. Sow17 uses precipitation and temperature data as inputs and generates rain-plus-melt or snow cover outflow as output. For an in-detail model description, readers are referred to the report of Anderson (2006). In this dissertation, the computational methods for calculating snow parameters are presented and the ranges of snow parameters are suggested based on the energy balance. The water balance representation of HL-RDHM is the National Weather Service SAC-SMA (Burnash, 1995) used in gridded mode as the distributed component (Koren et al., 2004). The National Weather Service SAC-SMA is comprised of two different layers: a lower layer and a relatively thin upper layer that supplies moisture for evapotranspiration demands. As both layers have free and tension water storage, they can interact to produce soil moisture states and water balance components. In the model, once the tension and free water storage of the upper layer are saturated, excess runoff occurs. After that, through hillslope and channel routing, the runoff is estimated for each grid in the HL-RDHM.

In the present application, the HL-RDHM is initially distributed with a resolution of $4\text{km} \times 4\text{km}$ using the HRAP grid over the study catchment of the Durango River basin in Colorado. Cell by cell, the gridded precipitation and temperature data are used to calculate snow melt and rain with Snow17. The precipitation excess is estimated in SAC-SMA using the snow melt and rain computed from Snow17 on each grid. Finally, we can obtain the runoff discharge at two different gauge locations (one is the outlet point at the study basin and another is an interior point) by accumulating the precipitation excess with routing.

3.2 Calibration Algorithms

For parameter estimation of snow and water balance components, the HL-RDHM is calibrated using single and multi-criteria calibration methods. As a single-criterion calibration algorithm, the SCEM global optimization method (Vrugt et al., 2003b) is employed for calibration using a snow variable or the outlet runoff. The algorithm is based on the Markov Chain Monte Carlo (MCMC) approach to estimating parameter uncertainty within a Bayesian framework. It is an effective MCMC sampler that is well-suited to searching the posterior probability distribution of hydrologic model parameters. With the SCEM, we can estimate uncertainty bounds on model simulation associated with parameter uncertainty. Sometimes single-criterion methods are limited (Gupta et al., 1999), so the MOSCEM algorithm (Vrugt et al., 2003a) is used for multi-criteria calibrations. MOSCEM is an extension of SCEM that uses the Pareto dominance concept; the MOSCEM is used to search the dominant Pareto set or non-inferior solution set to evolve the initial population of parameter points within the feasible parameter space. As a result, we can obtain the dominant Pareto set of the parameters for Snow 17 and SAC-SMA. The original papers have detailed descriptions of the algorithms, and the interested reader is referred to them for additional explanations.

For this study, the SCEM and MOSCEM are linked with HL-RDHM framework in C^{++} under a Linux environment. To address some of the problems that have arisen in previous research, various calibration cases will be tried in order to explore the parameter sets using a variety of objective functions and different levels of model distribution.

3.3 Study Area

The Durango River Basin, located in southwestern Colorado, is the chosen area of study because it has available data and is a snow-dominated basin. The basin is a relatively wide and elongated steep-sloping river valley approximately 97 km long, ranging in elevation from 2,100 m to 3,900 m. The basin has a drainage area of approximately 1,842 km^2 and is characterized by natural forested upland, both deciduous and evergreen, with sand and loam as dominant soil types. It has two different U.S Geological Survey (USGS) stream discharge stations: one is an internal station (USGS 08359010), called Q_2 in this study, and the other, called Q_1, is at the outlet of the basin (USGS 09361500). Furthermore, there are three different SNOTEL sites in the study site. The station names are Mineral Creek (Site Number 629), Molas Lake (Site Number 632), and Cascade (Site Number 386) from upstream to downstream. The elevations of the sites are 3,060 m, 3,200 m, and 2,700 m, respectively, as measured near the stream line. As mentioned earlier, the spatially distributed HL-RDHM model will be divided into a $4km \times 4km$ HRAP grid, so that 108 grid cells are produced over the catchment. Figure 1 depicts the location and the gridded cells on the basin. Figure 3.1 (a) shows the location of study catchment and associated runoff and SNOTEL observation sites. The gray parts are ignored for HRAP grids. Figure 3.1 (b, c, d, and e) depicts the signatures of Snow 17 and SAC-SMA for semi- and full-distributions, which will be described later in Chapter 4.

3.4 Available Data

In order to run the HL-RDHM we need gridded precipitation, temperature, and evaporation data over the Durango River basin as input data sets. The spatially distributed precipitation data estimates are available for the basin from radar information. The data are available at a temporal resolution of 6 hours and a spatial resolution of 4km$\times$4km over a HRAP grid based on a polar stereographic projection. The study basin consists of 108 HRAP cells and the precipitation and temperature values are available for each distributed cell. The data can be easily downloaded from the NOAA web site www.cbrfc.noaa.gov/outgoing/ cbrfc_precipitation_sets/6_hrly. For evaporation, NOAA provides estimates of free water surface evaporation values for the basin through the same website. These values are estimated from monthly multi-annual averages of station data, meaning the same evaporation values are repeated for every year. For this study, five years of data from October 1, 2001 to September 30, 2005 are used: the last water year (WY 04-05) is used to calibrate and the first water years (WY 01-04) are used to evaluate the model.

In the procedures of calibration and evaluation of HL-RDHM, we employ discharge from USGS gages 09361500 and 08359010 (Q_1, Q_2), remote sensing-based snow water equivalent generated by the National Snow and Ice Data Center (NSIDC) and snow water equivalent from three different SNOTEL stations in the study site as observations. Additionally, we compute a binary snow/no snow value (snow cover index) from the Snow Water Equivalent (SWE) at each cell and the snow cover extent (SCX-percent of basin area covered with snow from binary snow cover), which is very useful to compare snow information in distributed hydrological models (Carrera et al., 2010).

For the SWE, we use data from the NSIDC, which provides information over the entire Durango River basin with high spatial (1km$\times$1km) and temporal (1 hour) resolutions (Barrett, 2003). Because we use the HL-RDHM with 4km$\times$4km HRAP grid as the resolution in this study, we aggregate the resolution of snow water equivalent into the HRAP grid. However, the snow water equivalent data from NSIDC is provided only for WY 04-05 so it cannot be used for model evaluation. We should note that this SWE information is generated by a remote sensing model and those values are not necessarily correct. On the other hand, the binary snow cover is deemed much more reliable because the absence or presence of snow can be clearly determined from a remote sensing image. We have additional SWE information from SNOTEL sites in the Durango River basin. They have high quality SWE in situ data that can be used for model calibration. The observed SWE values are matched up for the computations at each cell in which the SNOTEL stations are located.

For the binary snow cover (SCV) we have generated two different sets of data. For the model calibration period, we use the SWE from NSIDC (snow if SWE > 0; otherwise no snow). Due to the model-generated limitation of this data set, the snow cover from NSIDC is used only for model calibration. For model verification, the snow cover data from the Moderate Resolution Imaging Spectroradiometer (MODIS) are utilized; however, the MODIS has different resolution than HRAP (500m$\times$500m), and the values are aggregated, when available, or are considered missing.

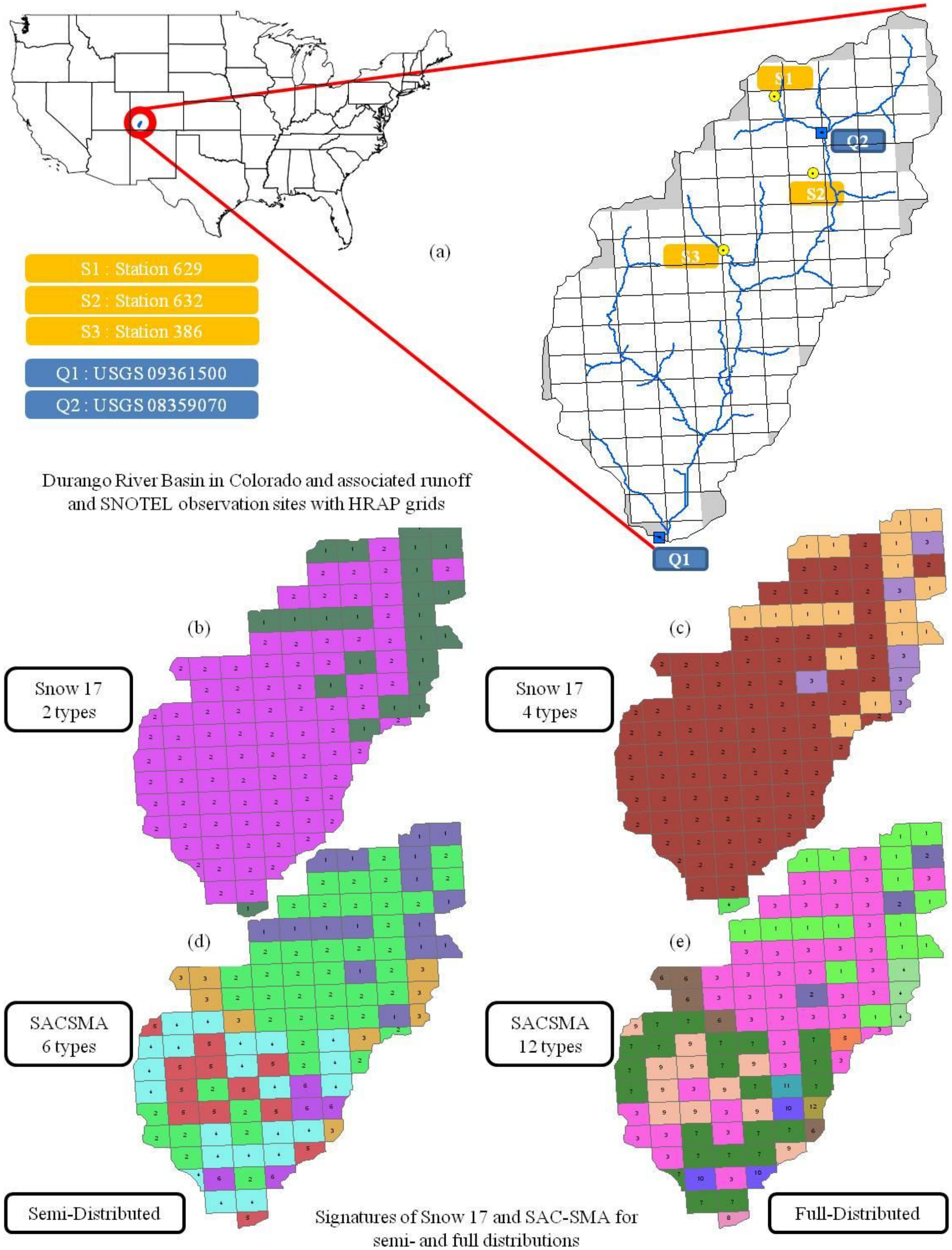

Figure 3.1 Durango River Basin (a) general location and location of discharge gages and SNOTEL sites (b) SNOW-17 signatures for “Semi-Distributed” (c) SNOW-17 signatures for “Full-Distributed” (d) SAC-SMA signatures for “Semi-Distributed” (e) SAC-SMA signatures for “Full-Distributed”.

CHAPTER 4

MODEL SIMULATIONS FOR EACH CALIBRATION

As mentioned above, the shift from lumped model calibration to distributed model calibration raises many important issues, such as parameterization, proper model complexity and appropriate closeness methods. In the procedures of parameterization, one of the most important issues is the reduction of the parameter dimensionality because the number of parameters to be optimized in a distributed hydrological model will be rapidly increased with the level of model distribution. In the present study we address the issue in the following manner: (1) based on previous studies, the most sensitive parameters for Snow 17 and SAC-SMA are selected (Hogue et al., 2000; Koren et al., 2000, 2003; Anderson, 2006; Franz et al., 2008a, 2008b, 2010; He et al., 2011a, 2011b; Zhang et al., 2011), which leaves 5 parameters and 13 parameters (respectively) in each cell for calibration (Table 4.1 shows the parameters to be optimized for HL-RDHM) and (2) areas with similar physical characteristics are ascribed same parameter values, such that if two different cells have the same physical characteristics, such as soil type and land cover, they will be treated as a single signature. In fact, one case of this study considers the entire catchment as one signature, i.e., all the cells have the same physical properties, but the model is still run on a cell-by-cell basis. To get an estimate of an appropriate level of model complexity, a “semi-distributed” model and a “Full-distributed” model are considered, with 2 snow and 6 water balance signatures and with 4 snow and 12 water balance signatures, respectively, based on the information about soil types, slopes, and vegetation cover (see Figure 3.1 for the identified signatures). The feasible search space for model parameter values, i.e., lower and upper bounds of parameters for Snow17 and SAC-SMA, define the a priori uncertainty in the model parameters associated with which there is an implicit uncertainty in the model outputs and is prescribed. It is clearly impossible to find a model to exactly match the data due to errors in input and output observations. However, the gap between computed and observed data for snow and discharge will be reduced through the calibration process.

4.1 Control Run using Default Parameter set

The parameter values for the a priori (starting point) are calculated for the snow and water balance components as a benchmark. Those computations are carried out as described in Anderson (2006) and Zhang et al. (2011). The former shows the calculation process and ranges for Snow 17 parameters based on an energy balance model. However, a priori parameters are estimated using only forest type, density, aspect and slope in each grid without considering energy fluxes such as radiation, sensible and latent heat, and so on due to limited data availability in the study site. On the other hand, the a priori parameter set for the water balance component has better conditions in data availability. The approach exploits map gridded information about antecedent soil moisture, hydrologic soil group from Natural Resource Conservation Service (NRCS), type of vegetation, and category of land use for spatially distributed cells in the study basin. The procedure to derive a priori parameters is described in detail by Zhang et al. (2011). In this study, we have a maximum of 4 different snow signatures and 12 different water balance signatures on the study catchment. Therefore, each cell has different initial parameter sets based on the physical characteristics within the cells. Table 4.1 includes the optimized ranges of parameters and a priori parameter set on each signature for Snow 17 and SAC-SMA.

4.2 Parameter Estimations for Each Calibration

Given that the focus of the paper is the study of the impact of snow information on the runoff simulations, for the single-criterion calibrations, only snow information is used, i.e. SWE, SCX, and SCV with different model distributions. On the other hand, snow and discharge information are used for the multi-criteria calibrations. We also look at the influence of different error functions to evaluate the differences between observations and simulations. As previously stated, a novel approach to properly compare the results from distributed models is used: the shape-matching error functions, Hausdorff and EMD. The traditional RMSE is utilized as well. In this dissertation, we present the results of five different single-criterion calibrations and eight different multi-criteria calibrations. In all, a total of 84 different calibration exercises, each with different error functions and levels of distribution, were considered, but only the 39 that provided better simulations were kept for further analysis. Table 4.2 shows all calibration cases as well as the sort of calibration cases (Selected No.) selected for this dissertation. NOAA means that the snow information from NSIDC remotely sensed data is used and SNOTEL means that the in situ SNOTEL information from the three different sites is used. The subscript determines the type of variable used and the superscript is associated with the type of objective functions. For instance, $NOAA_{SCX}^{RMSE}$ means that the SCX values from NSIDC remotely sensed information are calibrated with the traditional objective function RMSE. Remember that for the runoff observations, we have 2 different USGS stream stations on the study basin: Q_1 at the outlet point and Q_2 at an interior point. Hence, $Q_1^{RMSE} : Q_2^{RMSE} : SNOTEL_{SWE}^{RMSE}$ means a multi-criteria calibration using the two runoff discharges and SWE from SNOTEL with RMSE as objective function. In those abbreviations, we have 2 different kinds of Hausdorff values: Haus1 and Haus2. In the Haus1, the error values are calculated considering only the multiple time series simultaneously without considering location and elevation. Haus2 calculates the differences including time, location, elevation, and simulation variables simultaneously. Additionally, the matching number in Table 4.2 is described with the numbers on Figure 4.1 for single-, semi-distributed and full-distributed signature models.

4.3 Graphic User Interface (GUI) for Model Simulations

For the comparison of each calibration with different variables in terms of snow and runoff information, we have a total of 84 initial optimizations with different levels of distribution. Additionally, because the study basin has 108 HRAP grid cells, it is too hard to compare model parameters and outputs in both each point and the grid. In order to solve this problem, the Graphic User Interface (GUI) for each model optimization is invented with the MATLAB-GUI tool. Figure 4.2 is a sample of the interface. The cells (No. 0 – No. 107) represent the 108 HRAP grids on the study basin and dark gray boxes on the middle line represent the transect grids. The two green big boxes are runoff stations for the outlet and internal points. Also, the three smaller yellow boxes represent the SNOTEL stations on the study site. By putting SWE and SCV information on the interface, we can easily compare the runoff information as well as snow information for each optimization case. In particular, the variations of snow information according to time are investigated with the movie function. Therefore, we can easily see the variations in snow information for daily, monthly, and seasonal timeframes.

Table 4.1 HL-RDHM selected parameters for optimization, feasible space, and a priori parameter set for each signature.

Snow 17	Description	Ranges	A Priori Parameter			
			T1	T2	T3	T4
SCF	Snow correction factor (dimensionless)	0.50-1.50	1.05	1.05	1.05	1.05
MFMAX	Maximum melt factor (mm $^{o}C^{-1}$ $(6\ h)^{-1}$)	0.50-2.20	0.90	1.10	0.90	0.50
MFMIN	Minimum melt factor (mm $^{o}C^{-1}$ $(6\ h)^{-1}$)	0.05-0.60	0.50	0.05	0.05	0.45
NMF	Maximum negative melt factor (mm hPa^{-1} $(6\ h)^{-1}$)	0.05-0.50	0.20	0.20	0.20	0.20
UADJ	Wind function factor (mm hPa^{-1} $(6\ h)^{-1}$)	0.02-0.20	0.02	0.02	0.02	0.02

SAC-SMA	Description	Ranges	A Priori Parameter											
			T1	T2	T3	T4	T5	T6	T7	T8	T9	T10	T11	T12
UZTWM	Upper zone tension water capacity (mm)	1.00 - 150.00	41.885	10.000	108.284	10.048	100.523	132.427	90.807	54.131	150.000	150.000	64.957	45.049
UZFWM	Upper zone supplemental free water capacity (mm)	1.00 - 150.00	83.770	15.605	150.000	5.024	83.770	79.456	79.568	32.479	150.000	150.000	32.479	45.049
UZK	Fractional daily upper zone free water withdrawal rate (mm/hr)	0.10 - 0.50	0.500	0.500	0.500	0.130	0.357	0.255	0.318	0.200	0.357	0.500	0.130	0.310
PCTIM	Minimum impervious area (decimal fraction)	0.00 - 0.10	0.050	0.050	0.050	0.050	0.050	0.050	0.050	0.050	0.050	0.050	0.050	0.050
ADIMP	Additional impervious area (decimal fraction)	0.00 - 0.40	0.300	0.300	0.300	0.300	0.300	0.300	0.300	0.300	0.300	0.300	0.300	0.300
ZPERC	Maximum percolation rate coefficient (dimensionless)	1.00 - 250.00	21.520	21.520	21.520	56.577	32.120	40.523	29.049	41.434	24.977	24.656	56.577	25.684
REXP	Percolation equation exponent (dimensionless)	0.00 - 5.00	1.013	1.013	1.013	2.679	1.519	1.961	1.895	2.320	1.519	1.132	2.679	2.025
LZTWM	Lower zone tension water capacity (mm)	1.00 - 500.00	125.755	159.837	59.356	172.832	173.797	172.373	153.033	174.469	14.438	61.762	117.923	153.071
LZFSM	Lower zone supplemental free water capacity (mm)	1.00 - 1000.00	27.190	34.559	12.834	52.601	31.035	33.008	42.606	48.851	5.000	11.312	35.889	58.313
LZFPM	Lower zone primary free water capacity (mm)	1.00 - 1000.00	224.320	285.115	105.878	33.815	113.795	70.416	91.298	55.830	10.000	76.920	23.072	94.758
LZSK	Fractional daily supplemental withdrawal rate (mm/hr)	0.010 - 0.25	0.204	0.204	0.204	0.053	0.127	0.095	0.117	0.078	0.127	0.117	0.053	0.115
LZPK	Fractional daily primary withdrawal rate (mm/hr)	0.0001 - 0.025	0.025	0.025	0.025	0.025	0.025	0.025	0.025	0.025	0.025	0.025	0.025	0.025
PFREE	Fraction of percolated water going directly to lower zone free water storage (decimal fraction)	0.00 - 0.60	0.108	0.108	0.108	0.600	0.214	0.319	0.318	0.467	0.214	0.128	0.600	0.381

Table 4.2 All calibration cases and calibration cases selected with associated criteria. Single is considered the whole basin as one physical signature, but Semi- is 2 snow and 6 water balance signatures and Full- is 4 snow and 12 water balance signatures over the entire catchment. The Matching is the number depicted on Figure 4.1.

Selected No.	Calibration Cases	N. of Criteria	Matching Number		
			Single	Semi	Full
A	Q_1^{RMSE}	1	1	29	57
B	$NOAA_{SCX}^{RMSE}$	1	2	30	58
C	$NOAA_{SWE}^{EMD}$	1	3	31	59
D	$NOAA_{SWE}^{HAUS2}$	1	4	32	60
E	$NOAA_{SWE}^{RMSE}$	1	5	33	61
	$Q_1^{EMD} : Q_2^{EMD}$	2	6	34	62
	$Q_1^{HAUS1} : Q_2^{HAUS1}$	2	7	35	63
	$Q_1 Q_2^{EMD} : NOAA_{SCV}^{EMD}$	2	8	36	64
	$Q_1 Q_2^{EMD} : NOAA_{SWE}^{EMD}$	2	9	37	65
	$Q_1 Q_2^{EMD} : SNOTEL_{SWE}^{EMD}$	2	10	38	66
	$Q_1 Q_2^{EMD} : SNOTEL_{SWE}^{EMD} : NOAA_{SCV}^{EMD}$	3	11	39	67
	$Q_1 Q_2^{EMD} : SNOTEL_{SWE}^{EMD} : NOAA_{SWE}^{EMD}$	3	12	40	68
	$Q_1 Q_2^{HAUS1} : NOAA_{SCV}^{HAUS2}$	2	13	41	69
	$Q_1 Q_2^{HAUS1} : NOAA_{SWE}^{HAUS2}$	2	14	42	70
	$Q_1 Q_2^{HAUS1} : SNOTEL_{SWE}^{HAUS2}$	2	15	43	71
	$Q_1 Q_2^{HAUS1} : SNOTEL_{SWE}^{HAUS2} : NOAA_{SCV}^{HAUS2}$	3	16	44	72
	$Q_1 Q_2^{HAUS1} : SNOTEL_{SWE}^{HAUS2} : NOAA_{SWE}^{HAUS2}$	3	17	45	73
G	$Q_1^{RMSE} : NOAA_{SWE}^{HAUS2}$	2	18	46	74
H	$Q_1^{RMSE} : NOAA_{SWE}^{HAUS1}$	2	19	47	75
I	$Q_1^{RMSE} : NOAA_{SWE}^{RMSE}$	2	20	48	76
F	$Q_1^{RMSE} : Q_2^{RMSE}$	2	21	49	77
J	$Q_1^{RMSE} : Q_2^{RMSE} : NOAA_{SCX}^{RMSE}$	3	22	50	78
	$Q_1^{RMSE} : Q_2^{RMSE} : NOAA_{SWE}^{HAUS1}$	3	23	51	79
K	$Q_1^{RMSE} : Q_2^{RMSE} : NOAA_{SWE}^{HAUS2}$	3	24	52	80
L	$Q_1^{RMSE} : Q_2^{RMSE} : NOAA_{SWE}^{RMSE}$	3	25	53	81
M	$Q_1^{RMSE} : Q_2^{RMSE} : SNOTEL_{SWE}^{RMSE}$	3	26	54	82
	$Q_1^{RMSE} : SNOTEL_{SWE}^{HAUS2}$	2	27	55	83
	$Q_1^{RMSE} : SNOTEL_{SWE}^{RMSE}$	2	28	56	84

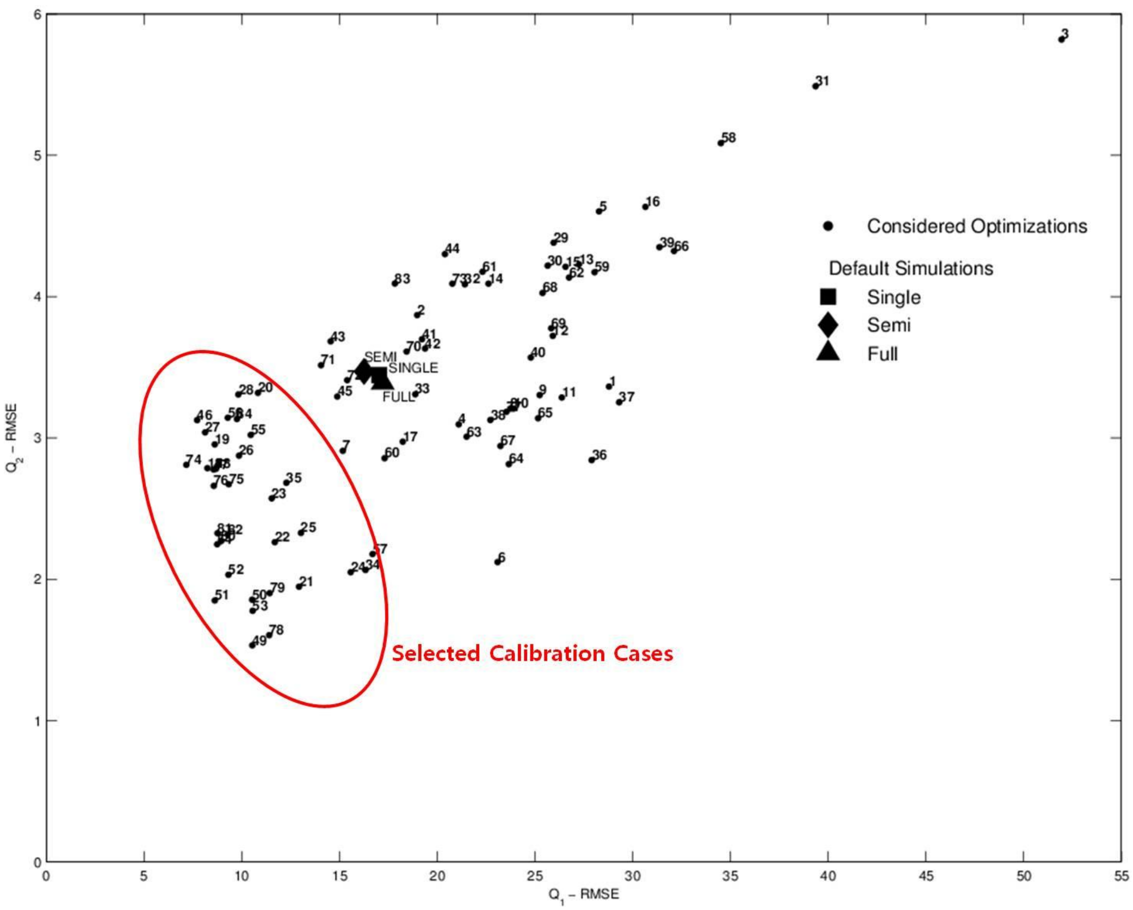

Figure 4.1 RMSE at the outlet (Q_1) and internal (Q_2) point discharges for the 84 initial optimizations considered and the a priori (default) simulations.

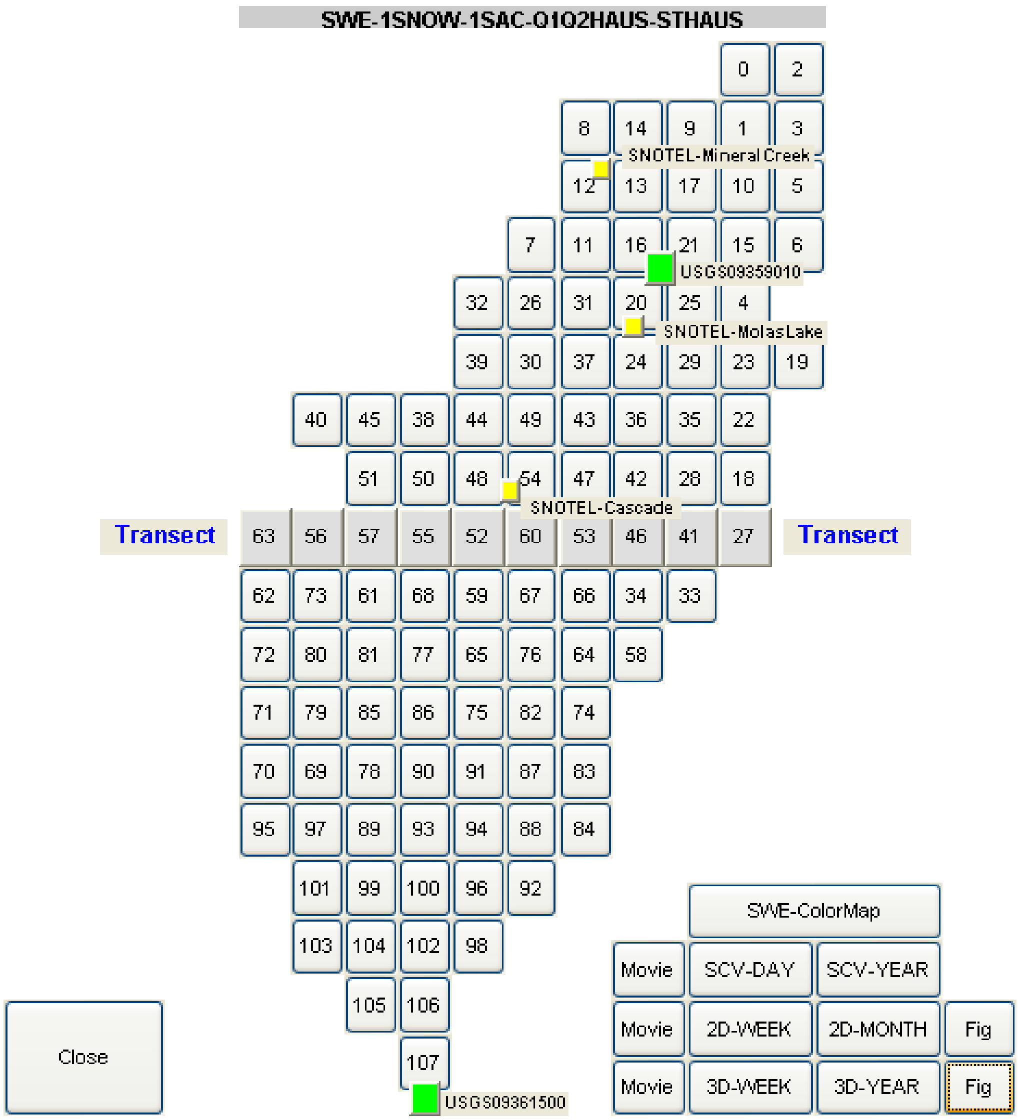

Figure 4.2 The sample of graphic user interface for one of the optimization cases. Each cell represents the HRAP grids, 2 green boxes are runoff gauges for both upstream and outlet points, and 3 yellow boxes are SNOTEL stations.

CHAPTER 5

DISTRIBUTED SPATIAL CALIBRATION AND EVALUATION FOR A HYDROLOGICAL MODEL USING SINGLE- AND MULTI-CRITERIA AUTOMATIC PROCEDURES IN SNOW DOMINATED AREAS

First, we carried out a total of 84 different exploratory optimizations (calibrations) using a variety of error functions and levels of model distribution. Because the optimization algorithms used are based on the Markov Chain Monte Carlo (MCMC) approach we get a distribution of the parameter values and a corresponding distribution of model outputs. The analysis of the parameter values and their distributions, as well as the uncertainty associated with them, will be addressed in the Chapter 6. Based on the performance of runoff simulations (see Figure 4.1) from different optimizations, we have chosen 13 optimizations for further analysis associated with each one of the three levels of distribution, i.e., a total of 39 optimizations are considered (see Table 4.2). Figure 4.1 shows Q_1 and Q_2 error values for all 84 exploratory cases. Most of the chosen 39 optimizations give better RMSE values in the three different levels of distribution than those of the benchmark default simulations except for some single-criterion calibrations of discharge or snow information only, such as optimization numbers 1 and 5, which correspond to Q_1^{RMSE} and $NOAA_{SWE}^{RMSE}$ (see Table 4.2 for a description of the optimizations). Also, due to the fact that multi-criteria optimizations end up with a number of solution points in the Pareto front, we have chosen a compromise solution based on the shortest Euclidean distance to the zero error origin for the parameter set to run the corresponding simulations. Those compromise parameter sets are used to evaluate the performance of the different calibrations. Q_1, Q_2, and snow information such as SCX, SCV, and SWE are analyzed to evaluate model performance. The single-signature, semi-distributed, and full-distributed models are calibrated and evaluated to investigate the effects of model complexity on model performances.

5.1 Snow Calibrations

In this section we analyze and evaluate the effects that snow calibrations have on the different snow variables considered: SCX, SCV, and SWE. We will also evaluate the effects that snow calibrations have on the other variables, Q_1 and Q_2, which are gauged at the locations depicted in the map in Figure 3.1.

5.1.1 Single Type Parameter Simulations (SINGLE)

The results of the optimizations considered here are presented in the SINGLE section of Tables 5.1 for the snow and discharge information of single type parameter modeling. Figure 5.1 also shows a bar chart for each calibration case. The values are normalized with respect to the default values, i.e., the default value is 1. Therefore, the improved calibration cases have values less than 1, and the deteriorated calibration cases have values greater than 1. We can see that the optimizations/calibrations using the different snow variables, such as SCX and SWE, result in an improvement in the model performance with respect to the performance associated with the default parameter values that hereinafter we will use as our benchmark. From the results shown in the SCX information part of Table 5.1 and in Figure 5.1, we can see that for the 13 chosen optimizations, including calibrations of discharge information only, there is always an improvement for the SINGLE modeling case in the simulations of the SCX. Those improvements are up to the order of 30% for the RMSE value, and 75% for the EMD.

These results show that the use of snow information, whether in the form of SCX or SWE, can be used to improve the overall performances of the snow simulations with the RDHM model. These results reveal that the SCX value can be improved with the calibration of discharge information only in the SINGLE modeling of RDHM model, as well. However, it is not possible to compare with Hausdorff values in the SCX of the calibration period because they have the same values. This is because of the characteristics of Hausdorff as a L_{∞} type norm.

Again from the results shown in Table 5.1 and Figure 5.1, the 13 chosen optimizations always yield an improvement over the default for the SINGLE modeling case on the SCV variable. The improvements are up to about 20% for the RMSE values, 100% for EMD, and 5% for Hit rate value. Herein, the Hit rate values are associated with the sum of the diagonal of the confusion matrix for the binary comparison, i.e., $Hit\ rate = true\ positive + true\ negative$. This result strongly suggests that with the use of snow information such as SCX and SWE, we can improve the overall snow information in the RDHM model. Also, the snow information can be improved with the calibrations of overall basin and sub-basin discharge information only.

Regarding the SWE simulations for the 13 chosen optimizations for the single type, we can see that some optimization cases improve on the benchmark but others deteriorate. In fact, the improvements are achieved up to an order of 20% for the RMSE and Hausdorff, and 60% for EMD, but it deteriorates up to around 50% for the RMSE, 90% for the Hausdorff and 160% for the EMD in the worst case.

In general for the single type case, Table 5.1 and Figure 5.1 show that all types of snow information, such as SCX, SCV, and SWE, can be improved with single- and multi-criteria calibrations. However, it would be relatively hard to improve the SWE when calibrating on SCX and discharge information only. In fact, the optimization cases related to the SCX and discharge information only, such as $NOAA_{SCX}^{RMSE}$, $Q_1^{RMSE} : Q_2^{RMSE} : NOAA_{SCX}^{RMSE}$, Q_1^{RMSE}, and $Q_1^{RMSE} : Q_2^{RMSE}$ could not be improved for RMSE, Hausdorff, and EMD values of SWE in the single type model.

Now we focus on the effects of snow calibrations, single- or multi-criteria, on runoff simulations. First, we investigate single-criterion calibrations on snow information only with the calibrations of discharge information only. According to the results for Q_1 (overall basin runoff) in Table 5.1 and Figure 5.1, all five single-criterion calibrations indicate inferior performances for RMSE, Hausdorff and EMD. Particularly, for the calibration of discharge information only, the single-criterion calibration Q_1^{RMSE} fails to improve the overall basin runoff simulation in a single type model. This result suggests that it is difficult to improve the overall basin runoff simulations with only the single-criterion calibrations of discharge or snow information only. For the sub-basin runoff, Q_2, most single-criterion calibrations on snow information only indicate inferior performances; only one, $NOAA_{SWE}^{HAUS2}$, improves in all of the error functions for sub-basin runoff simulations. The results show that the use of SWE information seems to produce better performances of runoff when the shape-matching functions, especially Hausdorff, are used for the single type model. In fact, the Hausdorff distance is reduced about 60% for sub-basin runoff simulations. For the single-calibration of discharge information only, Q_1^{RMSE}, the sub-basin runoff simulations are improved for RMSE and EMD, but not for Hausdorff.

Out of the five considered single-criterion calibrations, only one single-criterion calibration, $NOAA_{SCX}^{RMSE}$, uses the information of SCX as defined earlier in section 4.2. This calibration case uses the RMSE as an error function for the snow information of SCX over the entire catchment. For the single type modeling, we see that the simulations of Q_1 and Q_2 are actually deteriorated in all error function values with the calibration of $NOAA_{SCX}^{RMSE}$. These deteriorations are of the order of 15% for the RMSE of both overall basin and sub-basin runoff. The Hausdorff distance value is deteriorated around 25% for overall basin runoff and 5% for sub-basin runoff simulation. The EMD measure also indicates an inferior performance of the order of 65% and 15% for overall basin and sub-basin runoff, respectively. In general, it seems that the exclusive use of snow cover extent does not lead to an improvement in the simulations of both overall basin and sub-basin runoff. The single-criterion calibration using SWE, $NOAA_{SWE}^{HAUS2}$, shows better performances for Q_2. Perhaps it can be said that the use of the SWE information induces marginal improvements in the discharge simulations while the SCX does not.

Unlike the single-criterion calibrations on discharge or snow information only, all multi-criteria calibrations using snow and discharge information simultaneously yield superior performances for the overall basin and sub-basin runoff in error functions of RMSE and Hausdorff. They are improved up to a maximum of 75% for overall basin runoff and 65% for sub-basin runoff. In particular, of the eight different multi-criteria calibrations, only three calibrations of $Q_1^{RMSE} : NOAA_{SWE}^{RMSE}$, $Q_1^{RMSE} : NOAA_{SWE}^{HAUS1}$, and $Q_1^{RMSE} : NOAA_{SWE}^{HAUS2}$ use both snow and overall basin discharge information without sub-basin runoff information. Although they do not use the sub-basin discharge information, they make an improvement for sub-basin runoff simulations too while only using snow and overall basin discharge information. In fact, the sub-basin runoff simulations are improved for RMSE and Hausdorff with the three different calibrations mentioned above. However, of the three calibrations, $Q_1^{RMSE} : NOAA_{SWE}^{RMSE}$ shows inferior performance for the error function of EMD. In the multi-criteria calibration of discharge information only, $Q_1^{RMSE} : Q_2^{RMSE}$ overall and sub-basin runoff simulations are improved for RMSE and Hausdorff.

Based on these results, it is clear that the multi-criteria calibrations using both snow and runoff information are more efficient in improving both overall basin and sub-basin runoff simulations than single-criterion calibration of snow information only. Also, the sub-basin runoff simulations can be improved with the calibrations using both snow and overall basin discharge information for the single signature model.

5.1.2 2-Snow & 6 SAC-SMA Type Simulations (SEMI)

The results of semi-distributed calibrations are presented in the SEMI section of Table 5.1 and Figure 5.1 for the snow and discharge simulations. The results are shown in the SCX information part of Table 5.1 and Figure 4.1. All 13 chosen calibrations using the different snow variables make an improvement in the simulation of SCX when compared to the benchmark in the semi-distributed calibrations. The improvements are up to the order of 25% for the RMSE, and 75% for EMD. Therefore, we can say, again, that snow information such as SCX and SWE are very useful in improving the simulations of SCX through calibrations in the RDHM model. For the calibrations of discharge information only, although the single-criterion calibration - Q_1^{RMSE} makes an improvement in SCX simulations, the multi-criteria calibration does not. In fact, the multi-criteria calibration of $Q_1^{RMSE}:Q_2^{RMSE}$ is deteriorated up to 20% for RMSE and 30% for EMD. This result shows that the calibrations of discharge information only do not guarantee improvement in the simulation of SCX.

By examining the results of semi-distributed SCV information sections in Table 5.1 and Figure 5.1, we can see that the 13 chosen calibrations are always an improvement compared to the benchmark. These improvements are up to the order of 20% for the RMSE, 95% for EMD, and 5% for Hit rate values. The improvements are almost similar to those of the single type model; hence, it can be said that we can improve the SCV information by calibrating using snow information such as SCX and SWE in semi-distributed modeling. However, like SCX simulations, the multi-criteria calibration of discharge information only is deteriorated for RMSE, EMD, and Hit rate. Therefore, it can be confirmed that the calibration of discharge information only does not always make an improvement for snow information.

The semi-distributed SWE information sections in Table 5.1 and Figure 5.1 show that improvements up to the order of 15%, 5%, and 50% are achieved, with deteriorations of about 80%, 110%, and 60% in RMSE, Hausdorff, and EMD, respectively. In particular, as mentioned in numeral 4.2, of the 13 calibrations cases only $NOAA_{SCX}^{RMSE}$ and $Q_1^{RMSE}:Q_2^{RMSE}:NOAA_{SCX}^{RMSE}$ use the snow information of SCX. The calibration case using only SCX, $NOAA_{SCX}^{RMSE}$, does not make an improvement in SWE information in the semi-distributed model. The calibration case $Q_1^{RMSE}:Q_2^{RMSE}:NOAA_{SCX}^{RMSE}$ improves SWE for only EMD. This result shows that the SWE improvement is relatively difficult, especially in the calibration using snow information of SCX only. Additionally, the single- and multi-criteria calibrations of discharge information only fail to improve the simulations of SWE. Therefore, we can say again that improvements in SWE are difficult for the calibrations of discharge information only without considering single- or multi-criteria calibrations in semi-distributed HL-RDHM model.

For the investigation of the effects of snow calibrations on the discharge variables, we have five different single-criterion calibrations on discharge or snow information in the semi-distributed modeling (see Table 5.1 and Figure 5.1). Most calibrations fail to improve the overall basin runoff simulations, Q_1, for RMSE, Hausdorff, and EMD. However, the calibration of $NOAA_{SWE}^{RMSE}$ indicates superior performances in Hausdorff and EMD. In fact, they deteriorate from the benchmark up to the order of 150%, 170%, and 85% for RMSE, Hausdorff and EMD respectively. In particular, the calibration on SCX ($NOAA_{SCX}^{RMSE}$), does not improve upon the benchmark, i.e., it has very similar error values. As mentioned in 5.1.1, it seems that the exclusive use of snow cover extent is not generally efficient to improve the simulations of both overall basin and sub-basin runoff. The single-criterion calibration using SWE, $NOAA_{SWE}^{RMSE}$, shows better performances for Q_1. Given that we use a normalized value for each of the discharges, the difference in the performance measure may be due to the fact that the SWE is considered over the entire catchment, which is more directly related to the overall discharge, Q_1. Hence, we can say that the use of the SWE information is more efficient to improve the discharge simulations than SCX. In the calibration of discharge information only, the single-criterion calibration indicates inferior performances for overall basin runoff.

For the upstream sub-basin discharge, Q_2, we can see that the calibration case $NOAA_{SWE}^{RMSE}$ reduces the error function values up to around 10% for RMSE and EMD and 60% for Hausdorff. Also, the $NOAA_{SWE}^{EMD}$ case improves EMD about 10%. Therefore, it seems that the snow information of SWE is more efficient than SCX at improving the runoff simulations, especially in the upstream sub-basin, Q_2. For the calibration of discharge information only, the single-criterion calibration makes an improvement for EMD, but it does not improve the simulation of upstream sub-basin runoff for RMSE and Hausdorff.

All multi-criteria calibrations improve all considered error functions. In fact, improvements are on the order of 50% for RMSE and Hausdorff and 65% for EMD for overall basin discharge simulation, Q_1. Also, they show an improvement of 50% for RMSE, Hausdorff, and EMD on Q_2. This result suggests that the multi-criteria calibrations are more useful to improve both overall basin and upstream sub-basin runoff simulations. In particular, the calibrations using only snow and overall basin discharge decrease the error values for sub-basin runoff Q_2 in the semi-distributed model. As we can see in the SEMI sections in Table 5.1 and Figure 5.1, the calibrations related to the snow and overall basin runoff information only make an improvement in sub-basin runoff simulations for all error functions such as RMSE, Hausdorff, and EMD. This means that the calibrations using snow and overall basin runoff information can improve interior points discharge simulations. The sub-basin runoff simulations are improved up to 20%, 60%, and 25% for RMSE, Hausdorff, and EMD.

5.1.3 4-Snow & 12 SAC-SMA Type Simulations (FULL)

The results of the full-distributed optimizations are presented in the FULL sections of Table 5.1 and Figure 5.1. All calibration cases considered are an improvement in the SCX simulation except for the single-calibration of discharge information only. The improvements are up to the order of 25% for the RMSE and 75% for the EMD. However, due to the same values for all calibration cases, the Hausdorff values in the SCX of the calibration period could not be compared. Therefore, we can say that the use of snow information such as SCX and SWE, when available, appear to improve the overall snow simulations with the full-distributed HL-RDHM. We can also say that the single-calibration of discharge information only does not improve the SCX simulations.

For the SCV, we can see that all 13 chosen calibrations are an improvement up to the order of 20% for RMSE, 95% for EMD, and 5% for Hit rate. This result indicates that the SCX and SWE are useful to improve SCV simulations in full-distributed mode. However, in the calibrations using discharge information only, the single-criterion calibration of Q_1^{RMSE} fails to improve the SCV simulations.

For SWE some of the calibration cases are an improvement, while others are not. Therefore, we can say again that improving SWE is relatively difficult with the calibrations of single- or multi-criteria. In particular, the calibrations using snow information of SCX, $NOAA_{SCX}^{RMSE}$ and $Q_1^{RMSE}:Q_2^{RMSE}:NOAA_{SCX}^{RMSE}$ and discharge information only, Q_1^{RMSE} and $Q_1^{RMSE}:Q_2^{RMSE}$, fail to improve the snow information of SWE for all of error functions such as RMSE, Hausdorff, and EMD in the full-distributed HL-RDHM model.

Next we investigate the effects of snow-based calibrations on runoff discharges

Q_1 and Q_2 in the full distributed model with discharge-based calibrations (Table 5.1 and Figure 5.1, FULL sections). For the overall discharge Q_1, all four single-criterion calibrations on snow information result in inferior performances for RMSE and EMD. They deteriorate from the benchmark up to 100% for RMSE and 90% for EMD. The calibration $NOAA_{SCX}^{RMSE}$ does not improve the overall basin runoff simulations and stays at the benchmark as in the semi-distributed model. However, $NOAA_{SWE}^{HAUS2}$ shows improvement from the benchmark in terms of the Hausdorff error function. The single-calibration on discharge information shows superior performances in the error function of RMSE but not in Hausdorff and EMD.

For the upstream sub-basin runoff Q_2, the $NOAA_{SWE}^{HAUS2}$ case makes an improvement of about 50% for all the error functions considered. In terms of EMD, all calibrations yield improvements except for the case of $NOAA_{SWE}^{RMSE}$, which shows a deterioration on the order of 30%. According to the results, it seems that the SWE is the variable that provides the most information for improvement of Q_2 in the full-distributed model. For the calibration of discharge information only, the single-criterion calibration of Q_1^{RMSE} shows superior performances in RMSE and EMD.

On the other hand, the multi-criteria calibrations show superior performances for both Q_1 and Q_2 in terms of error functions of RMSE and EMD. However, some multi-criteria calibrations are deteriorated in the Hausdorff error function. This shows again the enhancing power of multi-criteria calibrations.

Furthermore, the sub-basin runoff simulations are improved when calibrating on snow and Q_1 only. The improvement of Q_2 is 25% for RMSE and 30% for EMD with the calibration of snow and Q_1 only. It is slightly greater than those of the semi-distributed model. Although the full-distributed model fails to show improvement in the Hausdorff, the semi-distributed model makes an improvement up to 60%.

5.2 Model Verification

In this section we verify the quality of model calibrations. For this purpose, as stated in section 3.4, we use three years of data (2001-2004) from the same USGS gages as before and snow information from the MODIS, given that the SWE is not available from the NSDIC for the same period; only the binary snow cover and the computed snow cover extent from it are used. The quality of optimizations is evaluated using compromise solutions of the Pareto front, for the multi-criteria calibrations, and the mode for the single objective optimizations.

5.2.1 Single Type Model Verification

The results of single type model verification are presented in the SINGLE sections of Table 5.2 and Figure 5.2. In the same manner as section 5.1.1., the error values are normalized with respect to the default; hence, the default values are 1. According to the results, most SCX simulations are improved up to 40% of RMSE, 25% of Hausdorff and 50% of EMD with the SCX information. For the SCV, most cases indicate superior performance in RMSE, Hausdorff, EMD, and Hit Rate with up to 20%, 10%, 50%, and 10%, respectively. These values are similar to the error values of the calibration period, although the Hausdorff is slightly different. In the calibration period, the multi-criteria calibration of discharge information only indicates superior performance, but it is deteriorated in the verification period. For Q_1, some calibration cases are an improvement in RMSE, Hausdorff and EMD, but other calibration cases show deterioration. In particular, the single-criterion calibrations on snow or discharge information only do not improve any of the error functions in the calibration period, but some of single-criterion calibrations show an improvement in the verification period. For the sub-basin discharge Q_2, some calibrations yield inferior performances for RMSE and Hausdorff, but all calibration cases except for $NOAA_{SWE}^{RMSE}$ indicate superior performances in the EMD.

Figures 5.3 and 5.4 show the hydrographs obtained for chosen simulations of the overall basin discharge, Q_1, for the calibration and verification periods. The simulations were chosen based on the RMSE criterion (see Table 5.1) and include the best, the overall basin runoff only (Q_1^{RMSE}), and the worst calibrations. The default simulation is also included. In Figure 5.3 the black lines correspond to the best simulation, cyan to the overall basin runoff, red to the worst, and green to the default. The red crosses are observed values. Using the same colors, the corresponding calibrations and error function values are also included. For example, for the single type model (1-SNOW 1-SACSMA), the optimization $Q_1^{RMSE} : NOAA_{SWE}^{HAUS2}$ is the best with an RMSE of 8.243 cms; the worst is $NOAA_{SWE}^{EMD}$ with an RMSE of 51.938 cms, while the default has an RMSE of 17.033 cms. The right panel is a scatter plot of observed versus computes values using the same colors. The time span is that of the calibration period. Figure 5.4 shows the same information but for the verification period. For example, in the Figure 5.4, we have the optimization $Q_1^{RMSE} : NOAA_{SWE}^{RMSE}$ as the best with an RMSE of 11.355 cms and $NOAA_{SWE}^{EMD}$ as the worst with an RMSE of 41.509 cms. Also, the default, green, shows an RMSE of 16.107 cms. As we can see in Figures 5.3 and 5.4, the best optimizations for the single signature model were not exactly consistent for calibration and verification periods, but the worst cases are the same. Furthermore, the calibration case of Q_1^{RMSE} (cyan) has almost similar error values for the single type model in both calibration and verification periods.

In a similar way, Figures 5.5 and 5.6 depict the same information for the sub-basin discharge, Q_2. In the single type model, the calibration case of $Q_1^{RMSE}:Q_2^{RMSE}$ is the best optimization with the RMSE of 1.948 cms. However, for the verification period the calibration case of $Q_1^{RMSE}:Q_2^{RMSE}:NOAA_{SWE}^{HAUS2}$ indicates the best RMSE value: 1.568 cms. In the worst case, $NOAA_{SWE}^{EMD}$ shows the worst performances for both the calibration and verification periods. It has RMSE values of 5.819 cms and 3.813 cms for calibration and verification periods, respectively. Like overall basin runoff, Q_1, the best cases are not same, but the worst cases are matched for sub-basin runoff, Q_2.

In Figure 5.7, we show the same graphs but for the SCX simulations for the optimization period. In the Figure 5.7 for the single type model (1-SNOW 1-SACSMA), the calibration of $NOAA_{SCX}^{RMSE}$ has the smallest RMSE of 0.147. Also, the calibration of $Q_1^{RMSE}:Q_2^{RMSE}$ is worst with a RMSE value of 0.179. As we can see in Figure 5.8 for the single type model, the best case for RMSE in the verification period is not same as that of optimization period, but the worst cases are same for both periods. For the verification period, the best RMSE case is $NOAA_{SWE}^{EMD}$ and worst case is $Q_1^{RMSE}:Q_2^{RMSE}$.

According to the results in the Q_1, Q_2, SCX, and SCV simulations for calibration and verification periods, we can say that the parameters to be optimized reflect the characteristics of the study basin for the single type model, in general.

5.2.2 Semi-Distributed Model Verification

The SEMI section of Table 5.2 and Figure 5.2 present the results of error functions for the verification period in the semi-distributed model. For the SCX snow information, by sorting the results shown in the semi-distributed snow information part for SCX in Table 5.2, we see that most calibrations are improved from the benchmark for RMSE and EMD, but not Hausdorff. In fact, the improvement is up to an order of 40% and the deterioration is up to an order of 25% for the RMSE and EMD. However, the Hausdorff values are decreased up to 10% and increased up to 40% in verification period. For SCV snow information, only two calibrations of $NOAA_{SWE}^{HAUS2}$ and $Q_1^{RMSE}:Q_2^{RMSE}$ show inferior performances for error functions, RMSE, EMD and Hit rate. In particular, all calibrations are improved from the benchmark in the Hausdorff error function.

For the overall basin runoff, Q_1, sorting the results shown in the Q_1 semi-distributed section in Table 5.2, shows that some calibration cases are improved for RMSE and Hausdorff, but all calibration cases are deteriorated for the EMD. The error values are improved up to an order of 20% and 80% for RMSE and EMD, but they are deteriorated from the benchmark up to 160%, 115%, and 250% for RMSE, Hausdorff, and EMD for overall basin runoff. For the sub-basin discharge Q_2, most calibrations except for only $NOAA_{SCX}^{RMSE}$ indicate the superior performances for Hausdorff and EMD, but all single-criterion calibrations indicate inferior performances in the error function of RMSE.

Furthermore, Figures 5.3 and 5.4, for the semi-distributed model (2-SNOW 6-SACSMA), show the calibration case of $Q_1^{RMSE} : NOAA_{SWE}^{HAUS2}$ as best RMSE value of overall basin discharge, Q_1, for both calibration and verification periods. The calibrations of best RMSE are the same, but the worst calibrations cases for RMSE are not matched for the calibration and verification periods. In fact, the worst case calibrations are $NOAA_{SWE}^{HAUS2}$ and $NOAA_{SWE}^{EMD}$, with RMSE values of 7.716 and 12.661 for calibration and verification periods, respectively. Also, the single-criterion calibration for overall basin runoff, Q_1^{RMSE}, indicates inferior performances with very similar RMSE values in both calibration and verification periods. The RMSE values are 25.953 for calibration period and 26.999 for verification period.

For the sub-basin discharge, Q_2, we can see in Figures 5.5 and 5.6 for the semi-distributed model that the calibration case of $Q_1^{RMSE} : Q_2^{RMSE}$ shows the best RMSE value for the calibration period, while the calibration case of $Q_1^{RMSE} : Q_2^{RMSE} : NOAA_{SCX}^{RMSE}$ shows the smallest RMSE value for the verification period. Although the calibrations of best RMSE do not match for the calibration and verification periods, the worst RMSE calibration cases are matched. The worst calibration is $NOAA_{SWE}^{EMD}$ with RMSE values of 4.381 cms and 2.659 cms for optimization and verification periods, respectively. Additionally, the single-criterion calibration on overall basin runoff shows inferior performances, with deterioration of about 20% from benchmark.

Lastly, the Figures 5.7 and 5.8, for the semi-distributed model (2-SNOW 6-SACSMA), show very similar patterns of SCX for the optimization and verification periods in that they show similar RMSE values in worst and overall basin runoff cases,

Q_1^{RMSE}. In fact, the calibration case of $Q_1^{RMSE}:Q_2^{RMSE}$ has the worst RMSE value of SCX for both the optimization and verification periods. Also, the single-criterion calibration of Q_1^{RMSE} makes an improvement from the benchmark with very similar RMSE values: 0.15 for calibration and verification periods. The calibration cases of $NOAA_{SCX}^{RMSE}$ and $NOAA_{SWE}^{EMD}$ show the best RMSE values of SCX for optimization and verification periods, respectively.

According to these statements, the parameters to be optimized are well-calculated, with the calibrations for optimization and verification periods showing similar trends for variables such as Q_1, Q_2, SCX, and SCV for both periods.

5.2.3 Full-Distributed Model Verification

For the results of full distributed model verification, the FULL sections of Table 5.2 and Figure 5.2 present the error function for each calibration case. In the error values of SCX snow information, sorting the results shown in the full-distributed snow information section of Table 5.2 shows that most calibration cases are improved up to 35% of RMSE and 60% of EMD in SCX. However, all of calibration cases fail to decrease the error function values of Hausdorff. The Hausdorff values are increased to about 30% from the benchmark.

For SCV, the trends of error values are very similar between the calibration and verification periods. Most calibrations except for Q_1^{RMSE} are improved from benchmark for RMSE, EMD, and Hit rate. The improvement of SCV is up to 20%, 60%, and 10% for RMSE, EMD, and Hit rate. These are very similar to of the calibration period. The Hausdorff values are improved for all calibrations in SCV.

For the overall basin discharge, Q_1, sorting the results shown in the full-distributed Q_1 information section of Table 5.2 shows that all single-criterion calibrations are deteriorated up to 80% of RMSE and 140% of EMD. In particular, without considering single- or multi-criteria calibrations, all calibrations except for $NOAA_{SWE}^{RMSE}$, have inferior performances for overall basin discharge in EMD error function. However, some calibrations show superior performances for Hausdorff, while others are not. The Hausdorff values are improved up to 80% and deteriorated up to 80% in overall basin discharge.

On the other hand, sorting the results shown in the full-distributed Q_2 information section of Table 5.2 shows all calibrations are increased for Hausdorff, with deterioration of 240%. Also, most calibrations except for only $NOAA_{SWE}^{RMSE}$ indicate superior performances for EMD error function. The improvement is 50% and the deterioration is 15% for sub-basin runoff. In the error function of RMSE, some calibrations are decreased up to 50%, but some single-criterion calibrations on snow information only fail to reduce the error values from the default.

For the convenience of comparison, Figures 5.3 and 5.4 show the model output performances of overall basin runoff, Q_1, for optimization and verification periods. In Figures 5.3 and 5.4, for the full-distributed model (4-SNOW 12-SACSMA), the calibration of $Q_1^{RMSE} : NOAA_{SWE}^{HAUS2}$ shows the best RMSE value for both calibration and verification periods. However, the optimization and verification periods have different calibration cases as the worst case. The calibration case $NOAA_{SWE}^{EMD}$ shows the worst RMSE value for the optimization period. For the verification period, $NOAA_{SCX}^{RMSE}$

indicates the worst RMSE with a value of 33.646 cms. Therefore, the calibration of best RMSE is exactly the same for the calibration period but not for verification period. The calibration of overall basin runoff only Q_1^{RMSE} shows superior performances for error function of RMSE in both periods, as well.

Figures 5.5 and 5.6, for the full-distributed model (4-SNOW 12-SACSMA) show the sub-basin discharge Q_2 performances for optimization and verification periods. In both figures, the best RMSE cases are different; the calibration of $Q_1^{RMSE} : Q_2^{RMSE} : NOAA_{SCX}^{RMSE}$ is best RMSE for the calibration period, while the calibration on overall basin runoff only Q_1^{RMSE} shows the smallest RMSE value for the verification period. Although the best RMSE cases are different, the worst RMSE cases are exactly the same for both periods. The calibration of $NOAA_{SCX}^{RMSE}$ with the RMSE is 5.086 cms and 3.977 cms for calibration and verification periods, respectively.

Lastly, Figures 5.7 and 5.8, for the full-distributed model (4-SNOW 12-SACSMA), depict the time-series of SCX for both periods. The calibration of $NOAA_{SCX}^{RMSE}$ indicates the best RMSE, 0.142 cms, for the optimization period, while the calibration of $NOAA_{SWE}^{EMD}$, 1.333 cms, is the best for the verification period. Although the best RMSE does not match, the calibration of overall basin runoff information only shows the smallest RMSE values for both periods: 0.232 and 0.265.

According to these statements, the trends of output variables are sometimes slightly different for both periods, but most variables have same calibrations as best or worst RMSE in full-distributed modeling. Hence, we can say, again, that they are calculated to properly describe the characteristics of the study basin.

5.3 Degree of Distribution (Model Complexity)

In distributed hydrological models, the degree of distribution is, in a way, a component of model complexity. In the present case, we disregard the complexity of the model formulation and parameterization, as they remain the same under all conditions, and consider the complexity exclusively associated with the degree of distribution or the number of different types of parameters that are included in the model. This is also closely related to the efficiency and effectiveness of the parameter identification because the number of unknown parameters to be optimized rapidly increases with the model complexity. Therefore, a decision on the appropriate level of distribution is very important. In this section, the error function values are calculated based on the degrees of distribution. Hence, we can check which distribution is proper for the case study.

Figure 5.9 depicts the ranges of error values for each degree of distribution. Given that we use normalized values with respect to the default for each of error functions, the bars describe the minimum and maximum error values of calibration cases for each of distributions in the variables: Q_1, Q_2, SCX, SCV, and SWE. In the overall basin runoff, Q_1, the full-distributed model shows the relatively smaller uncertainty as having narrow bar, while the single signature model has wide bars for the RMSE, Hausdorff, and EMD error functions. In the error function EMD, the full-distributed model show relatively greater uncertainty for some of variables, such as Q_2, SCX, SCV, and SWE.

For the convenience of comparison, Table 5.3 shows the Euclidean distance to the zero error origin for the minimum and maximum error values of each calibration case. That is, by calculating the distance values with 5 different minimums or maximums for each variable, we can easily compare which distribution is closer to the observations, in general. In the error function of RMSE in Table 5.3, the full-distributed model has better distance values for both minimum and maximum error values. However, the single-signature model has greater distance values for both minimum and maximum error values. This means that the full-distributed model is more precise with respect to the observations; therefore, the full-distributed model has smaller uncertainty and is closer to observations. However, the Hausdorff and EMD show a more complex phase. That is, the single-signature model has better distance for minimum error values, while the semi-distributed model has smaller maximum error values. Also, the difference between minimum and maximum is largest in the single-signature model for Hausdorff. This means that the single-signature model is closer to observation but has greater uncertainty for the Hausdorff error function. In the same way, the full-distributed model has better distance in minimum error values, but larger uncertainty.

It is difficult to decide which distribution is best for each calibration, but generally the distributed models show better performances as smaller distance values and differences between Euclidean distances of minimum and maximum error values. For the case study, the appropriate level of model complexity is decided for model calibration and evaluation with this process.

Table 5.1 Error function values of each variable according to the optimization cases for the calibration period (WY 04-05). Default vales are the error function values from the a priori parameter set (benchmark).

CALIBRATION PERIOD			Q_1			Q_2			SCX			SCV				SWE		
			RMSE	HAUS1	EMD	RMSE	HAUS1	EMD	RMSE	HAUS1	EMD	RMSE	HAUS2	EMD	Hit Rate	RMSE	HAUS2	EMD
SINGLE	A	Q_1^{RMSE}	28.78860	0.57270	0.06600	3.36349	0.65782	0.04302	0.15416	0.46433	0.029035	0.29647	0.55863	0.02787	0.91210	130.73816	0.45473	0.05721
	B	$NOAA_{SCX}^{RMSE}$	18.97690	0.32660	0.04180	3.86960	0.44790	0.09100	0.14750	0.46433	0.02170	0.28746	0.55863	0.00562	0.91747	121.71452	0.43869	0.05093
	C	$NOAA_{SWE}^{EMD}$	51.93850	1.13240	0.04780	5.81900	1.52760	0.07080	0.14940	0.46433	0.02220	0.29023	0.55863	0.00383	0.91582	85.34584	0.24767	0.01112
	D	$NOAA_{SWE}^{HAUS2}$	21.10060	0.29940	0.03350	3.09660	0.18330	0.06480	0.16200	0.46433	0.04260	0.30781	0.55863	0.04254	0.90538	87.89819	0.22918	0.01720
	E	$NOAA_{SWE}^{RMSE}$	28.28350	0.45210	0.05590	4.60290	0.68600	0.10410	0.14790	0.46433	0.02180	0.28969	0.55863	0.00883	0.91613	80.72119	0.21281	0.01194
	F	$Q_1^{RMSE}: Q_2^{RMSE}$	12.93237	0.20858	0.02794	1.94759	0.25196	0.05018	0.17924	0.46433	0.05853	0.32838	0.55863	0.05847	0.89216	140.72338	0.46375	0.06130
	G	$Q_1^{RMSE} : NOAA_{SWE}^{HAUS2}$	8.24302	0.06747	0.01101	2.78595	0.20835	0.06454	0.16375	0.46433	0.03892	0.31222	0.55863	0.03802	0.90252	90.79956	0.21242	0.01258
	H	$Q_1^{RMSE} : NOAA_{SWE}^{HAUS1}$	8.61660	0.07451	0.01506	2.95445	0.41084	0.06853	0.17164	0.46433	0.05080	0.32062	0.55863	0.05078	0.89727	88.17098	0.21626	0.01389
	I	$Q_1^{RMSE} : NOAA_{SWE}^{RMSE}$	10.83173	0.12678	0.01688	3.31901	0.38568	0.07967	0.15072	0.46433	0.02418	0.29404	0.55863	0.01944	0.91354	82.30207	0.21614	0.01421
	J	$Q_1^{RMSE} : Q_2^{RMSE} : NOAA_{SCX}^{RMSE}$	11.68956	0.09852	0.02321	2.26316	0.30508	0.05550	0.16174	0.46433	0.03401	0.30728	0.55863	0.03242	0.90568	129.82043	0.44038	0.04736
	K	$Q_1^{RMSE} : Q_2^{RMSE} : NOAA_{SWE}^{HAUS2}$	15.57492	0.22236	0.03597	2.04997	0.16195	0.04564	0.17883	0.46433	0.05530	0.32829	0.55863	0.05513	0.89233	105.01008	0.28066	0.02559
	L	$Q_1^{RMSE} : Q_2^{RMSE} : NOAA_{SWE}^{RMSE}$	13.02898	0.13982	0.03073	2.32846	0.21872	0.05285	0.16607	0.46433	0.04242	0.31381	0.55863	0.04183	0.90153	101.79993	0.29527	0.02349
	M	$Q_1^{RMSE} : Q_2^{RMSE} : SNOTEL_{SWE}^{RMSE}$	9.85694	0.08236	0.01772	2.87469	0.28254	0.06668	0.14925	0.46433	0.02232	0.29141	0.55863	0.00846	0.91511	100.45610	0.29794	0.02345
		DEFAULT	**17.03300**	**0.26340**	**0.02570**	**3.44389**	**0.42706**	**0.07915**	**0.19800**	**0.46433**	**0.07600**	**0.35564**	**0.55863**	**0.07609**	**0.87358**	**97.61794**	**0.25245**	**0.02427**
SEMI	A	Q_1^{RMSE}	25.95302	0.67116	0.03484	4.38113	1.13918	0.04890	0.15784	0.46433	0.03640	0.31838	0.55863	0.01202	0.89863	134.51587	0.48362	0.03730
	B	$NOAA_{SCX}^{RMSE}$	25.65279	0.52822	0.04986	4.21860	0.78180	0.08640	0.14280	0.46433	0.01950	0.29317	0.55863	0.01027	0.91414	130.86553	0.28476	0.02826
	C	$NOAA_{SWE}^{EMD}$	39.35654	0.52620	0.03232	5.48780	1.16820	0.04570	0.14770	0.46433	0.01940	0.28505	0.55863	0.00481	0.91885	96.13777	0.39555	0.01247
	D	$NOAA_{SWE}^{HAUS2}$	21.41524	0.33975	0.02976	4.08750	0.49340	0.08910	0.18000	0.46433	0.06210	0.32239	0.55863	0.06203	0.89613	87.75603	0.24385	0.02190
	E	$NOAA_{SWE}^{RMSE}$	18.87931	0.13028	0.01375	3.30850	0.15710	0.07430	0.14560	0.46433	0.02090	0.28333	0.55863	0.01725	0.91987	79.30918	0.22226	0.01849
	F	$Q_1^{RMSE}: Q_2^{RMSE}$	10.54425	0.24882	0.01371	1.53299	0.20829	0.03118	0.21485	0.46433	0.08888	0.36183	0.55863	0.08881	0.86907	161.23486	0.48955	0.03726
	G	$Q_1^{RMSE} : NOAA_{SWE}^{HAUS2}$	7.71641	0.16527	0.01006	3.12587	0.21907	0.07235	0.15367	0.46433	0.02840	0.29896	0.55863	0.02569	0.91079	88.17453	0.22614	0.01404
	H	$Q_1^{RMSE} : NOAA_{SWE}^{HAUS1}$	8.55506	0.15243	0.01086	2.77692	0.18203	0.06206	0.16482	0.46433	0.04127	0.30655	0.55863	0.04124	0.90612	86.81668	0.26203	0.01543
	I	$Q_1^{RMSE} : NOAA_{SWE}^{RMSE}$	8.68336	0.19152	0.01180	2.78155	0.17826	0.06493	0.15854	0.46433	0.03368	0.29895	0.55863	0.03342	0.91071	86.56012	0.28508	0.01289
	J	$Q_1^{RMSE} : Q_2^{RMSE} : NOAA_{SCX}^{RMSE}$	10.53604	0.23532	0.01315	1.85570	0.16875	0.03937	0.15575	0.46433	0.03900	0.30933	0.55863	0.03906	0.90436	155.67361	0.47186	0.01974
	K	$Q_1^{RMSE} : Q_2^{RMSE} : NOAA_{SWE}^{HAUS2}$	9.31776	0.17245	0.01652	2.03197	0.12129	0.04111	0.17639	0.46433	0.05142	0.32241	0.55863	0.05121	0.89614	115.32442	0.34574	0.03615
	L	$Q_1^{RMSE} : Q_2^{RMSE} : NOAA_{SWE}^{RMSE}$	10.55814	0.23205	0.01546	1.77786	0.17836	0.03745	0.17209	0.46433	0.04838	0.31287	0.55863	0.04841	0.90214	107.24456	0.42259	0.03668
	M	$Q_1^{RMSE} : Q_2^{RMSE} : SNOTEL_{SWE}^{RMSE}$	8.74437	0.13900	0.01425	2.24840	0.20314	0.04585	0.15484	0.46433	0.02274	0.29772	0.55863	0.01715	0.91140	120.86963	0.42980	0.02754
		DEFAULT	**16.25420**	**0.24880**	**0.02710**	**3.47058**	**0.48273**	**0.08082**	**0.18390**	**0.46433**	**0.06990**	**0.34222**	**0.55863**	**0.06999**	**0.88297**	**90.27334**	**0.23385**	**0.02332**
FULL	A	Q_1^{RMSE}	16.68883	0.26116	0.03470	2.17829	0.24861	0.03695	0.23176	0.46433	0.10339	0.38119	0.55863	0.10360	0.85469	173.90671	0.47900	0.09528
	B	$NOAA_{SCX}^{RMSE}$	34.51595	0.36892	0.02708	5.08580	0.89590	0.05830	0.14220	0.46433	0.01880	0.29039	0.55863	0.00872	0.91574	133.19481	0.28584	0.03078
	C	$NOAA_{SWE}^{EMD}$	28.04664	0.33590	0.02774	4.17290	0.57710	0.04440	0.14920	0.46433	0.02210	0.29214	0.55863	0.00362	0.91477	94.73270	0.39722	0.00997
	D	$NOAA_{SWE}^{HAUS2}$	17.30657	0.21450	0.02569	2.85630	0.11710	0.06150	0.17020	0.46433	0.05570	0.31812	0.55863	0.05573	0.89885	93.53479	0.21332	0.01819
	E	$NOAA_{SWE}^{RMSE}$	22.31766	0.25649	0.04687	4.17630	0.44520	0.09870	0.14640	0.46433	0.02170	0.28348	0.55863	0.01899	0.91975	78.43259	0.22510	0.01232
	F	$Q_1^{RMSE}: Q_2^{RMSE}$	23.54240	0.19252	0.01334	3.18511	0.12496	0.05009	0.16283	0.46433	0.03319	0.31778	0.55863	0.02382	0.89901	133.23031	0.34189	0.03133
	G	$Q_1^{RMSE} : NOAA_{SWE}^{HAUS2}$	7.16713	0.17216	0.01101	2.81031	0.20441	0.05617	0.15714	0.46433	0.03544	0.31658	0.55863	0.01878	0.89989	101.61850	0.23193	0.01386
	H	$Q_1^{RMSE} : NOAA_{SWE}^{HAUS1}$	9.33474	0.18064	0.01064	2.67276	0.19546	0.06080	0.17553	0.46433	0.05468	0.31698	0.55863	0.05466	0.89963	84.87253	0.23105	0.01520
	I	$Q_1^{RMSE} : NOAA_{SWE}^{RMSE}$	8.56621	0.12854	0.01133	2.66128	0.19676	0.05866	0.15855	0.46433	0.03611	0.29962	0.55863	0.03601	0.91026	86.26733	0.25630	0.01692
	J	$Q_1^{RMSE} : Q_2^{RMSE} : NOAA_{SCX}^{RMSE}$	11.40467	0.24570	0.02386	1.60479	0.16591	0.02126	0.16138	0.46433	0.03458	0.31736	0.55863	0.02812	0.89931	132.74456	0.44334	0.02622
	K	$Q_1^{RMSE} : Q_2^{RMSE} : NOAA_{SWE}^{HAUS2}$	8.93662	0.20583	0.01129	2.27009	0.21236	0.04681	0.16863	0.46433	0.04412	0.31282	0.55863	0.04398	0.90221	109.50904	0.27746	0.02161
	L	$Q_1^{RMSE} : Q_2^{RMSE} : NOAA_{SWE}^{RMSE}$	8.75749	0.09855	0.01227	2.32576	0.22366	0.05155	0.16809	0.46433	0.04777	0.30937	0.55863	0.04775	0.90439	99.08466	0.36621	0.02082
	M	$Q_1^{RMSE} : Q_2^{RMSE} : SNOTEL_{SWE}^{RMSE}$	9.28427	0.12367	0.01335	2.31749	0.26624	0.04357	0.16850	0.46433	0.04590	0.31199	0.55863	0.04593	0.90275	105.05680	0.28344	0.01847
		DEFAULT	**17.20770**	**0.25360**	**0.02490**	**3.39119**	**0.17810**	**0.07693**	**0.18450**	**0.46433**	**0.07150**	**0.34404**	**0.55863**	**0.07148**	**0.88172**	**89.98313**	**0.23385**	**0.02325**

Table 5.2 Error function values of each variable according to the optimization cases for verification period (WY 01-04). Default vales are the error function values from the a priori parameter set (benchmark).

VERIFICATION PERIOD			Q_1			Q_2			SCX			SCV			
			RMSE	HAUS1	EMD	RMSE	HAUS1	EMD	RMSE	HAUS1	EMD	RMSE	HAUS2	EMD	Hit Rate
SINGLE	A	Q_1^{RMSE}	27.80819	1.63506	0.11213	2.46222	0.27440	0.00814	0.17347	0.20370	0.08717	0.38097	0.12864	0.09750	0.85485
	B	$NOAA_{SCX}^{RMSE}$	12.14897	0.33712	0.02622	2.31353	0.62180	0.03389	0.14537	0.20190	0.06978	0.35612	0.12864	0.07924	0.87326
	C	$NOAA_{SWE}^{EMD}$	41.50949	2.55421	0.07613	3.81339	0.61461	0.02661	0.13060	0.19780	0.05456	0.34203	0.12864	0.06147	0.88307
	D	$NOAA_{SWE}^{HAUS2}$	24.34742	1.55100	0.06352	2.31921	0.33870	0.02391	0.18082	0.15740	0.09803	0.39017	0.12864	0.10952	0.84783
	E	$NOAA_{SWE}^{RMSE}$	14.21785	0.33305	0.02323	2.53471	0.57101	0.03900	0.14116	0.20262	0.06390	0.35194	0.12864	0.07292	0.87623
	F	$Q_1^{RMSE}: Q_2^{RMSE}$	20.78182	0.67704	0.07476	1.68539	0.30441	0.01447	0.20581	0.20370	0.10670	0.41086	0.12864	0.12037	0.83119
	G	$Q_1^{RMSE} : NOAA_{SWE}^{HAUS2}$	11.40612	0.15215	0.06241	1.89076	0.53139	0.02587	0.17680	0.20190	0.07816	0.38122	0.12864	0.09039	0.85479
	H	$Q_1^{RMSE} : NOAA_{SWE}^{HAUS1}$	11.86648	0.16983	0.05157	2.03841	0.60756	0.02880	0.18750	0.20370	0.09462	0.39356	0.12864	0.10664	0.84513
	I	$Q_1^{RMSE} : NOAA_{SWE}^{RMSE}$	11.35488	0.28587	0.03308	2.11248	0.63408	0.03318	0.15298	0.20085	0.07332	0.36258	0.12864	0.08322	0.86865
	J	$Q_1^{RMSE} : Q_2^{RMSE} : NOAA_{SCX}^{RMSE}$	16.70662	0.50452	0.06523	1.71166	0.48923	0.01860	0.18151	0.20340	0.08635	0.38662	0.12864	0.09736	0.85052
	K	$Q_1^{RMSE} : Q_2^{RMSE} : NOAA_{SWE}^{HAUS2}$	17.07039	0.54340	0.08927	1.56847	0.42120	0.01668	0.20147	0.20814	0.09935	0.40514	0.12864	0.11264	0.83596
	L	$Q_1^{RMSE} : Q_2^{RMSE} : NOAA_{SWE}^{RMSE}$	13.56164	0.31304	0.06925	1.57598	0.47718	0.02199	0.18570	0.20191	0.08640	0.38982	0.12864	0.09894	0.84808
	M	$Q_1^{RMSE} : Q_2^{RMSE} : SNOTEL_{SWE}^{RMSE}$	16.01342	0.32865	0.05090	2.02103	0.63626	0.02599	0.14661	0.20021	0.06991	0.35771	0.12864	0.07917	0.87218
		DEFAULT	**16.10696**	**0.92604**	**0.02907**	**2.34693**	**0.38735**	**0.03410**	**0.20333**	**0.20340**	**0.10087**	**0.40841**	**0.13719**	**0.11528**	**0.83332**
SEMI	A	Q_1^{RMSE}	26.99921	0.95578	0.08799	2.65919	0.25590	0.01707	0.15389	0.19759	0.06631	0.36803	0.12864	0.07543	0.86454
	B	$NOAA_{SCX}^{RMSE}$	13.08448	0.20059	0.03286	2.48087	0.74330	0.03622	0.14130	0.20085	0.05150	0.36143	0.12864	0.06092	0.86945
	C	$NOAA_{SWE}^{EMD}$	37.34101	1.75001	0.08998	3.74400	0.40868	0.02656	0.13120	0.20191	0.04829	0.33975	0.12864	0.05556	0.88468
	D	$NOAA_{SWE}^{HAUS2}$	19.93720	1.30717	0.04213	2.55913	0.15958	0.03257	0.20991	0.14814	0.11640	0.41263	0.12864	0.13023	0.82982
	E	$NOAA_{SWE}^{RMSE}$	19.35910	0.94314	0.04555	2.25726	0.52876	0.02766	0.14687	0.20191	0.06568	0.35602	0.12864	0.07743	0.87332
	F	$Q_1^{RMSE}: Q_2^{RMSE}$	15.35005	0.44580	0.05598	1.45327	0.30828	0.01327	0.24677	0.14814	0.13567	0.44114	0.12864	0.15175	0.80539
	G	$Q_1^{RMSE} : NOAA_{SWE}^{HAUS2}$	12.66122	0.30668	0.04402	2.12130	0.58826	0.02923	0.16535	0.20191	0.07760	0.37311	0.12864	0.08848	0.86084
	H	$Q_1^{RMSE} : NOAA_{SWE}^{HAUS1}$	13.85977	0.42214	0.04513	2.04133	0.53532	0.02289	0.18510	0.20370	0.09205	0.38854	0.12864	0.10294	0.84912
	I	$Q_1^{RMSE} : NOAA_{SWE}^{RMSE}$	13.74730	0.38582	0.04526	2.05879	0.47440	0.02397	0.17562	0.20191	0.07411	0.37625	0.12864	0.08634	0.85858
	J	$Q_1^{RMSE} : Q_2^{RMSE} : NOAA_{SCX}^{RMSE}$	12.94446	0.35295	0.05671	1.39060	0.39914	0.01347	0.17596	0.14814	0.08513	0.39876	0.12864	0.10161	0.84106
	K	$Q_1^{RMSE} : Q_2^{RMSE} : NOAA_{SWE}^{HAUS2}$	15.93002	0.49047	0.06592	1.91464	0.49901	0.01600	0.19970	0.20998	0.10065	0.40271	0.12864	0.11306	0.83786
	L	$Q_1^{RMSE} : Q_2^{RMSE} : NOAA_{SWE}^{RMSE}$	15.62006	0.50488	0.06704	1.46464	0.43284	0.01620	0.20251	0.20370	0.10064	0.40259	0.12864	0.11243	0.83802
	M	$Q_1^{RMSE} : Q_2^{RMSE} : SNOTEL_{SWE}^{RMSE}$	16.54016	0.45449	0.06161	1.88901	0.55601	0.01563	0.16716	0.20021	0.07352	0.37155	0.12864	0.08283	0.86201
		DEFAULT	**14.60108**	**0.83213**	**0.02872**	**2.24031**	**0.61457**	**0.03460**	**0.19848**	**0.15740**	**0.10883**	**0.40812**	**0.13719**	**0.12247**	**0.83352**
FULL	A	Q_1^{RMSE}	18.83504	0.67158	0.08058	1.28817	0.40184	0.01673	0.26513	0.15740	0.15129	0.46256	0.15033	0.17320	0.78603
	B	$NOAA_{SCX}^{RMSE}$	33.64612	2.04729	0.05759	3.97735	0.81938	0.02273	0.13713	0.20085	0.05333	0.35714	0.12864	0.06145	0.87253
	C	$NOAA_{SWE}^{EMD}$	28.64215	1.17570	0.07201	2.88100	0.37855	0.02355	0.13331	0.19780	0.04886	0.34097	0.15033	0.05654	0.88387
	D	$NOAA_{SWE}^{HAUS2}$	21.57733	0.87218	0.06130	2.09875	0.50068	0.02290	0.19244	0.15740	0.10564	0.40338	0.15033	0.11994	0.83743
	E	$NOAA_{SWE}^{RMSE}$	22.12693	1.14693	0.03241	2.75981	0.26199	0.03509	0.15123	0.18518	0.06906	0.35983	0.12864	0.08073	0.87052
	F	$Q_1^{RMSE}: Q_2^{RMSE}$	25.24808	1.26319	0.05848	2.83463	0.49109	0.02332	0.16860	0.20000	0.06977	0.37228	0.12864	0.07927	0.86140
	G	$Q_1^{RMSE} : NOAA_{SWE}^{HAUS2}$	13.10970	0.23964	0.05334	2.03585	0.64704	0.02256	0.15538	0.19780	0.06849	0.36863	0.12864	0.07838	0.86414
	H	$Q_1^{RMSE} : NOAA_{SWE}^{HAUS1}$	14.35681	0.46989	0.04552	1.94766	0.53379	0.02322	0.20131	0.15740	0.10597	0.40335	0.12864	0.11844	0.83743
	I	$Q_1^{RMSE} : NOAA_{SWE}^{RMSE}$	14.26709	0.42661	0.04688	1.92622	0.58157	0.02213	0.17859	0.18518	0.08865	0.38327	0.12864	0.09934	0.85323
	J	$Q_1^{RMSE} : Q_2^{RMSE} : NOAA_{SCX}^{RMSE}$	17.96686	0.62942	0.08221	1.61918	0.49418	0.02069	0.17171	0.20085	0.07675	0.38228	0.12864	0.08892	0.85399
	K	$Q_1^{RMSE} : Q_2^{RMSE} : NOAA_{SWE}^{HAUS2}$	15.74972	0.42641	0.05667	1.94585	0.60285	0.01977	0.18787	0.20340	0.09069	0.39042	0.12864	0.10232	0.84766
	L	$Q_1^{RMSE} : Q_2^{RMSE} : NOAA_{SWE}^{RMSE}$	14.95856	0.28970	0.05199	1.88681	0.57142	0.02039	0.18872	0.18518	0.09289	0.39403	0.12864	0.10615	0.84473
	M	$Q_1^{RMSE} : Q_2^{RMSE} : SNOTEL_{SWE}^{RMSE}$	13.90406	0.31631	0.06414	1.85002	0.62244	0.01938	0.19442	0.20370	0.10273	0.39732	0.12864	0.11361	0.84221
		DEFAULT	**18.97373**	**1.14997**	**0.03526**	**2.50780**	**0.24452**	**0.03115**	**0.19839**	**0.15740**	**0.11127**	**0.40922**	**0.16373**	**0.12477**	**0.83253**

Table 5.3 Euclidean distance to zero error origin of normalized minimum and maximum error values for the three degrees of distribution.

	RMSE		Hausdorff		EMD	
	Minimum	Maximum	Minimum	Maximum	Minimum	Maximum
SINGLE	3.430	8.009	3.477	11.713	1.766	7.948
SEMI	3.399	8.014	3.725	9.211	1.638	7.082
FULL	3.356	7.802	3.958	10.533	1.446	10.159

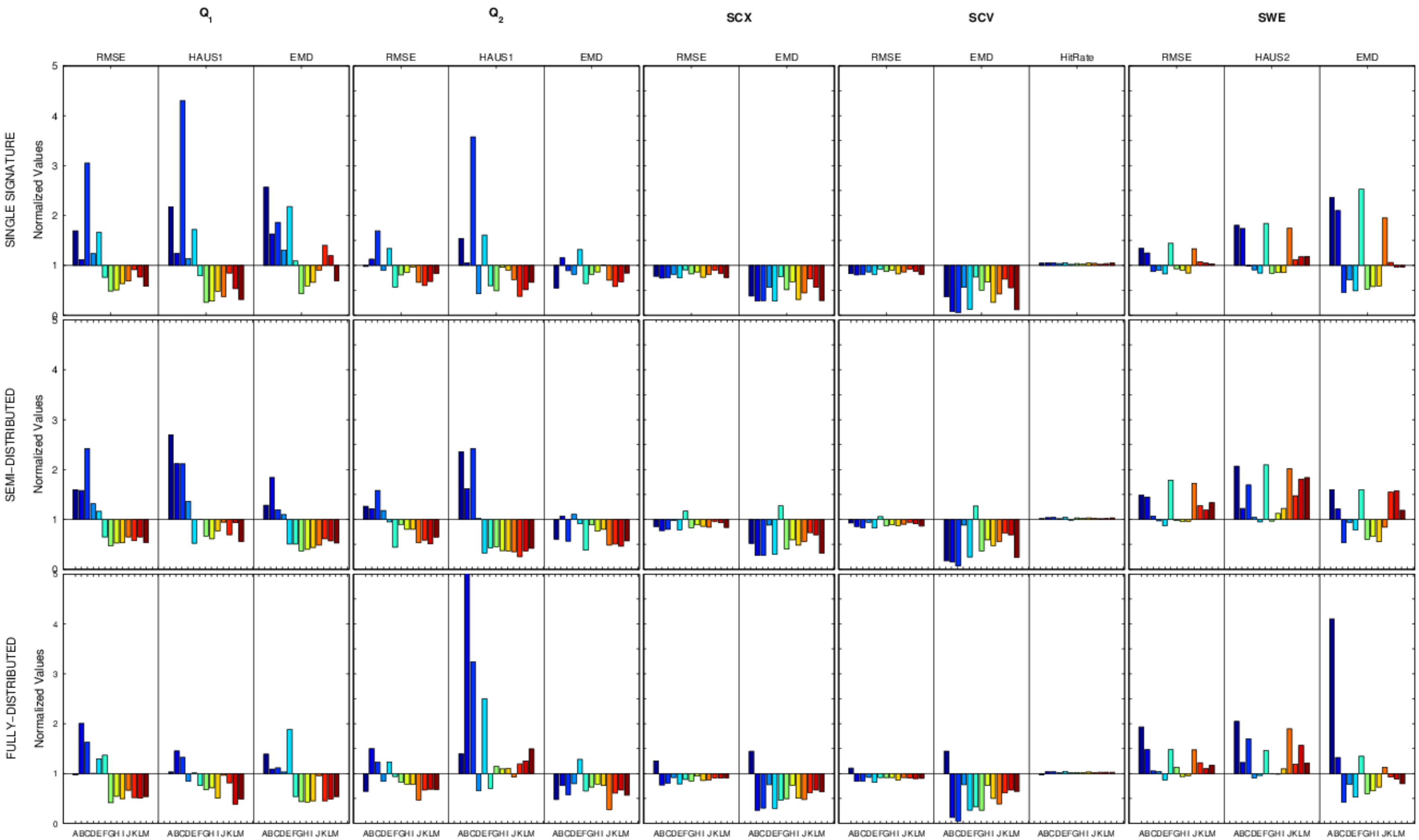

Figure 5.1 Normalized with respect to default simulation (Value > 1: improvement; value < 1: deterioration) for the considered optimization cases in the calibration period.

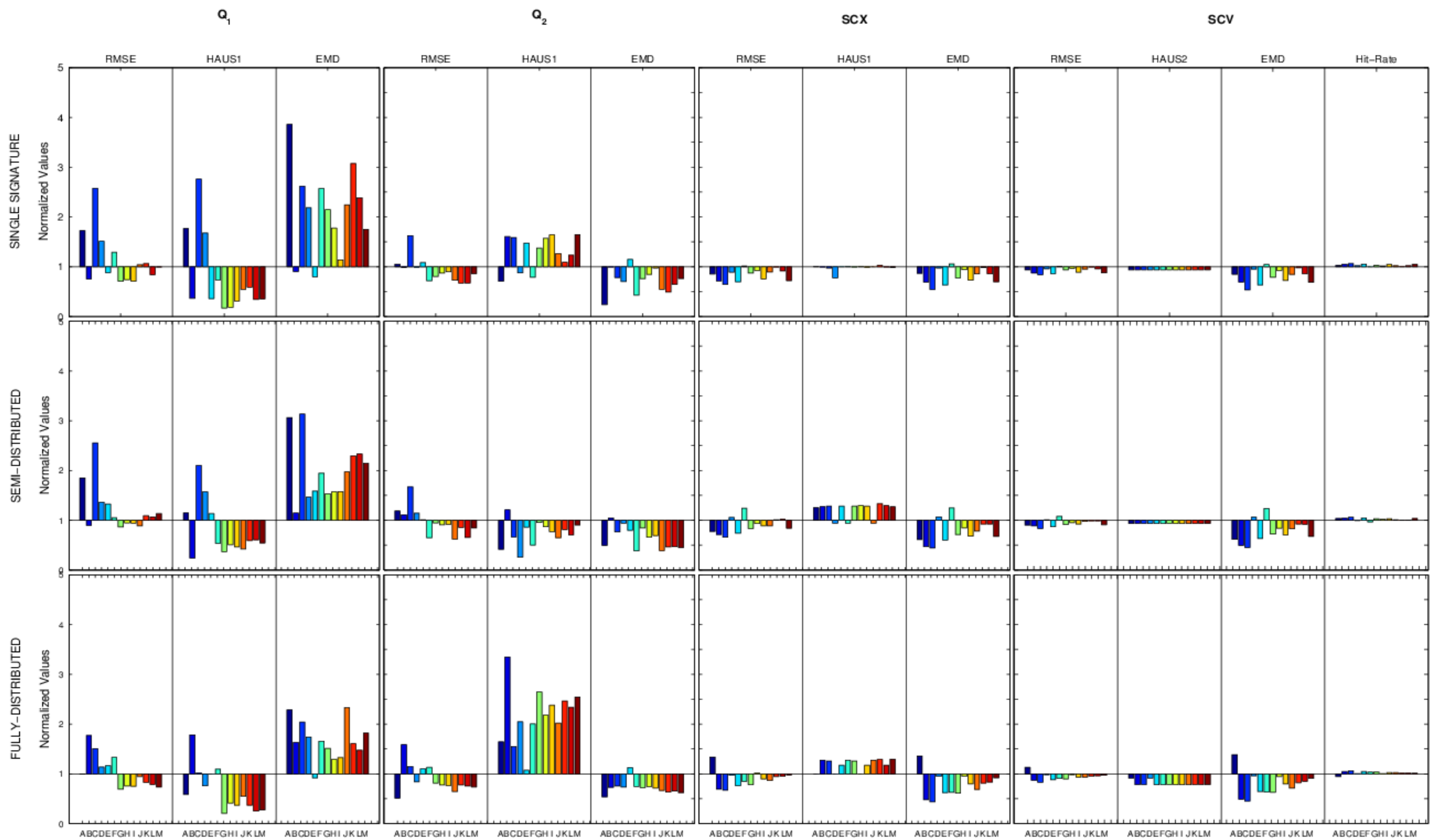

Figure 5.2 Normalized with respect to default simulation (Value > 1: improvement; value < 1: deterioration) for the considered optimization cases in the verification period.

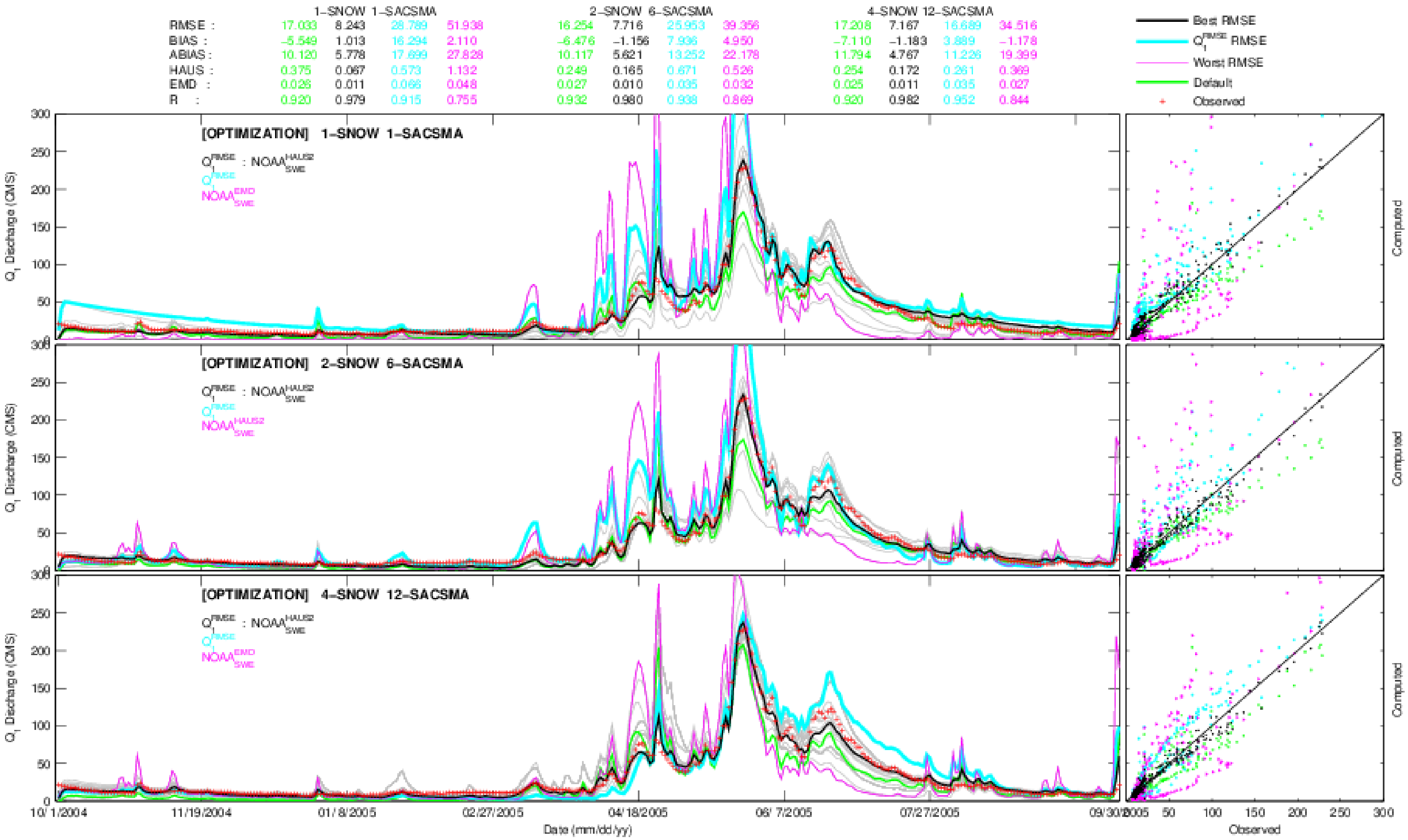

Figure 5.3 Outlet discharge (Q_1) simulation for different levels of distribution. Black is Best RMSE, Cyan is Q_1^{RMSE} Optimization, Magenta is Worst RMSE and Red cross is Observed values at the top of the figure compared to different error functions for the chosen optimizations in the calibration period.

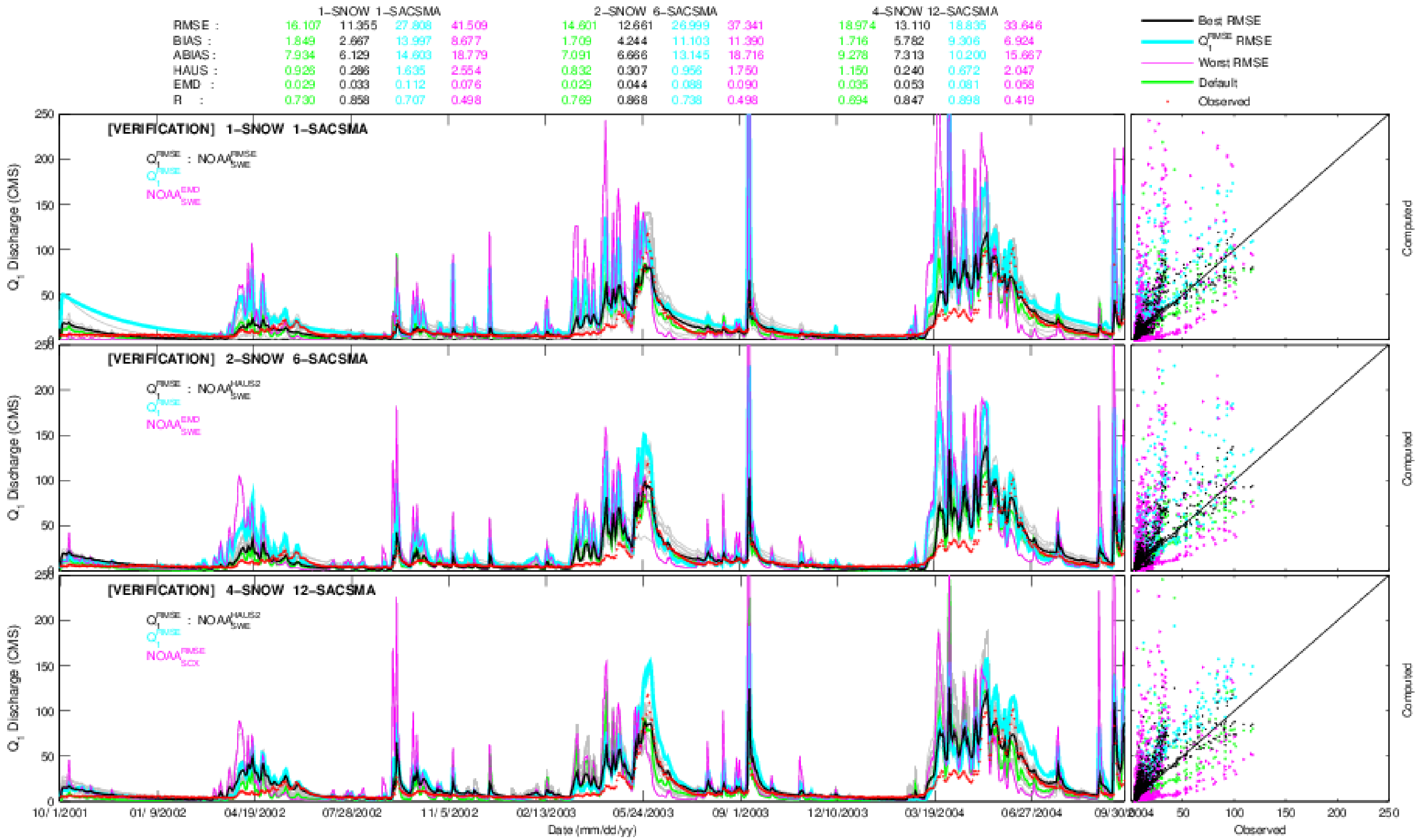

Figure 5.4 Outlet discharge (Q_1) simulation for different levels of distribution. Black is Best RMSE, Cyan is Q_1^{RMSE} Optimization, Magenta is Worst RMSE and Red cross is Observed values at the top of the figure compared to different error functions for the chosen optimizations in the verification period.

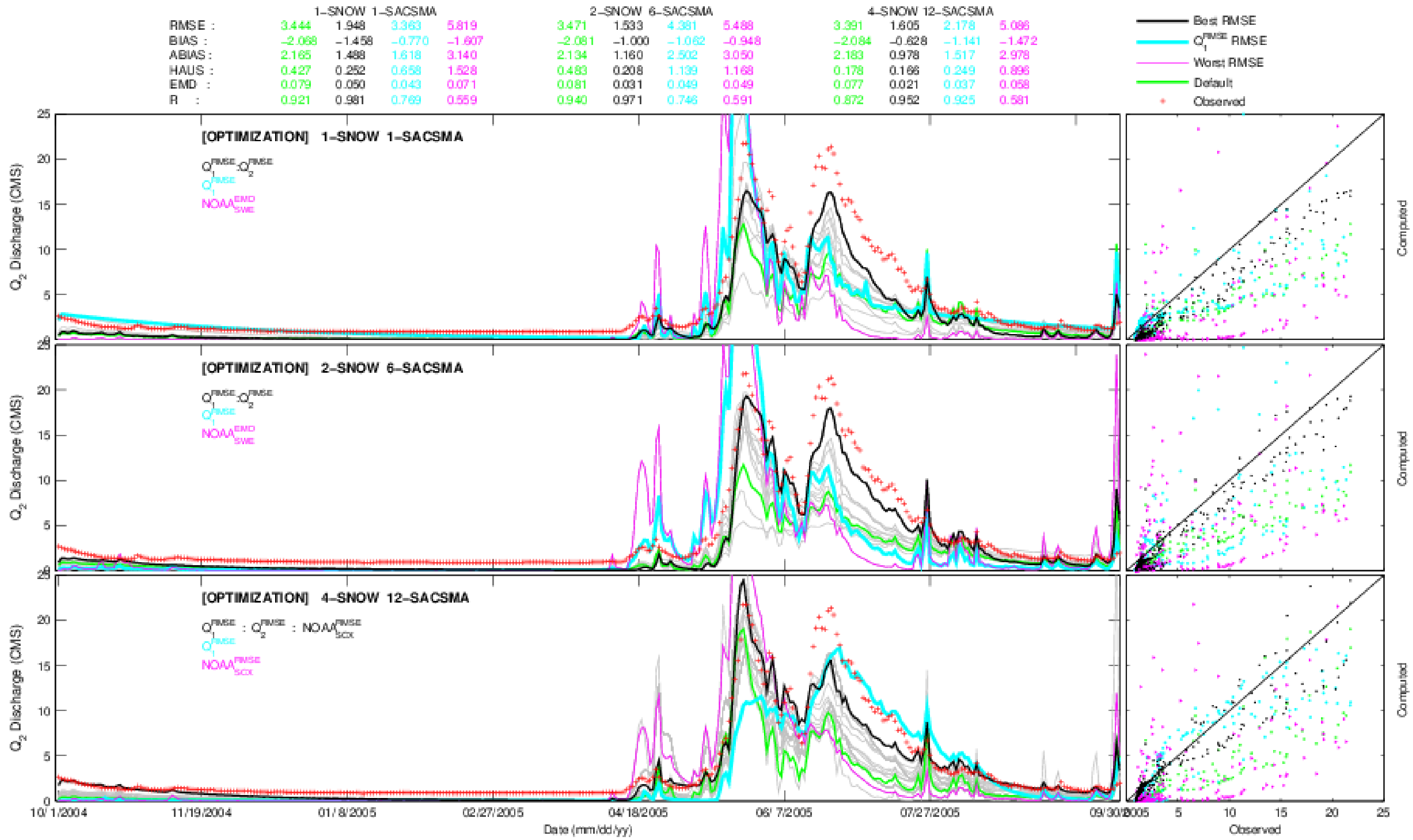

Figure 5.5 Upstream sub-basin discharge (Q_2) simulation for different levels of distribution. Black is Best RMSE, Cyan is Q_1^{RMSE} Optimization, Magenta is Worst RMSE and Red cross is Observed values at the top of the figure compared to different error functions for the chosen optimizations in the calibration period.

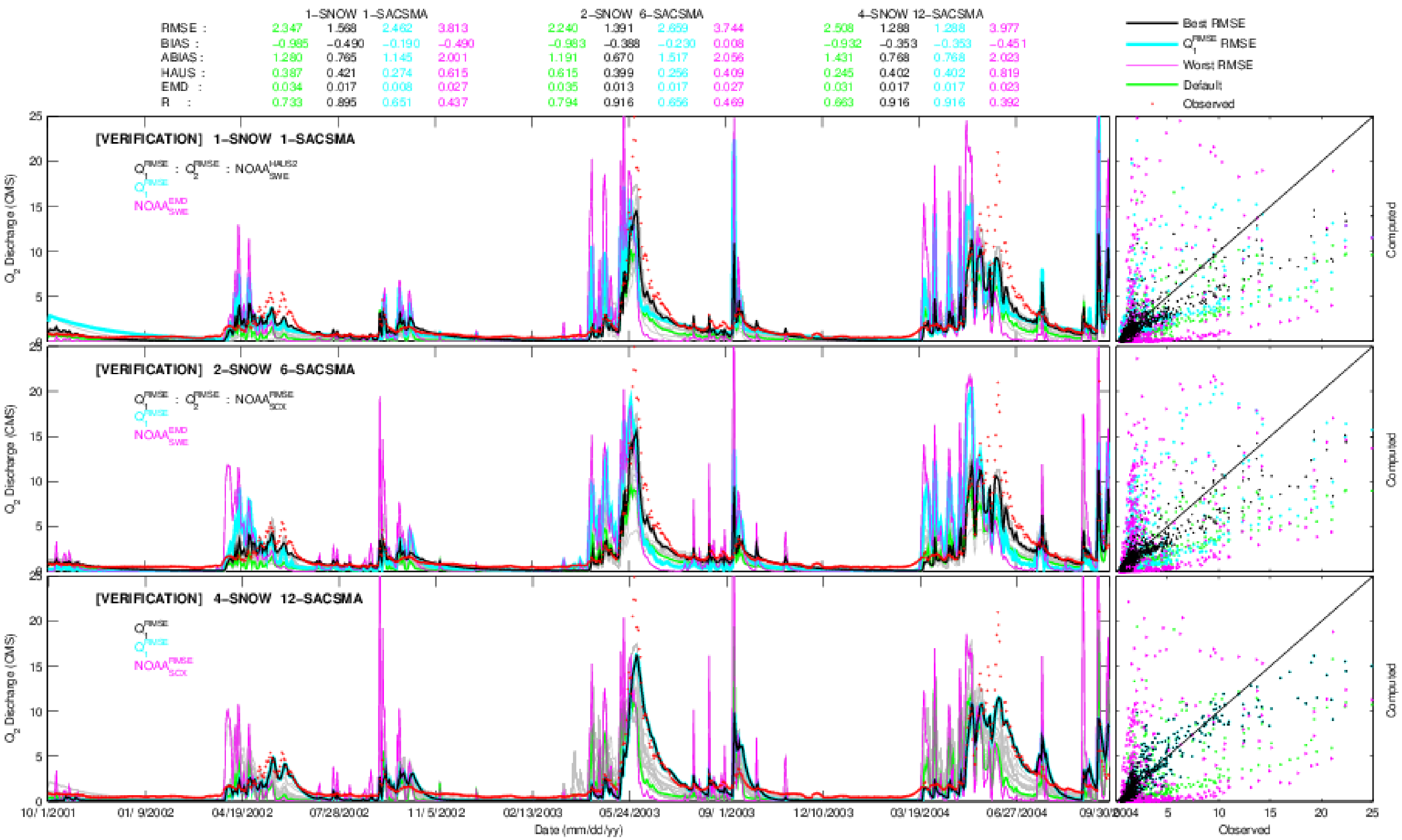

Figure 5.6 Upstream sub-basin discharge (Q_2) simulation for different levels of distribution. Black is Best RMSE, Cyan is Q_1^{RMSE} Optimization, Magenta is Worst RMSE and Red cross is Observed values at the top of the figure compared to different error functions for the chosen optimizations in the verification period.

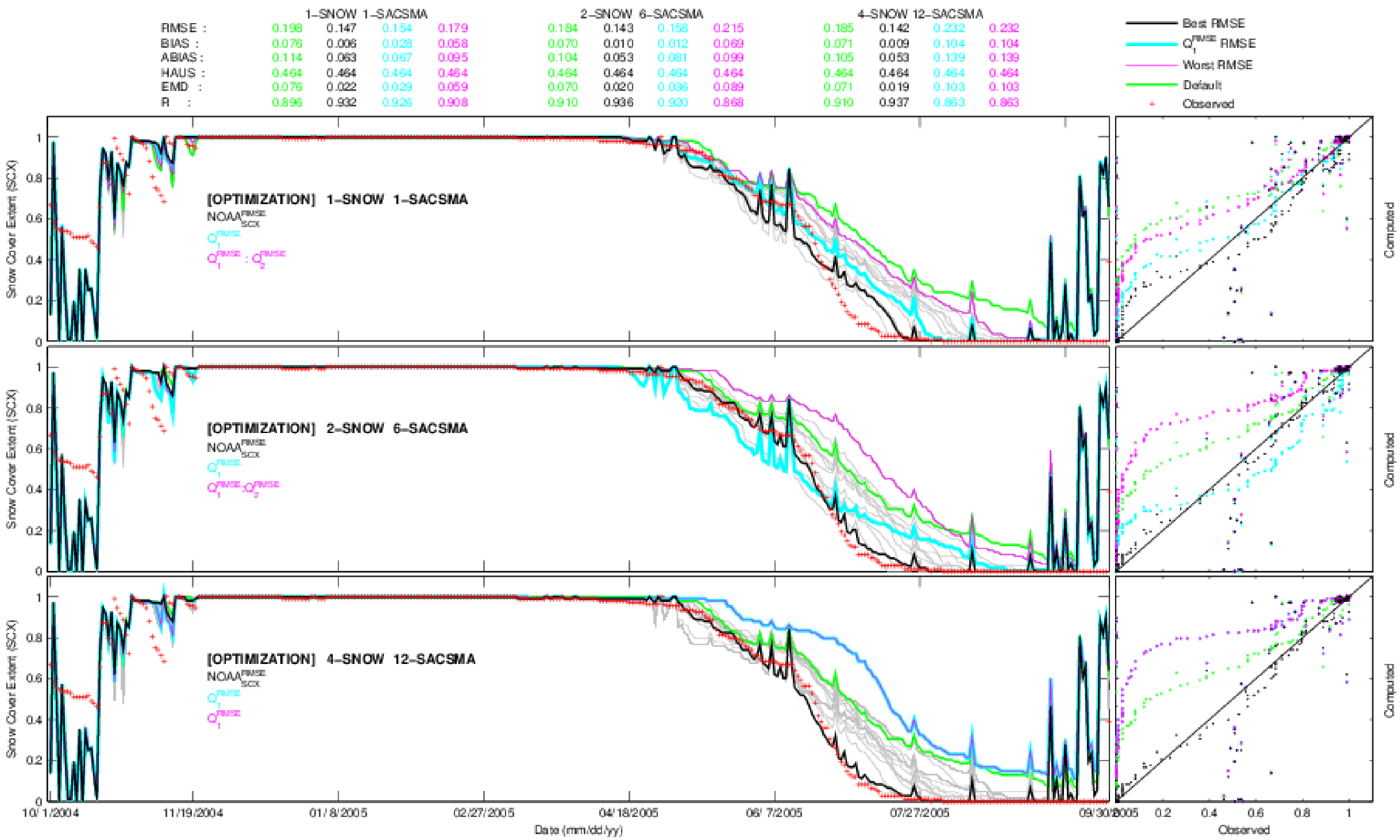

Figure 5.7 Snow Cover eXtent (SCX) simulation for different levels of distribution. Black is Best RMSE, Cyan is Q_1^{RMSE} Optimization, Magenta is Worst RMSE and Red cross is Observed values at the top of the figure compared to different error functions for the chosen optimizations in the calibration period.

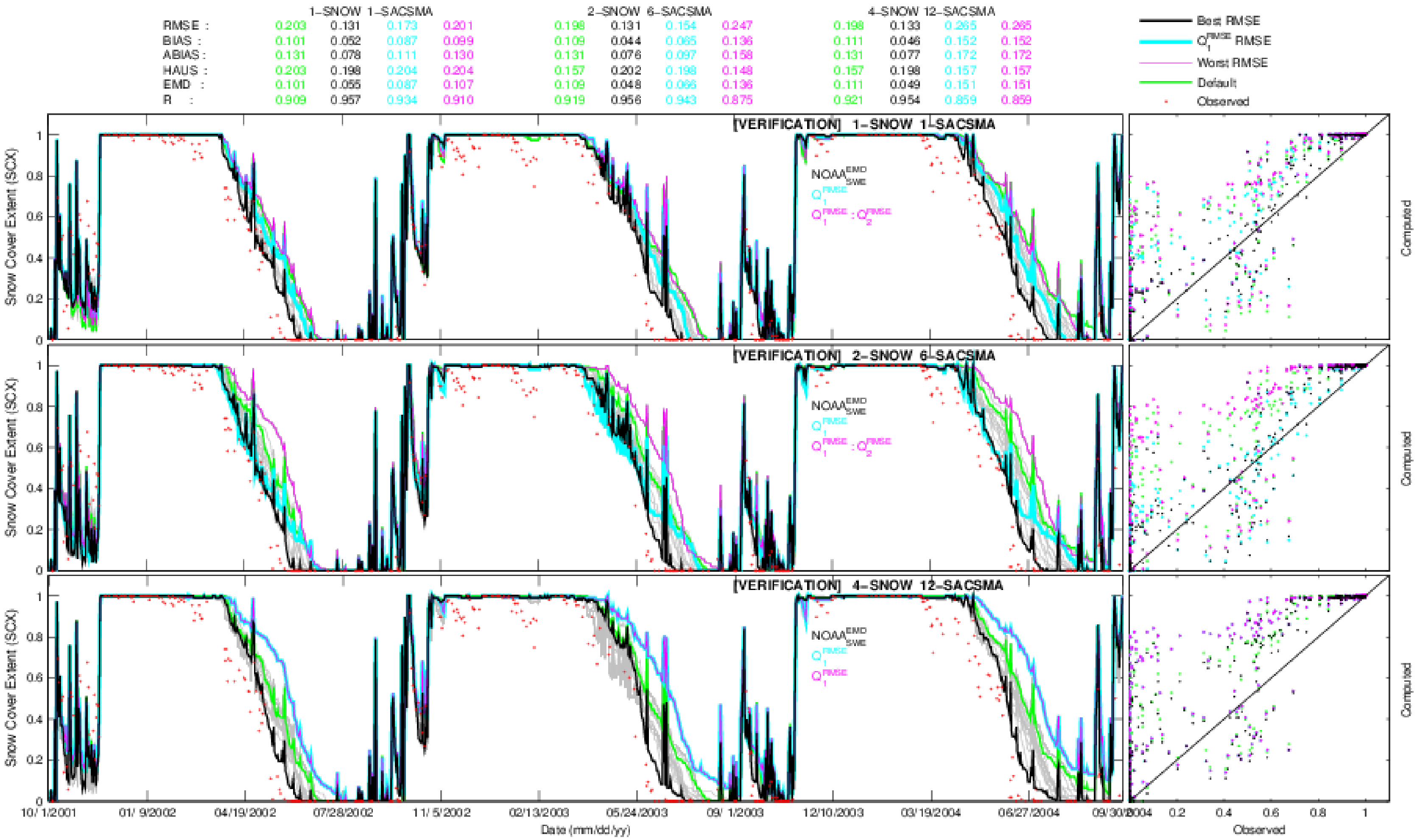

Figure 5.8 Snow Cover eXtent (SCX) simulation for different levels of distribution. Black is Best RMSE, Cyan is Q_1^{RMSE} Optimization, Magenta is Worst RMSE and Red cross is Observed values at the top of the figure compared to different error functions for the chosen optimizations in the verification period.

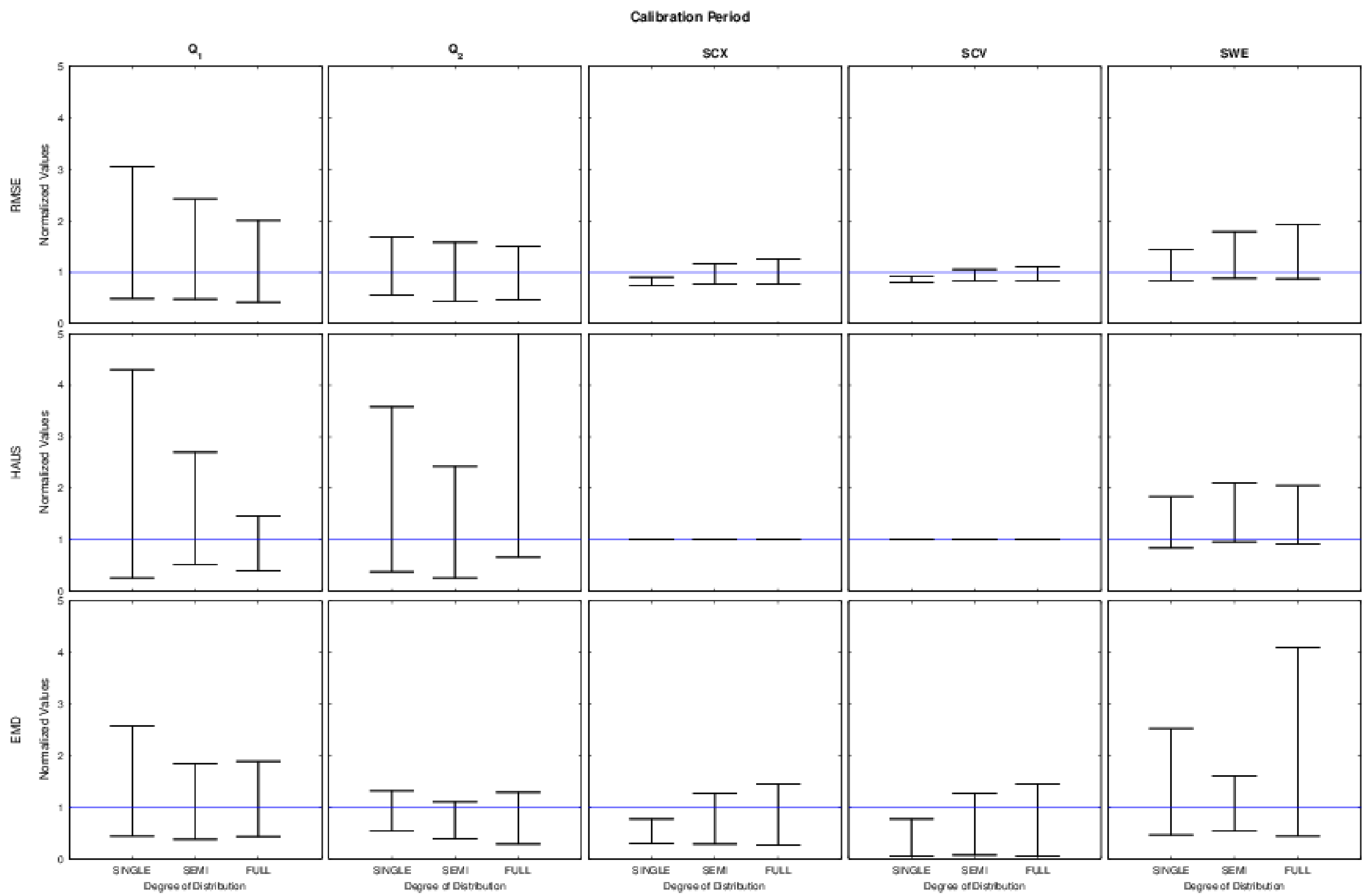

Figure 5.9 Normalized ranges of variation of three error function values for the 13 chosen optimizations.

CHAPTER 6

PARAMETER ESTIMATIONS AND UNCERTAINTY ANALYSIS FOR A SPATIALLY DISTRIBUTED HYDROLOGICAL MODEL

Hydrological model uncertainty includes input data, parameter, and model structural errors (Vrugt et al., 2008). In this dissertation, we do not consider forcing data uncertainty and assuming that model structure is perfect to simulate model output; instead, the model uncertainty is considered with parameter estimations. In order to reduce the model uncertainty, the model parameters are estimated with appropriate values (Bastidas et al., 1999; Gupta et al., 1999). As mentioned in Chapter 5, we have a parameter distribution and a corresponding distribution of model outputs with the optimization algorithms based on the MCMC approach. Ideally, the parameter distributions should always be physically the same, regardless of calibration cases, error functions or degrees of distribution. In this section, we carry out the analysis of the parameter values and their distributions as well as the uncertainty associated with them based on the single- and multi-criteria calibrations.

6.1 Parameter Estimations by Model Calibrations

To explore the parameter set, we have carried out a total of 84 different optimizations (calibrations) using a variety of objective functions and levels of model distribution. This section is only focused on the parameter values and their distributions; the uncertainty associated with them and evaluation of model performance will be addressed in Section 6.3. For the parameter set, we have chosen 13 optimizations as selected in Table 4.2. In this dissertation, we investigate the parameter distributions based on single signature, semi, or full-distributed models with single objective or multi-objective through estimated parameter ranges, spread and Hausdorff values.

For the single-criterion calibrations, only snow information or runoff information is used, i.e., SWE, SCX, and SCV or runoff discharges at the outlet point with different model distributions. On the other hand, discharge information, as well as snow information, is used for the multi-criteria calibrations. We will also utilize the different error functions to evaluate the differences between observation and simulation. As a novel approach to properly compare the results from distributed models, the Hausdorff and EMD are used. In this dissertation, we present 5 different single-criterion calibrations and 8 different multi-criteria calibrations. All parameters are normalized from 0 to 1, with minimum and maximum parameter values, to calculate the Hausdorff and EMD values.

6.1.1 Single Type Parameter Estimations

As mentioned above, we present only 13 different calibration cases for this dissertation. Of the 13 different calibrations, 5 optimizations are single-criterion with snow or runoff discharge at outlet point information and 8 are multi-criteria calibrations using both runoff discharge and snow information. The parameters to be optimized for HL-RDHM are presented in the Table 4.1 with a priori values and parameter ranges. Through the calibrations, the optimized parameter sets considered here are depicted in Figure 6.1 for single type, (a) Snow 17 and (b) SAC-SMA. In Figure 6.1, we have different box plots for single-criterion and multi-criteria calibrations because they use different concept for calibrations. In fact, the 5 box plots are single-criterion optimizations using SCEM, and the next 8 box plots depict the parameters of the multi-criteria calibrations using MOSCEM. For the single-criterion plots, the box plots are a normal box plot, such that the gray box means minimum and maximum ranges of each parameter. Also, the red line represents the mode values for each parameter distribution. However, for the multi-criteria calibrations the black boxes are 100% Pareto ranges, gray boxes are 90% Pareto ranges, and red lines mean compromised solutions.

In the single-criterion calibrations for Snow 17 parameters with single-signature modeling in Figure 6.1 (a), there is only one calibration case for runoff only: Q_1^{RMSE}. Although this case uses only runoff information at an outlet point, the trends of parameters are similar to those of other single-criterion calibrations of snow information only. Also, we have only one single-criterion calibration for SCX: $NOAA_{SCX}^{RMSE}$. The parameter of T1-SCF and T1-MFMAX are very similar ranges for both runoff only and SCX only calibrations. In particular, we have 3 different SWE calibrations with traditional and shape-matching error functions. All snow parameters are very similar patterns with similar parameter uncertainty; however, the T1-MFMAX is a different range for the calibration of $NOAA_{SWE}^{HAUS2}$. As mentioned in section 4.2, the error function of HAUS2 includes the locations and elevations in the procedures of comparison.

For the multi-criteria calibrations of single signature, of 8 multi-criteria calibrations, only one case, $Q_1^{RMSE} : Q_2^{RMSE}$, uses the runoff without snow information. The 90% ranges for Pareto set are similar patterns to runoff only calibration in the parameters of T1-SCF, T1-MFMIN, and T1-UADJ. In particular, we have 2 different calibrations (G and H) for Hausdorff with runoff information at an outlet point. The calibration of $Q_1^{RMSE} : NOAA_{SWE}^{HAUS2}$ (G) has relatively smaller uncertainty than that of $Q_1^{RMSE} : NOAA_{SWE}^{HAUS1}$ (H) in Snow 17 parameters. It seems that the Hausdorff with spatial coordinates (HAUS2) is efficient to constrain parameters in single signature models of HL-RDHM. Additionally, the multi-criteria calibrations with 2 different runoff information sets and snow information (J, K, L, and M) show very similar patterns and uncertainties for Snow 17 parameters without considering variables and error functions.

For the parameters of the water balance component in HL-RDHM, Figure 6.1 (b) shows the parameter uncertainty of single- or multi-criteria calibrations for single signature modeling. In the single-criterion calibrations, the SAC-SMA parameters are very changeable; in particular, the efficiency of single-criterion calibration is doubtful, as the mode values of some parameters are exclusive from box plots. On the other hand, the multi-criteria calibrations with 2 runoff information data sets and snow information show very similar trends for single signature modeling. However, they have relatively larger parameter uncertainties than those of other multi-criteria calibrations using runoff at the outlet point and snow information.

6.1.2 Semi-Distributed Parameter Estimations

As model distributions become more complex from single signature to semi-distribution, the number of parameters to be optimized rapidly increases, and it becomes hard to control the parameters and to analyze each one. In the semi-distributed modeling, we have 2 different snow component types and 6 different water balance component types. As a result, we have 10 and 78 parameter to be optimized for snow and water balance components in HL-RDHM.

For the convenience of comparison for each calibration case, Figure 6.2 (a) depicts the box plotting Snow 17 parameters in the semi-distributed HL-RDHM. Although the parameters should be physically the same regardless of calibration case, the Snow 17 parameters from single-criterion calibrations are changeable in semi-distributed modeling. However, the multi-criteria calibrations reveal very similar trends, especially in Type 1. In particular, the calibration using 2 different runoff discharges (F) has similar parameter uncertainty to that of the calibrations using snow and 2 different runoff discharges. Generally, the multi-criteria calibrations using 3 variables have relatively larger uncertainties, but are well-constrained with Snow 17 parameters in the semi-distributed HL-RDHM model.

For the SAC-SMA parameters in semi-distributed HL-RDHM modeling, the Figure 6.2 (b) represents the box plotting for each calibration case. Like single signature, some of the mode values from single-criterion calibrations are exclusive of the normal box. Therefore, we can say that the single-criterion calibrations using runoff or snow information only could not guarantee the parameter convergence. The SAC-SMA parameters are similar patterns for the multi-criteria calibrations in the semi-distributed HL-RDHM model. In particular, the calibrations with Hausdorff error functions show relatively smaller uncertainties in some of parameters for water balance component in the HL-RDHM model.

6.1.3 Full-Distributed Parameter Estimations

For the full-distributed HL-RDHM modeling, we have 20 parameters for Snow 17 and 156 parameters for SAC-SMA depended on the type of signatures. Figure 6.3 presents the comparison of parameters for (a) snow and (b) water balance component parameters in HL-RDHM.

In the single-criterion calibrations of Figure 6.3 (a), some of the snow parameters look to be well-constrained with traditional and shape-matching error functions.

However, the mode values in calibrations of Q_1^{RMSE} and $NOAA_{SWE}^{HAUS2}$ are exclusive of minimum and maximum ranges for optimized parameters in some signatures. Therefore, it is difficult to reflect the physical characteristics for the snow balance component with mode values of optimized parameters using the single-criterion calibrations in full-distributed HL-RDHM modeling. In the multi-criteria calibrations for Snow 17 parameters, the calibration of $Q_1^{RMSE} : NOAA_{SWE}^{HAUS2}$ shows smaller uncertainties for parameters of Type 1 signature. However, as the mode value of T2-MFMAX in calibration of $Q_1^{RMSE} : Q_2^{RMSE}$ is exclusive of the 90% percentile. It means that the calibration using runoff discharge information only, even though it is a multi-criteria calibration, could not estimate proper parameter ranges for the snow component. In the same ways as single signature and semi-distributed modeling, the multi-criteria calibrations using snow and 2 different runoff discharges are well-constrained with Snow 17 parameters, but the uncertainties are relatively larger in the full-distributed HL-RDHM model.

With the SAC-SMA parameters in the full-distributed HL-RDHM, the single-criterion calibrations have some outliers in the mode values. Therefore, it seems that the single-criterion calibrations using snow information only or runoff information only could not select the appropriate parameter ranges for the water balance component in HL-RDHM model. For the multi-criteria calibrations, a few SAC-SMA parameters with compromised solutions are exclusive of the 90 percentile of optimized parameter ranges. However, the multi-criteria calibrations are well constrained, with 90 percentile parameter ranges as compared to single-criterion calibrations.

6.2 Parameter Distributions for Model Calibrations and Complexity

In section 6.1, we have roughly investigated the parameters for single-signature, semi-distributed, and full-distributed HL-RDHM model. In particular, increasing the number of parameters to be optimized and analyzed in distributed models makes investigating the parameters very complicated. In this section, we control only parameters for Signature 1 (Type 1) to analyze the effect of distributions on the HL-RDHM model. Regardless of the degree of distributions, the parameters in Type1 are always physically the same for snow and water balance components. Therefore, we are able to investigate whether the calibrations are well-constrained with the parameters as compared with the parameters in Type 1 for each distribution. To compare the parameters for Signature 1 from each calibration, the Hausdorff values are used with parameter ranges / spread for single- and multi-criteria calibrations.

6.2.1 Single-Criterion Calibrations

For the single-criterion calibrations the SCEM optimization algorithm is used with runoff or snow information only, using traditional or shape-matching error functions. The Figure 6.4 (a) single-criterion calibrations are parallel plots of Snow 17 and SAC-SMA parameters. The black, blue, and red transparencies represent the 90 percentile ranges of optimized parameters for single-signature, semi-distributed, and full-distributed modeling, respectively. Also, the thick lines represent mode values for each parameter distribution. The Table 6.1 single-criterion shows the Hausdorff values to compare the parameter distributions from each distribution. With the Hausdorff values we compare the parameters from single-signature, semi-distributed, and full-distributed models.

Of 5 different single-criterion calibrations, the calibration of Q_1^{RMSE} is used for runoff information only. For the results of Q_1^{RMSE} in Figure 6.4 (a), the Snow 17 parameters have their own distributions for each distribution. The Snow 17 parameters other than T1-MFMIN, such as T1-SCF, T1-MFMAX, T1-NMF, and T1-UADJ, show similar trends and uncertainties for single-signature, semi-distributed, and full-distributed HL-RDHM models. Although the calibration uses runoff only at an outlet point, the parameters in terms of water balance component are changeable for all distributions. In fact, the parameter patterns for each model have their own distributions for SAC-SMA parameters. With the Table 6.1 single-criterion, we affirm that the parameters for the water balance component are relatively more flexible in the calibration of Q_1^{RMSE}.

For the single-criterion calibration of $NOAA_{SCX}^{RMSE}$, the Snow 17 parameters have slightly different patterns for all distributions. In particular, the parameters of T1-SCF, T1MFMIN, and T1-NMF have different ranges in the single-signature, semi-distributed, and full-distributed models, respectively. Moreover, although this calibration uses snow information only, the parameters for Snow 17 reveal greater Hausdorff values in Table 6.1 single-criterion than those for SAC-SMA parameters. Hence, it appears to be difficult to select proper parameters for SAC-SMA, as well as Snow 17, with the calibrations using SCX information only.

The Snow 17 parameters from the calibration of $NOAA_{SWE}^{EMD}$ show similar tendencies for single-signature and full-distributed models, but the parameter of T1-MFMIN in semi-distributed model is estimated to different ranges and values for 90 percentile and mode. The parameters for the water balance component are still changeable depending on the degree of distributions.

We have 2 other single-criterion calibrations: $NOAA_{SWE}^{HAUS2}$ and $NOAA_{SWE}^{RMSE}$. Both calibrations are useful to constrain the Snow 17 parameters as showing very similar tendencies of ranges and mode values for semi- and full- distributions in Figure 6.4 for single-criterion calibrations. In fact, both calibration cases have relatively smaller values for Hausdorff [0.113 and 0.063] compared semi- and full-distributed modeling. However, the Snow 17 parameter of T1-MFMAX has different ranges and mode values for both calibrations. Also, in calibration case of $NOAA_{SWE}^{HAUS2}$, the parameter of T1-MFMAX shows different ranges in single-signature. The calibration of $NOAA_{SWE}^{RMSE}$ has different distribution of 90 percentile for the parameter of T1-MFMAX in the single-signature model. In the Table 6.1 single-criterion, the calibrations of $NOAA_{SWE}^{HAUS2}$ and $NOAA_{SWE}^{RMSE}$ still show large Hausdorff values [0.231 to 0.479] for water balance component.

According to the results in this section, it would not be easy to estimate proper parameter ranges with single-criterion calibration for HL-RDHM, in general; however, the calibrations using SWE with RMSE and Hausdorff and including time and spatial coordinate variables are relatively useful to constrain the parameters for the snow component in the HL-RDHM model.

6.2.2 Multi-criteria Calibrations

The MOSCEM optimization algorithm is used for multi-criterion calibrations with both runoff and snow information. The Figure 6.4 (b) multi-criteria calibrations are parallel plots of Snow 17 and SAC-SMA parameters for multi-criterion calibrations. The black, blue, and red transparencies depict the 90 percentile of Pareto ranges for optimized parameters for single-signature, semi-distributed, and full-distributed modeling, respectively. Also, the thick lines represent compromised solutions for each parameter distribution.

Of the 8 different multi-criteria calibrations, the $Q_1^{RMSE} : Q_2^{RMSE}$ calibration uses runoff information only, without snow information. In the Figure 6.4 (b) multi-criteria calibrations, the $Q_1^{RMSE} : Q_2^{RMSE}$ calibration shows very similar parameter uncertainties for semi- and full-distributed models. In fact, they have Hausdorff values of 0.0684 and 0.092 for snow and water balance components in HL-RDHM. However, the parameter uncertainties are relatively larger in semi- and full-distributed models than in the single signature model.

In this dissertation, we have 3 different calibrations using SWE information and runoff information on the outlet point with different error functions. All calibrations show their own parameter uncertainties for Snow 17 and SAC-SMA. In particular, the calibration of $Q_1^{RMSE} : NOAA_{SWE}^{HAUS2}$ has different trends of Snow 17 in the semi-distributed model. Also, the parameters of T1-MFMAX and T1-MFMIN have different parameter distributions in semi-distributed modeling for the calibrations of $Q_1^{RMSE} : NOAA_{SWE}^{HAUS1}$ and $Q_1^{RMSE} : NOAA_{SWE}^{RMSE}$. In Table 6.1 for multi-criteria, the calibrations using SWE and runoff information on the outlet point (F, G, and H) improve the Hausdorff values for the parameters of snow and water balance components, in general. They have Hausdorff values from 0.169 to 0.330 for Snow 17 parameters and from 0.164 to 0.528 for SAC-SMA.

There are 4 other multi-criteria calibrations that use snow and 2 different runoff discharges. In Figure 6.4 (b) multi-criteria calibrations, the calibrations using both snow and 2 different runoff discharges show very similar parameter uncertainties for snow and water balance components. In particular, the parameters for Snow 17 and SAC-SMA have similar distributions between semi- and full-distributed models. In Table 6.1 for multi-criteria, the Hausdorff values are 0.018 - 0.116 for snow parameters and 0.039 - 0.112 when comparing semi- and full-distributed models.

As results, the multi-criteria calibrations are very useful for estimating parameter ranges and spread for the HL-RDHM model. When we use the multi-criteria calibrations with distributed models, the parameters are especially well-constrained to simulate the HL-RDHM model.

6.3 Model Uncertainty with Parameters

In this dissertation, we describe and evaluate the procedure that accounts for hydrologic model uncertainty associated with parameter uncertainty using Hausdorff values. The model output uncertainty is estimated based on the 90 percentile ranges of estimated parameter sets, and then overall Hausdorff values are calculated with 3 different model outputs, such as runoff discharges at both internal and outlet points and SCX information. With the Hausdorff values, we can check how close the model outputs are to their observations with the parameter estimations. For the single-criterion calibrations, the 90 percentile ranges of optimized parameters are selected to calculate the model output uncertainty. Also, the 90 percentile ranges of optimized Pareto front are used for multi-criteria calibrations. Table 6.2 presents the Hausdorff values considering overall basin runoff, sub-basin runoff, and SCX information for each calibration. In this table, the Hausdorff values are calculated for the mode or compromised solutions as well as the 90 percentile ranges (Min/Max).

6.3.1 Single Type Uncertainty

In the single-signature type in Table 6.2, the Hausdorff values for all compromised solutions and 90 percentile ranges of multi-criteria calibrations are improved from the default (benchmark) values. Furthermore, all Hausdorff values for 90 percentile of optimized parameters for single-criterion calibrations are reduced from default values. This means that the observations are covered with the mode outputs from 90 percentile of optimized parameters in both single- and multi-criteria calibrations. However, most of Hausdorff values for mode of single-criterion calibrations are deteriorated from default values except for the calibration of $NOAA_{SCX}^{RMSE}$. Figure 6.5 (a) depicts the model output ranges from the calibration of $Q_1^{RMSE} : NOAA_{SWE}^{HAUS2}$, which is the best Hausdorff value for compromised solution and output ranges in the single-signature model. Figure 6.5 (a) shows the model output uncertainty with 90 percentile parameter ranges for the optimization period. For multi-criteria calibrations, the light and darker gray ranges are 100 and 90 percentile model outputs from parameter distributions of optimized parameters. Also, the green lines are default values (benchmark), the blue lines are compromised solutions for parameter distribution, and the red dots are observations. In Figure 6.5 (a), the output values from the calibrations of $Q_1^{RMSE} : NOAA_{SWE}^{HAUS2}$ cover the observations. In particular, 90 percentile ranges are covered, with observations for overall basin runoff and SCX. However, the 90 percentile ranges for sub-basin runoff are exclusive of observations for single-signature model.

6.3.2 Semi-Distributed Model Uncertainty

For the semi-distributed modeling of HL-RDHM, the Hausdorff values on Table 6.2 for SEMI indicate superior performances for all of calibrations with 90 percentile model outputs. However, the mode values from the single-criterion calibrations fail to improve the Hausdorff values from default parameters, except for the calibration of $NOAA_{SWE}^{RMSE}$. In particular, the multi-criteria calibrations using snow and 2 different runoff discharges indicate smaller Hausdorff values than those of single-criterion calibrations and other multi-criteria calibrations using snow and overall basin runoff information. It seems that the multi-criteria calibrations using snow and 2 different runoff discharges are more useful to match the observations. However, Figure 6.5 (b) depicts the model simulations for overall basin, upstream sub-basin runoff, and SCX information from the calibration of $Q_1^{RMSE} : Q_2^{RMSE}$ as the best Hausdorff in the semi-distributed modeling of HL-RDHM. In Figure 6.5 (b), the SCX information is exclusive of observations compared with default values for 90 percentile ranges and compromised solutions. On the other hand, the observations for both runoff discharges are relatively included within the 90 percentile ranges, indicating better Hausdorff values. Hence, the simulations of snow information are not covered with this calibration in spite of better performances for overall basin and sub-basin runoff information.

6.3.3 Full-Distributed Model Uncertainty

In the same manner as with single-signature and semi-distributed modeling, the full-distributed model indicates an improvement from default Hausdorff values for single- and multi-criteria calibrations on Table 6.2 for FULL. However, most single-criterion calibrations fail to improve the Hausdorff values. As we can see, the Figure 6.5 (c) 90 percentile ranges of optimized parameters from calibration of $Q_1^{RMSE} : Q_2^{RMSE} : NOAA_{SWE}^{HAUS2}$ show better performances than those of single-signature and semi-distributed modeling of HL-RDHM including observations. Furthermore, comparing the Hausdorff values in Table 6.2 indicates better performances in semi- and full-distributed models with multi-criteria calibrations. According to the results, we could say that the multi-criteria calibrations are useful to calibrate HL-RDHM with distributed modeling.

Table 6.1 The Hausdorff values to compare Snow 17 and SAC-SMA parameter distributions of Signature 1 (Type 1) for single-signature, semi-, and full-distributed models.

Calibrations			Snow 17 Parameters			SAC-SMA Parameters		
			Single : Semi	Single : Full	Semi : Full	Single : Semi	Single : Full	Semi : Full
Single Criterion	A	Q_1^{RMSE}	0.27490	0.27450	0.42390	0.75030	0.46950	0.61690
	B	$NOAA_{SCX}^{RMSE}$	0.44750	0.44500	0.40610	0.46650	0.29980	0.39020
	C	$NOAA_{SWE}^{EMD}$	0.31470	0.11960	0.34710	0.30140	0.27000	0.29260
	D	$NOAA_{SWE}^{HAUS2}$	0.30070	0.28650	0.11300	0.47890	0.28950	0.34120
	E	$NOAA_{SWE}^{RMSE}$	0.25740	0.28790	0.06340	0.23690	0.23100	0.24270
Multi Criteria	F	$Q_1^{RMSE} : Q_2^{RMSE}$	0.42260	0.39970	0.06840	0.27760	0.25610	0.09280
	G	$Q_1^{RMSE} : NOAA_{SWE}^{HAUS2}$	0.22250	0.29440	0.31030	0.52830	0.59540	0.37610
	H	$Q_1^{RMSE} : NOAA_{SWE}^{HAUS1}$	0.25240	0.19010	0.23140	0.25080	0.23530	0.29880
	I	$Q_1^{RMSE} : NOAA_{SWE}^{RMSE}$	0.33000	0.16940	0.30020	0.16360	0.34700	0.20570
	J	$Q_1^{RMSE} : Q_2^{RMSE} : NOAA_{SCX}^{RMSE}$	0.40520	0.40260	0.03900	0.22410	0.21400	0.05870
	K	$Q_1^{RMSE} : Q_2^{RMSE} : NOAA_{SWE}^{HAUS2}$	0.34140	0.35000	0.04000	0.22920	0.23290	0.11230
	L	$Q_1^{RMSE} : Q_2^{RMSE} : NOAA_{SWE}^{RMSE}$	0.16980	0.18790	0.01820	0.16600	0.12290	0.05110
	M	$Q_1^{RMSE} : Q_2^{RMSE} : SNOTEL_{SWE}^{RMSE}$	0.08640	0.11470	0.11600	0.20960	0.19340	0.03910

Table 6.2 The Hausdorff values for 3 different observations (SCX, overall basin and sub-basin runoff) from mode or compromised solution and 90 percentile of optimized parameters for single-signature, semi-, and full-distributed models.

Hausdorff			Calibration Period		
Distribution	Calibrations		Default	Mode/Compromised	Min/Max
SINGLE	A	Q_1^{RMSE}	0.62020	0.82668	0.47731
	B	$NOAA_{SCX}^{RMSE}$		0.57991	0.52410
	C	$NOAA_{SWE}^{EMD}$		1.90166	0.47118
	D	$NOAA_{SWE}^{HAUS2}$		0.62233	0.53373
	E	$NOAA_{SWE}^{RMSE}$		0.82207	0.51095
	F	$Q_1^{RMSE} : Q_2^{RMSE}$		0.46575	0.49390
	G	$Q_1^{RMSE} : NOAA_{SWE}^{HAUS2}$		0.46555	0.47150
	H	$Q_1^{RMSE} : NOAA_{SWE}^{HAUS1}$		0.49723	0.51352
	I	$Q_1^{RMSE} : NOAA_{SWE}^{RMSE}$		0.61088	0.47237
	J	$Q_1^{RMSE} : Q_2^{RMSE} : NOAA_{SCX}^{RMSE}$		0.46568	0.50867
	K	$Q_1^{RMSE} : Q_2^{RMSE} : NOAA_{SWE}^{HAUS2}$		0.50879	0.53366
	L	$Q_1^{RMSE} : Q_2^{RMSE} : NOAA_{SWE}^{RMSE}$		0.46599	0.50095
	M	$Q_1^{RMSE} : Q_2^{RMSE} : SNOTEL_{SWE}^{RMSE}$		0.52602	0.50928
SEMI	A	Q_1^{RMSE}	0.66537	1.32482	0.47045
	B	$NOAA_{SCX}^{RMSE}$		0.96235	0.47126
	C	$NOAA_{SWE}^{EMD}$		1.27046	0.47210
	D	$NOAA_{SWE}^{HAUS2}$		0.70751	0.58263
	E	$NOAA_{SWE}^{RMSE}$		0.57818	0.47782
	F	$Q_1^{RMSE} : Q_2^{RMSE}$		0.46628	0.47028
	G	$Q_1^{RMSE} : NOAA_{SWE}^{HAUS2}$		0.58724	0.54476
	H	$Q_1^{RMSE} : NOAA_{SWE}^{HAUS1}$		0.56702	0.56877
	I	$Q_1^{RMSE} : NOAA_{SWE}^{RMSE}$		0.53785	0.49206
	J	$Q_1^{RMSE} : Q_2^{RMSE} : NOAA_{SCX}^{RMSE}$		0.46887	0.49086
	K	$Q_1^{RMSE} : Q_2^{RMSE} : NOAA_{SWE}^{HAUS2}$		0.46909	0.48305
	L	$Q_1^{RMSE} : Q_2^{RMSE} : NOAA_{SWE}^{RMSE}$		0.46648	0.48401
	M	$Q_1^{RMSE} : Q_2^{RMSE} : SNOTEL_{SWE}^{RMSE}$		0.48350	0.49881
FULL	A	Q_1^{RMSE}	0.59656	0.48208	0.51486
	B	$NOAA_{SCX}^{RMSE}$		0.95699	0.49516
	C	$NOAA_{SWE}^{EMD}$		0.65741	0.47007
	D	$NOAA_{SWE}^{HAUS2}$		0.55257	0.56325
	E	$NOAA_{SWE}^{RMSE}$		0.64158	0.54444
	F	$Q_1^{RMSE} : Q_2^{RMSE}$		0.46836	0.47955
	G	$Q_1^{RMSE} : NOAA_{SWE}^{HAUS2}$		0.46820	0.47082
	H	$Q_1^{RMSE} : NOAA_{SWE}^{HAUS1}$		0.58493	0.50043
	I	$Q_1^{RMSE} : NOAA_{SWE}^{RMSE}$		0.57640	0.50414
	J	$Q_1^{RMSE} : Q_2^{RMSE} : NOAA_{SCX}^{RMSE}$		0.47202	0.49158
	K	$Q_1^{RMSE} : Q_2^{RMSE} : NOAA_{SWE}^{HAUS2}$		0.46726	0.47891
	L	$Q_1^{RMSE} : Q_2^{RMSE} : NOAA_{SWE}^{RMSE}$		0.46676	0.48889
	M	$Q_1^{RMSE} : Q_2^{RMSE} : SNOTEL_{SWE}^{RMSE}$		0.46510	0.49707

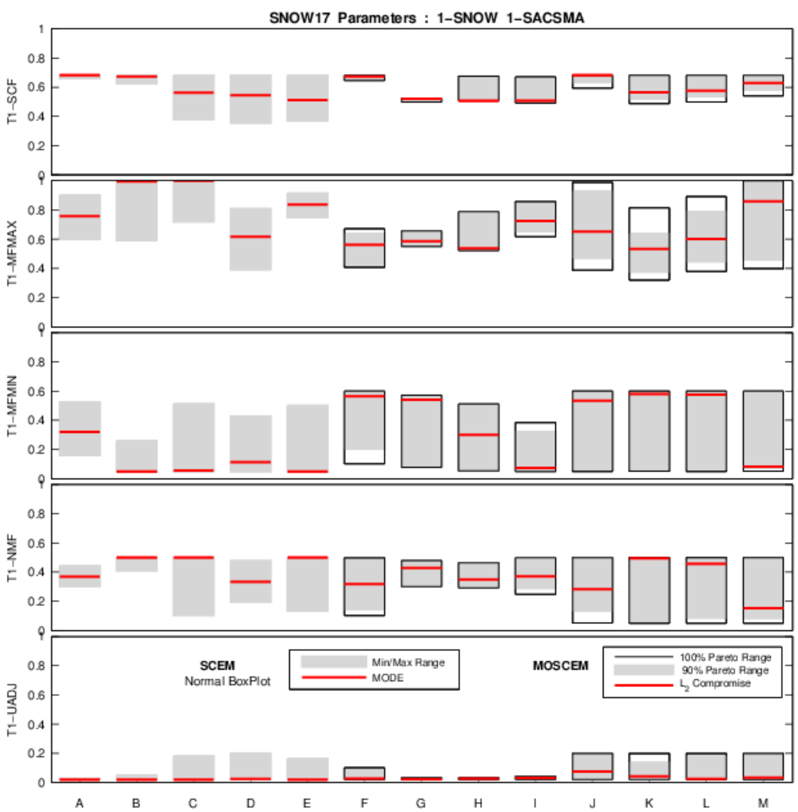

(a) Single-Signature Snow 17 parameters.

Figure 6.1 Box plotting for Normalized Parameter Estimations of Single-Signature HL-RDHM. For the single-criterion calibrations using SCEM, normal box plot is used so that the red line mode values for parameter distributions. For multi-criteria calibrations using MOSCEM the box plot is parameter ranges of 100 percentile, gray box is 90 percentile ranges of optimized parameters and red line represents compromised solutions.

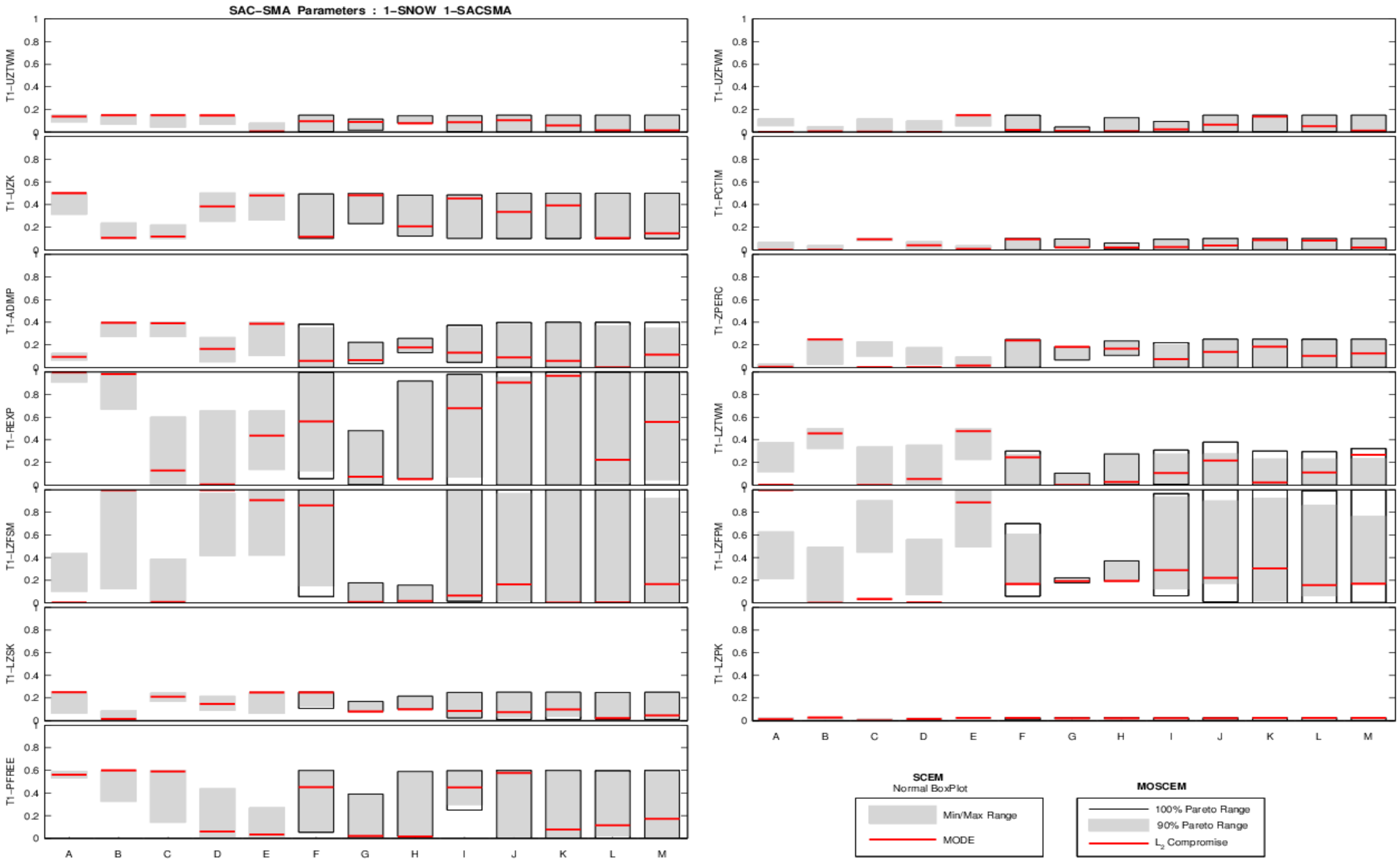

(a) Single-Signature SAC-SMA parameters.

Figure 6.1 Cont.

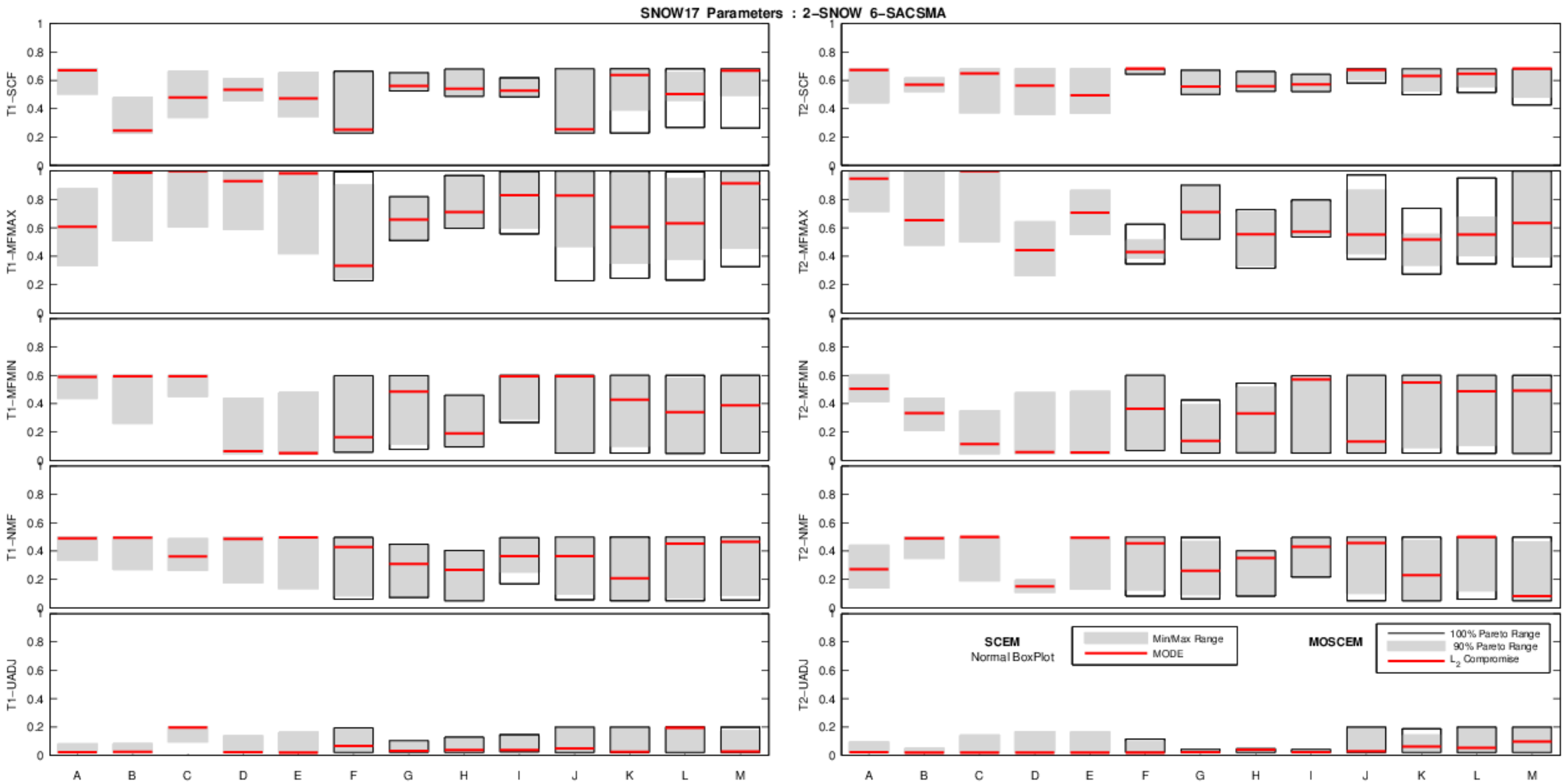

(a) Semi-Distributed Snow 17 parameters – Signature 1 & 2.

Figure 6.2 Box plotting for Normalized Parameter Estimations of Semi-Distributed HL-RDHM. For the single-criterion calibrations using SCEM, normal box plot is used so that the red line mode values for parameter distributions. For multi-criteria calibrations using MOSCEM the box plot is parameter ranges of 100 percentile, gray box is 90 percentile ranges of optimized parameters and red line represents compromised solutions.

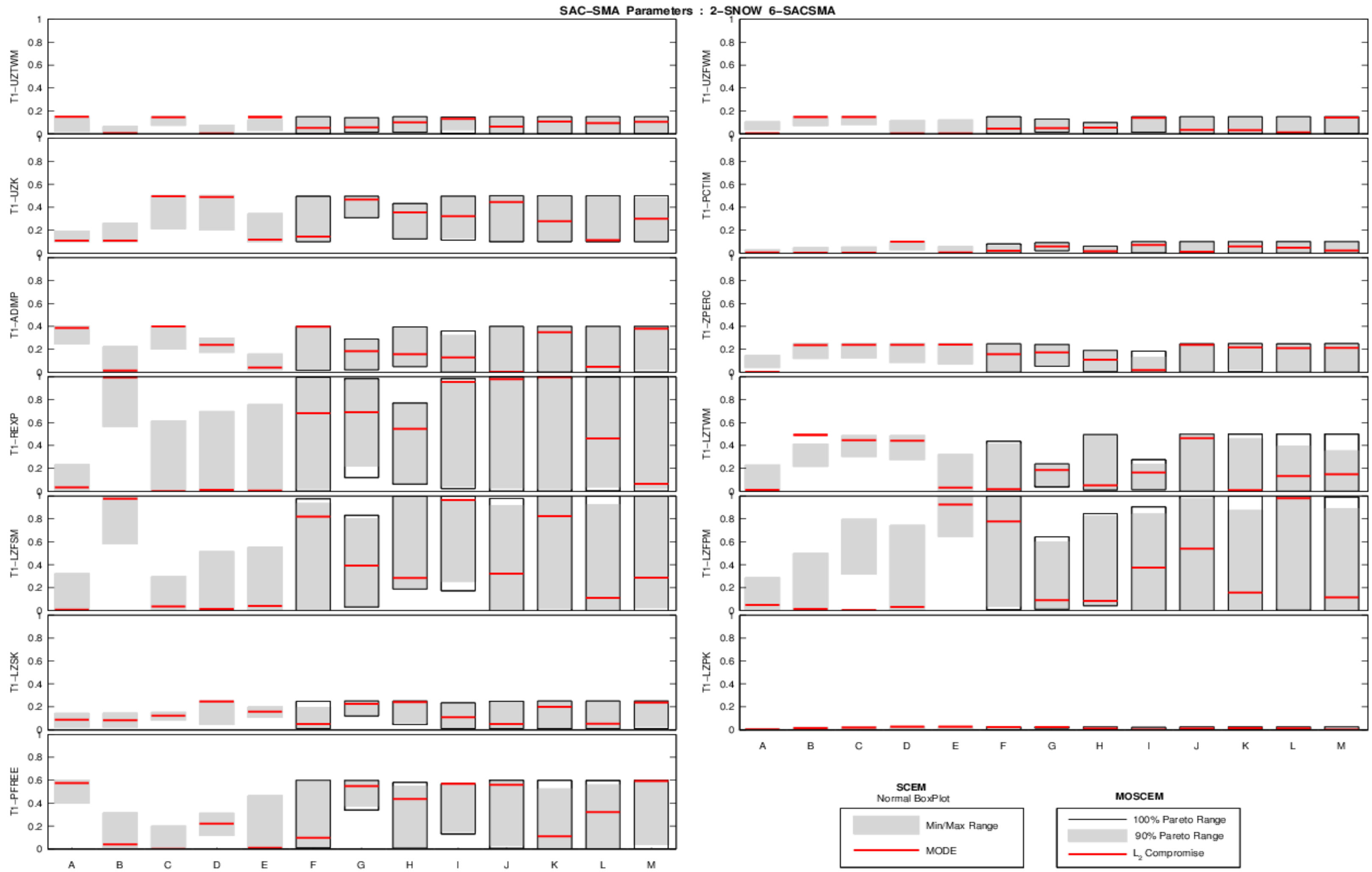

(b) Semi-Distributed SAC-SMA parameters – Signature 1.

Figure 6.2 Cont.

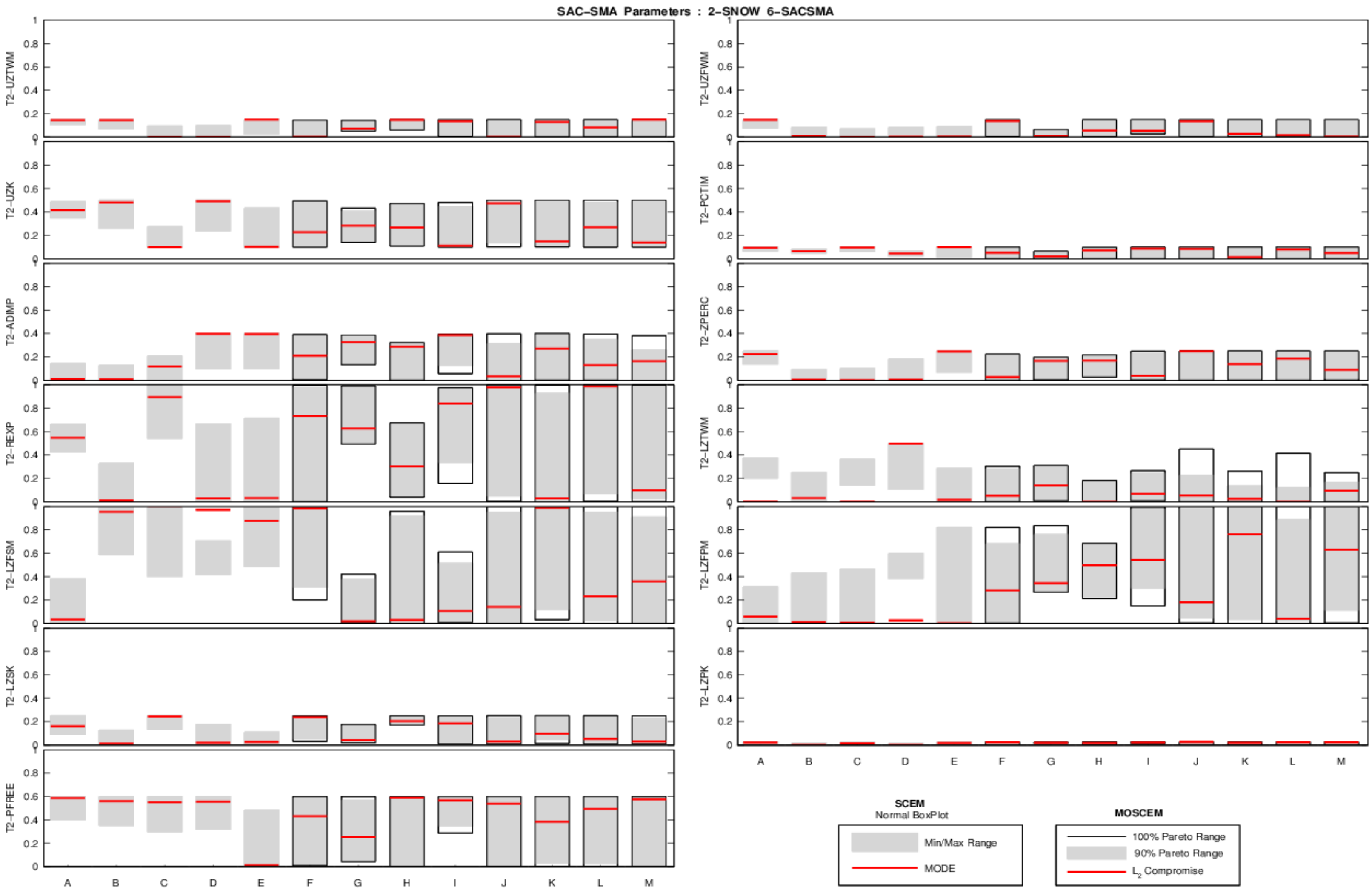

(b) Semi-Distributed SAC-SMA parameters – Signature 2.

Figure 6.2 Cont.

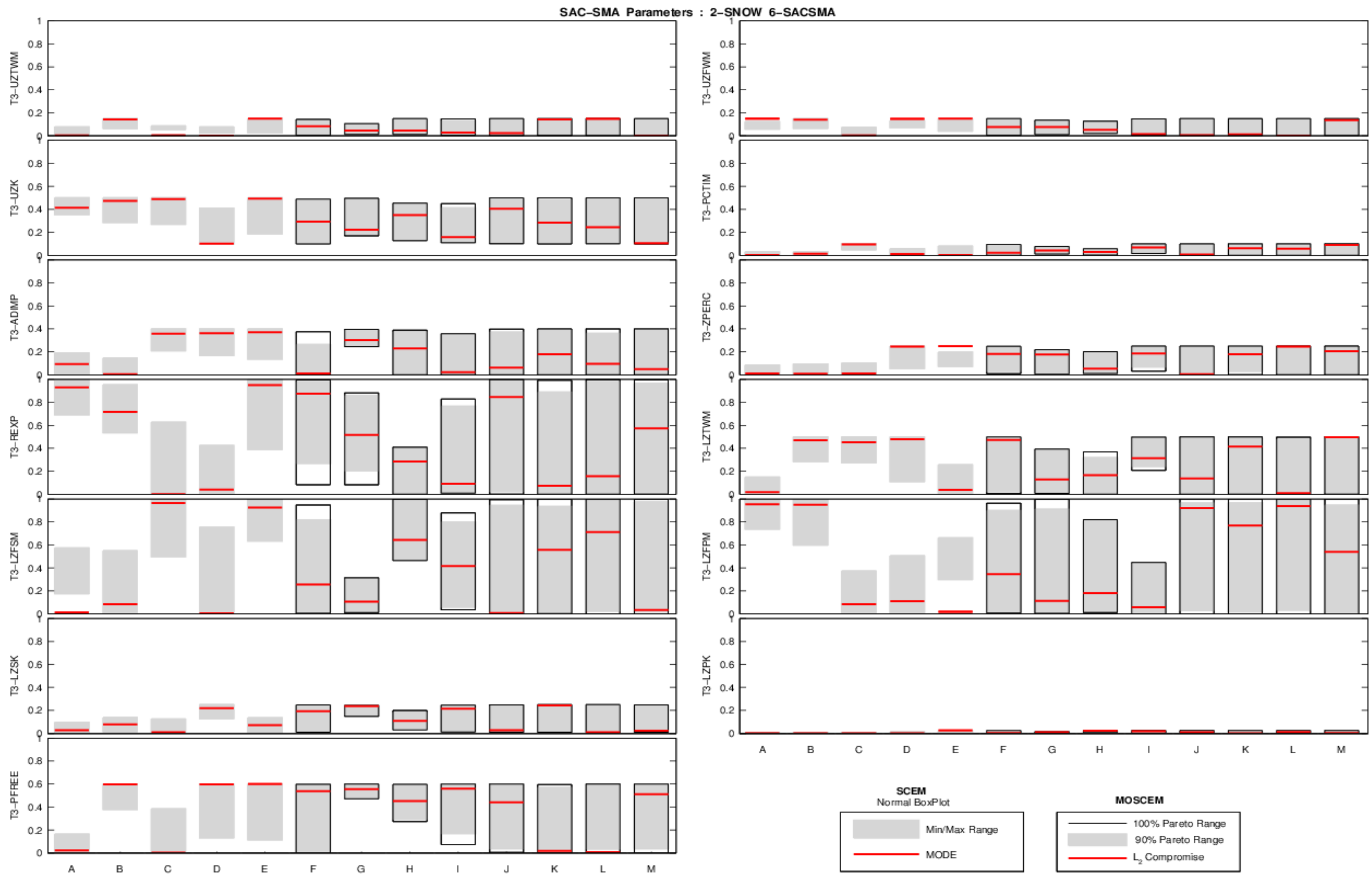

(b) Semi-Distributed SAC-SMA parameters – Signature 3.

Figure 6.2 Cont.

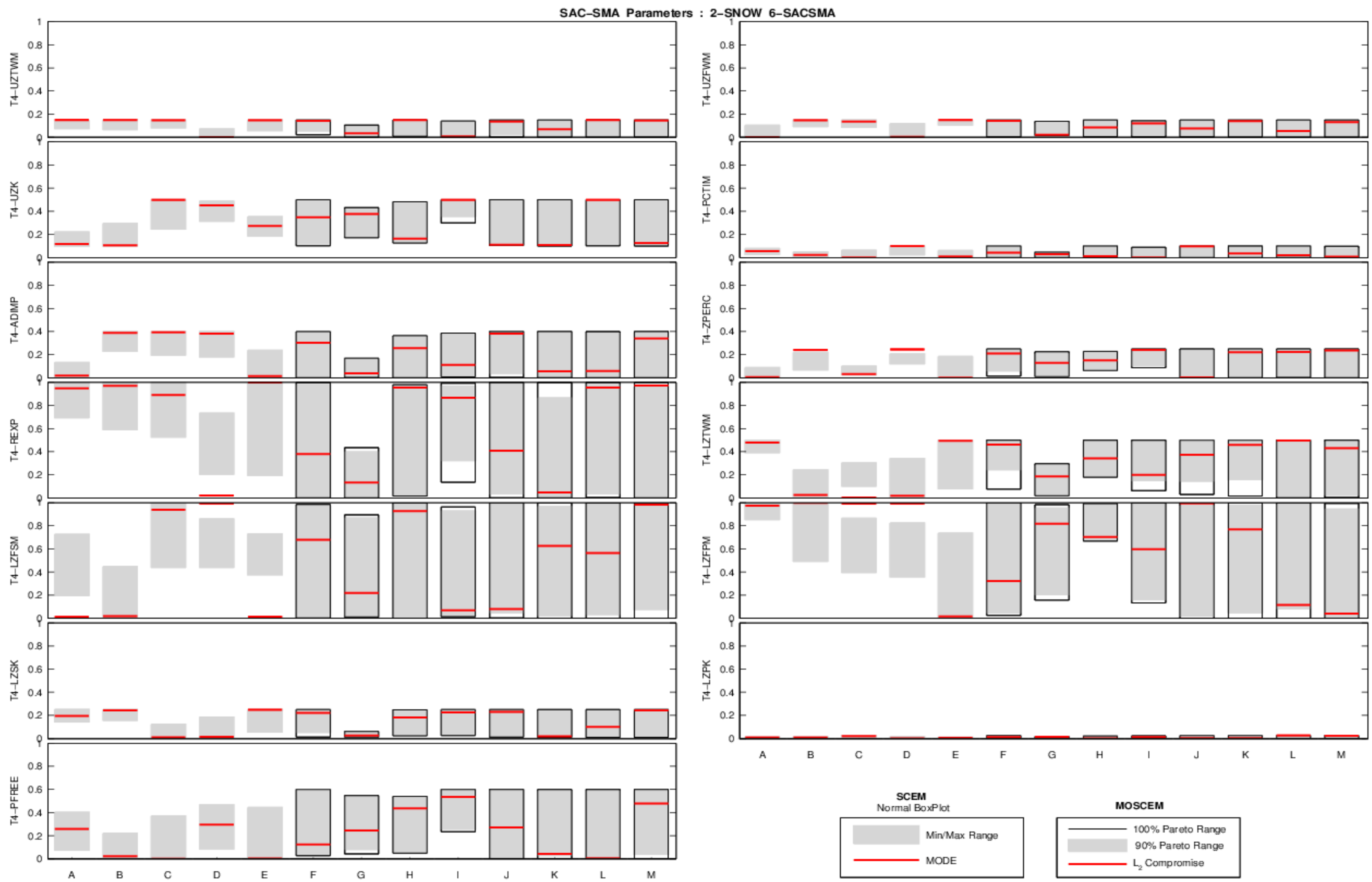

(b) Semi-Distributed SAC-SMA parameters – Signature 4.

Figure 6.2 Cont.

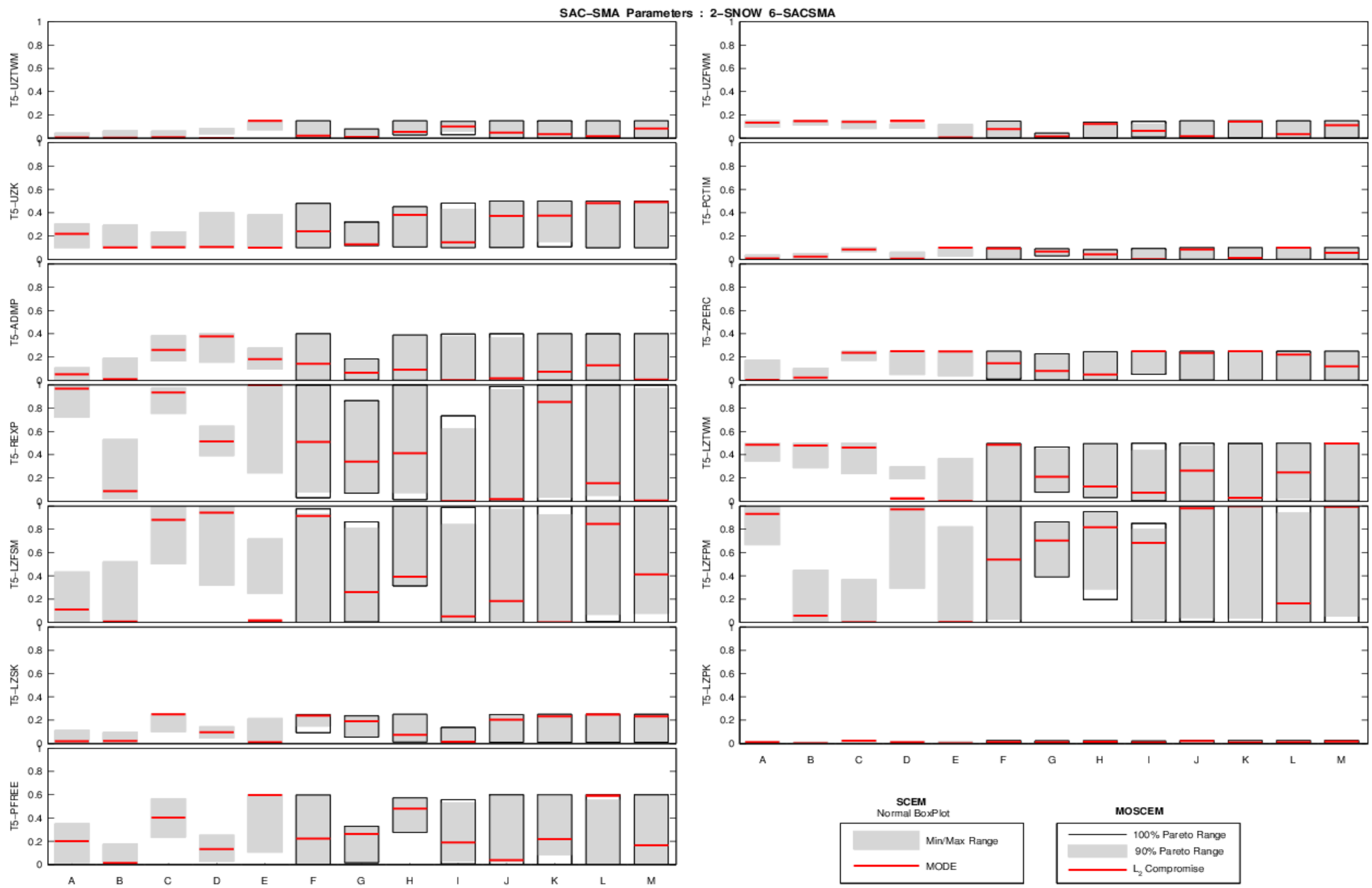

(b) Semi-Distributed SAC-SMA parameters – Signature 5.

Figure 6.2 Cont.

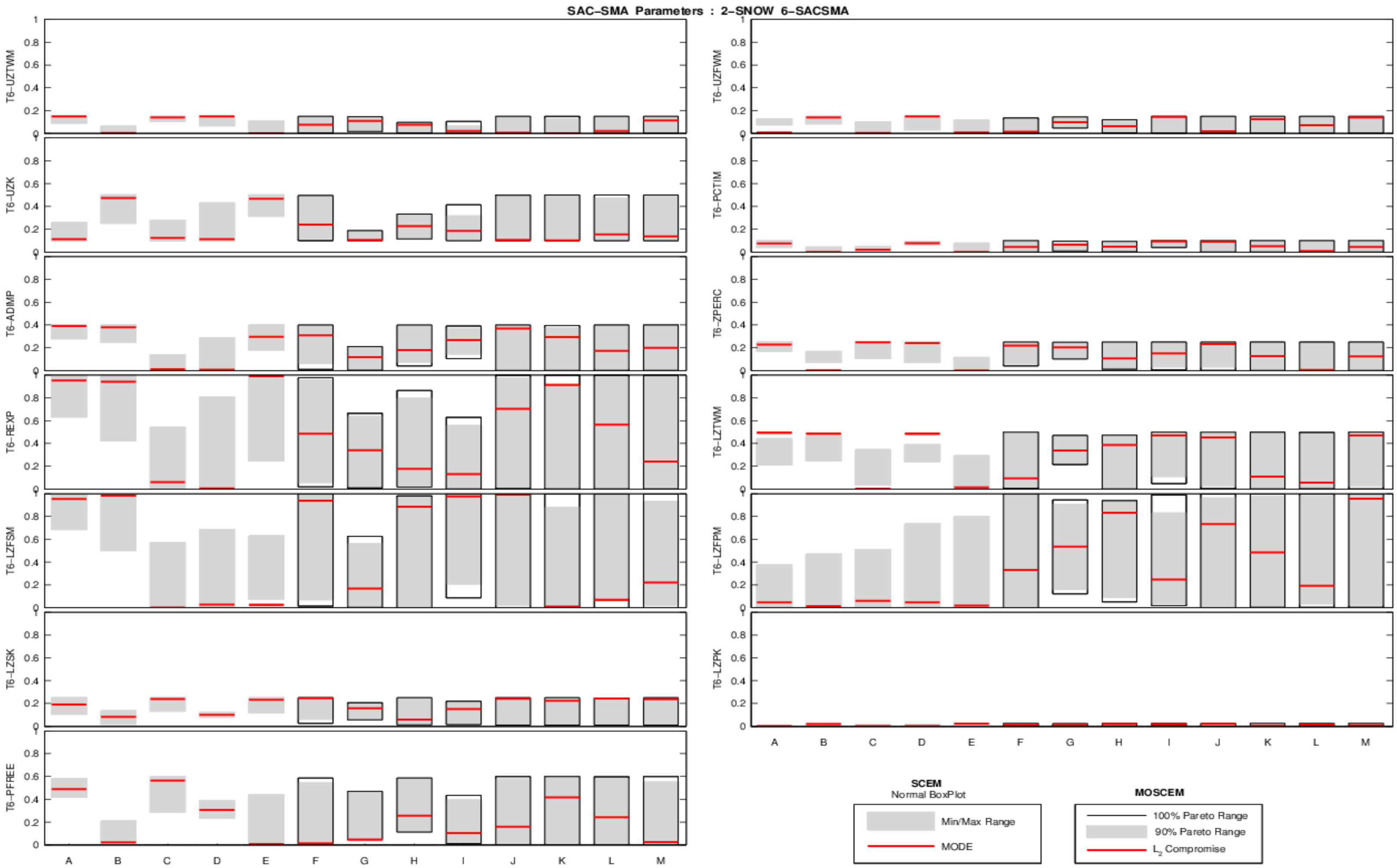

(b) Semi-Distributed SAC-SMA parameters – Signature 6.

Figure 6.2 Cont.

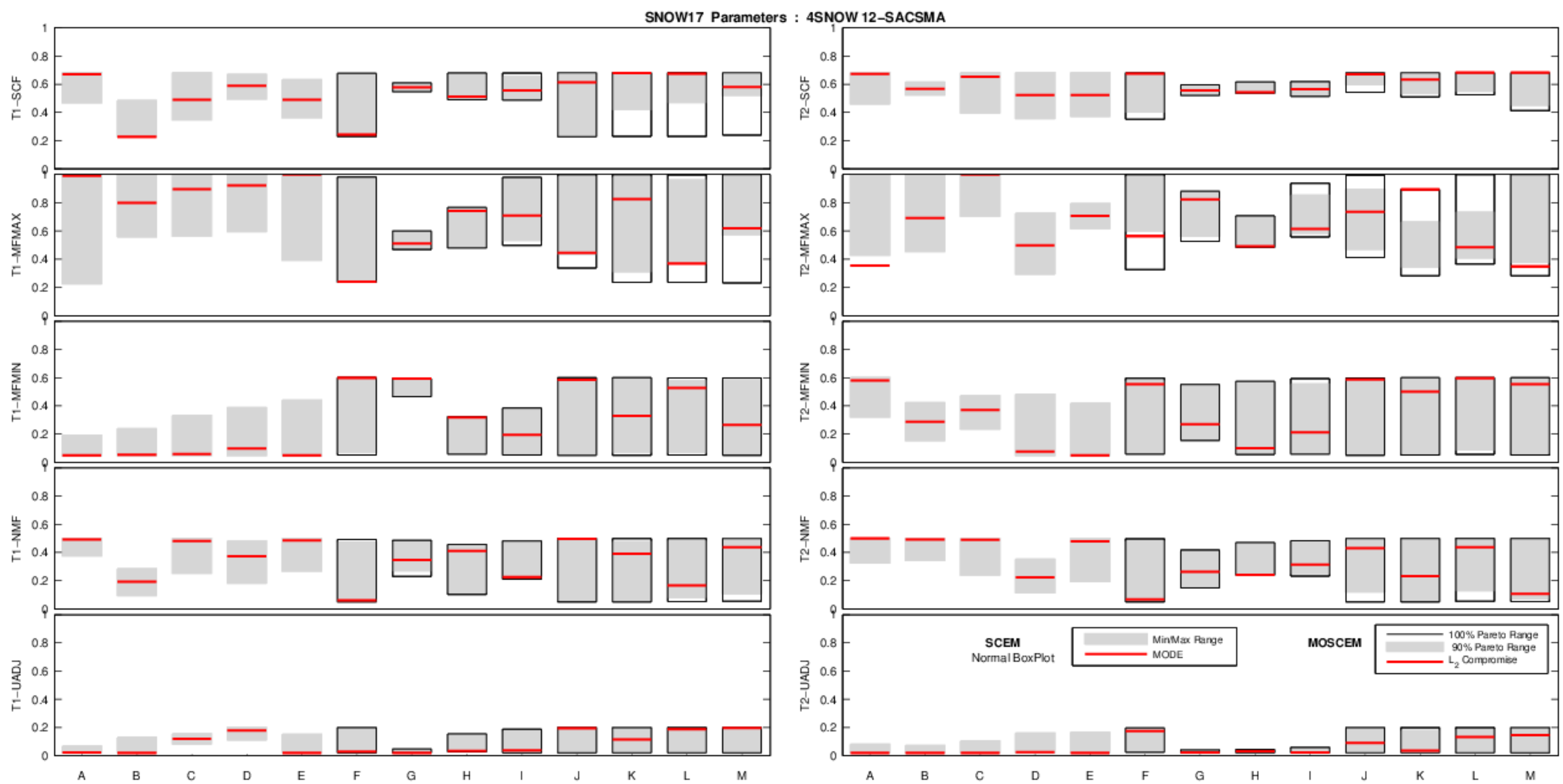

(a) Full-Distributed Snow 17 parameters – Signature 1 & 2.

Figure 6.3 Box plotting for Normalized Parameter Estimations of Full-Distributed HL-RDHM. For the single-criterion calibrations using SCEM, normal box plot is used so that the red line mode values for parameter distributions. For multi-criteria calibrations using MOSCEM the box plot is parameter ranges of 100 percentile, gray box is 90 percentile ranges of optimized parameters and red line represents compromised solutions.

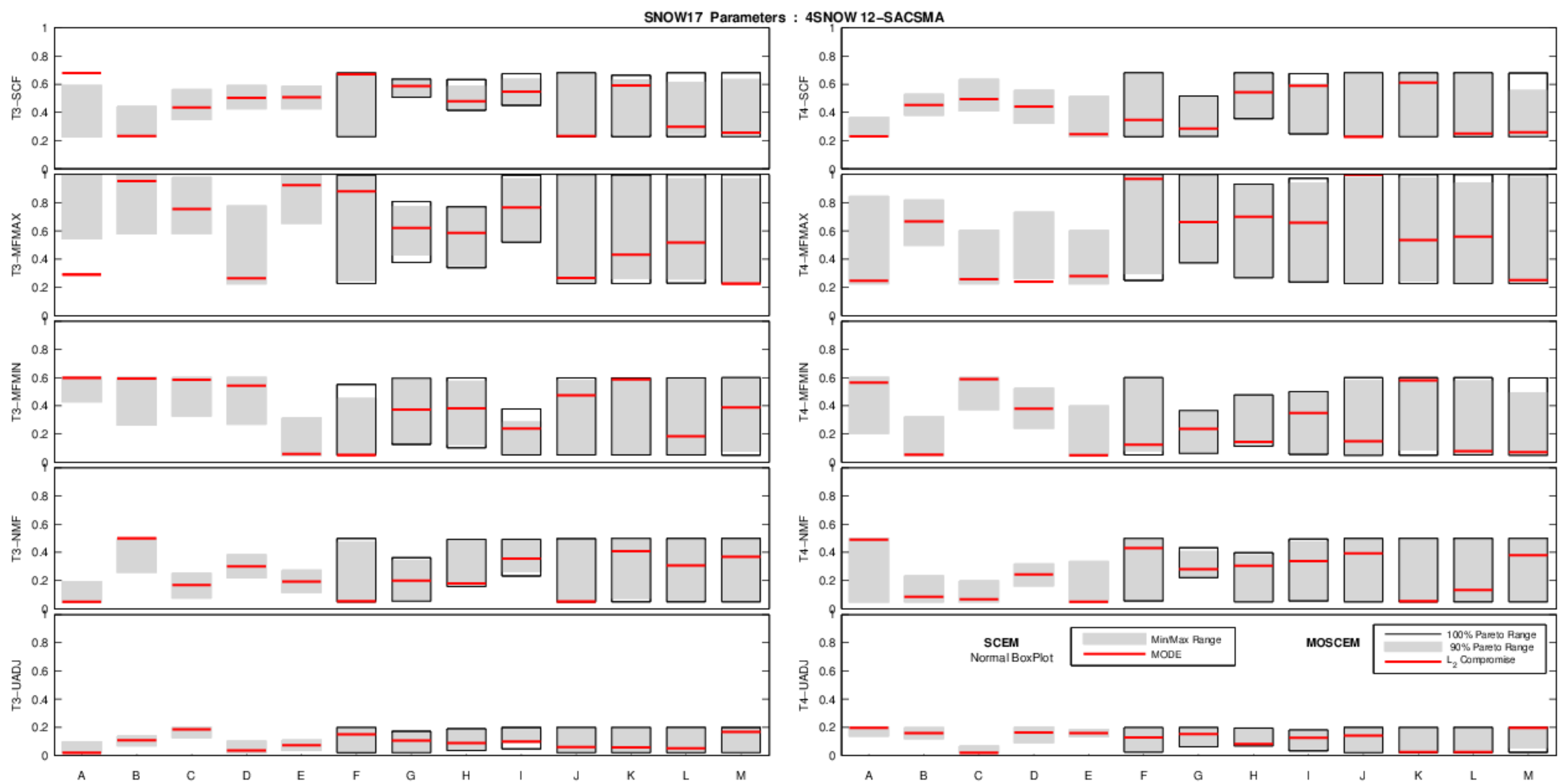

(a) Full-Distributed Snow 17 parameters – Signature 3 & 4.

Figure 6.3 Cont.

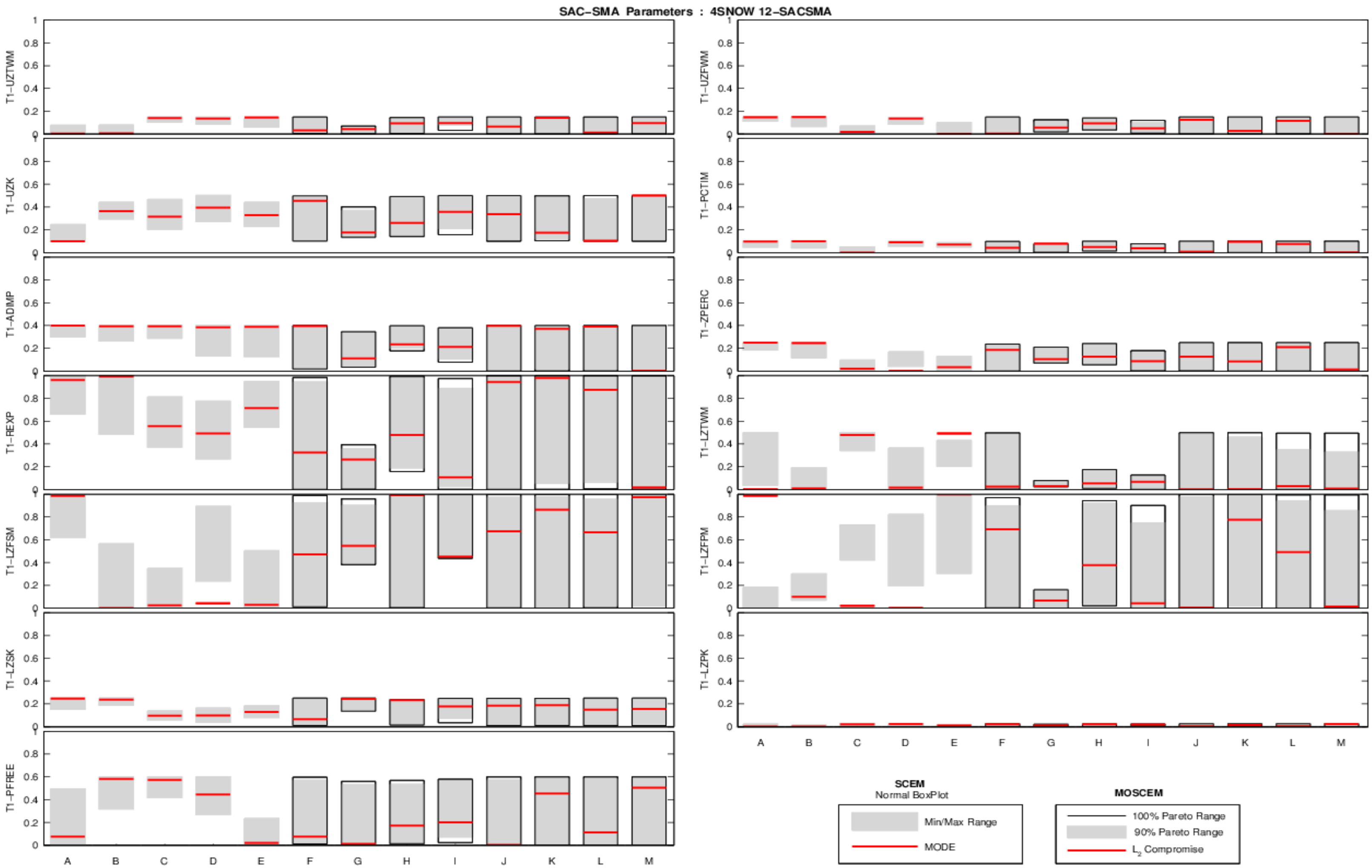

(b) Full-Distributed SAC-SMA parameters – Signature 1.

Figure 6.3 Cont.

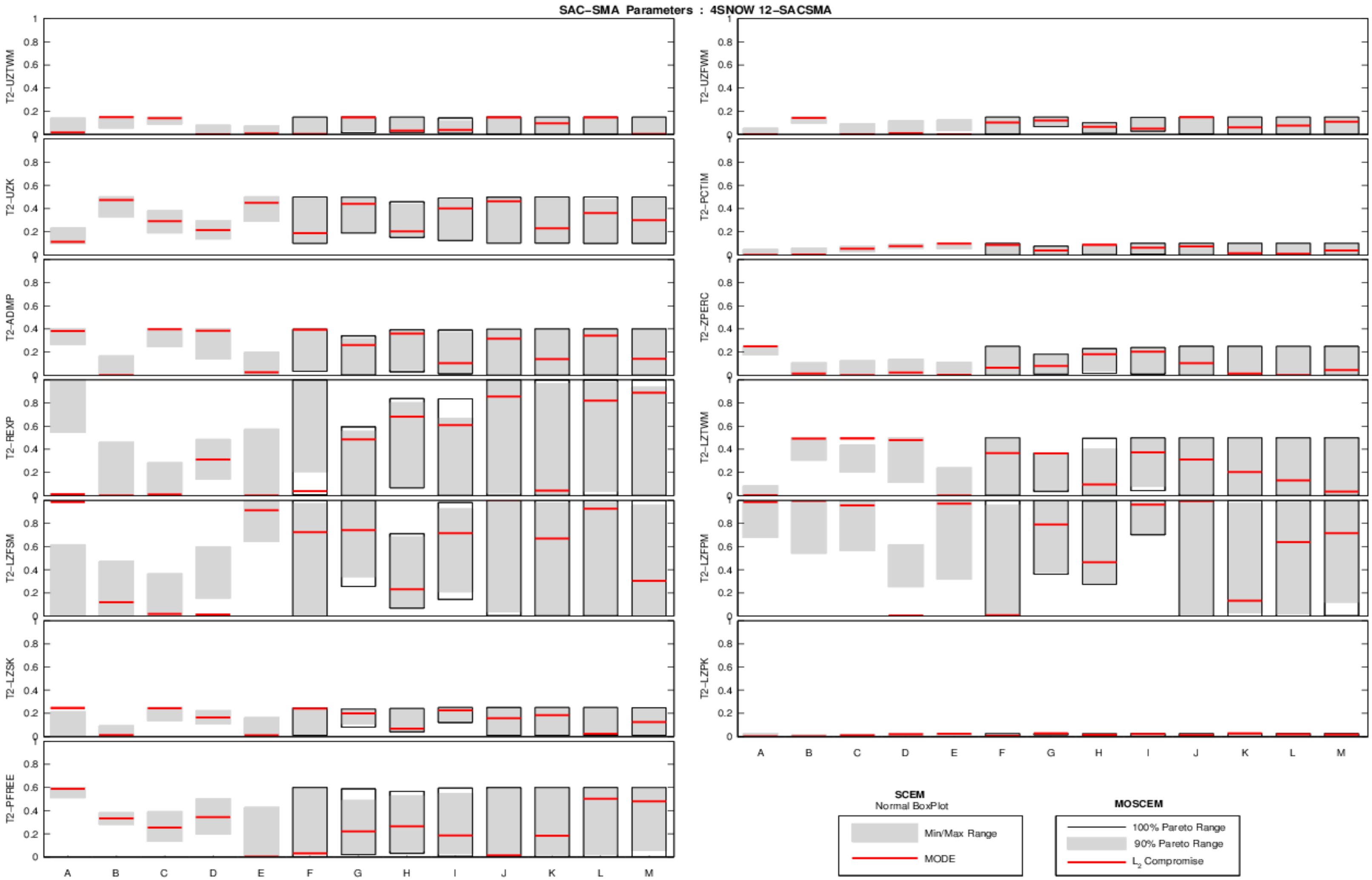

(b) Full-Distributed SAC-SMA parameters – Signature 2.

Figure 6.3 Cont.

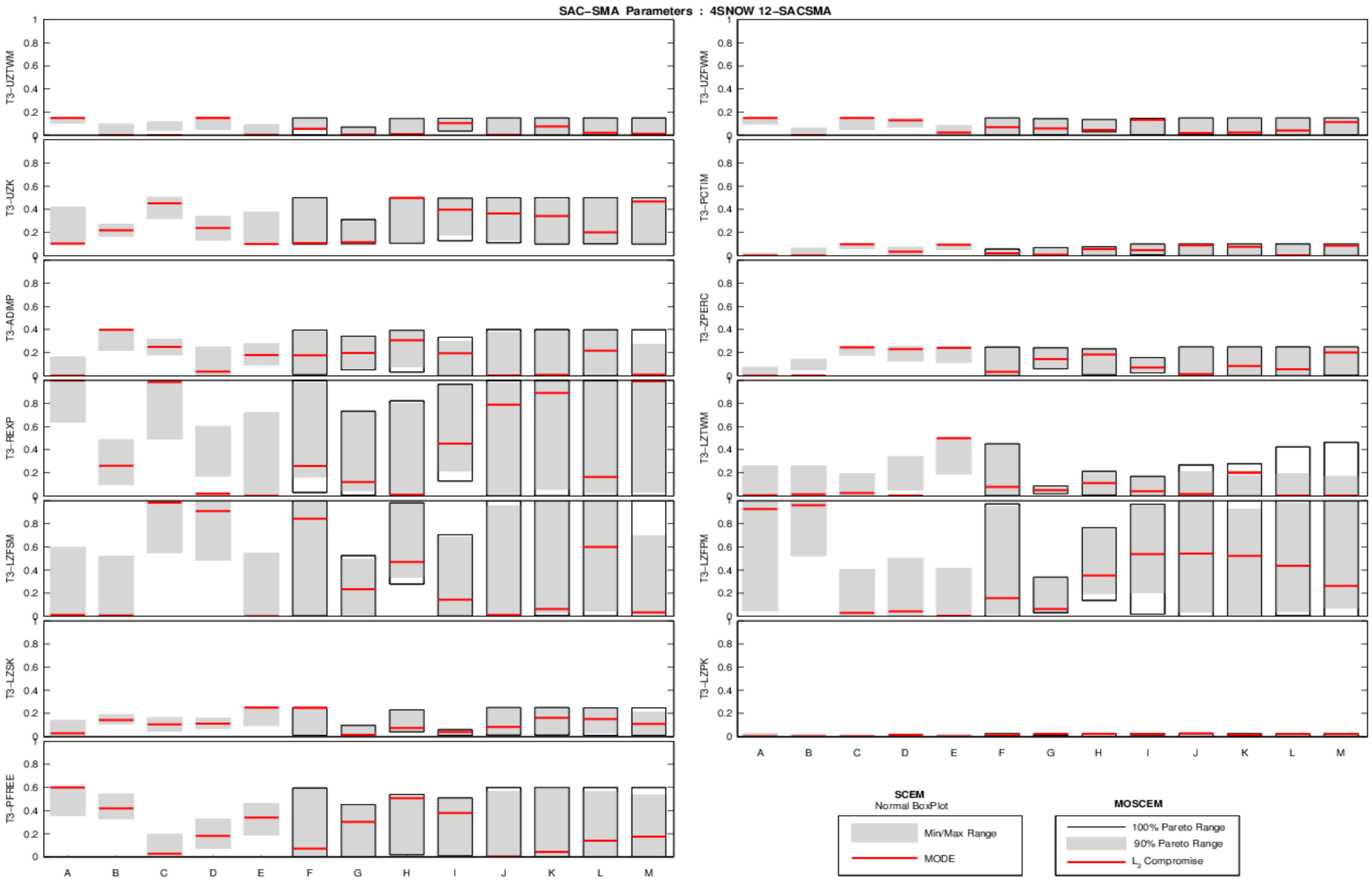

(b) Full-Distributed SAC-SMA parameters – Signature 3.

Figure 6.3 Cont.

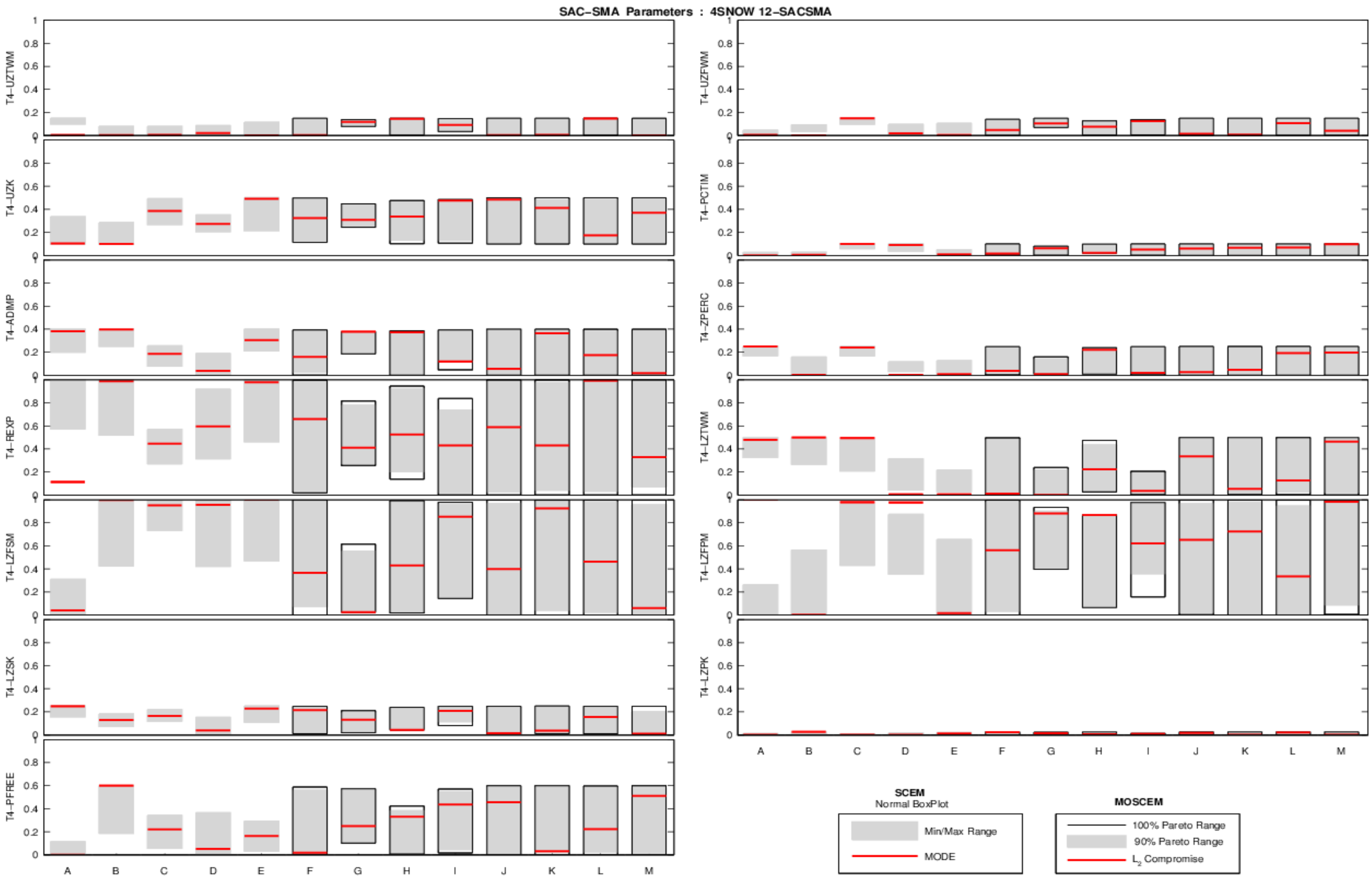

(b) Full-Distributed SAC-SMA parameters – Signature 4.

Figure 6.3 Cont.

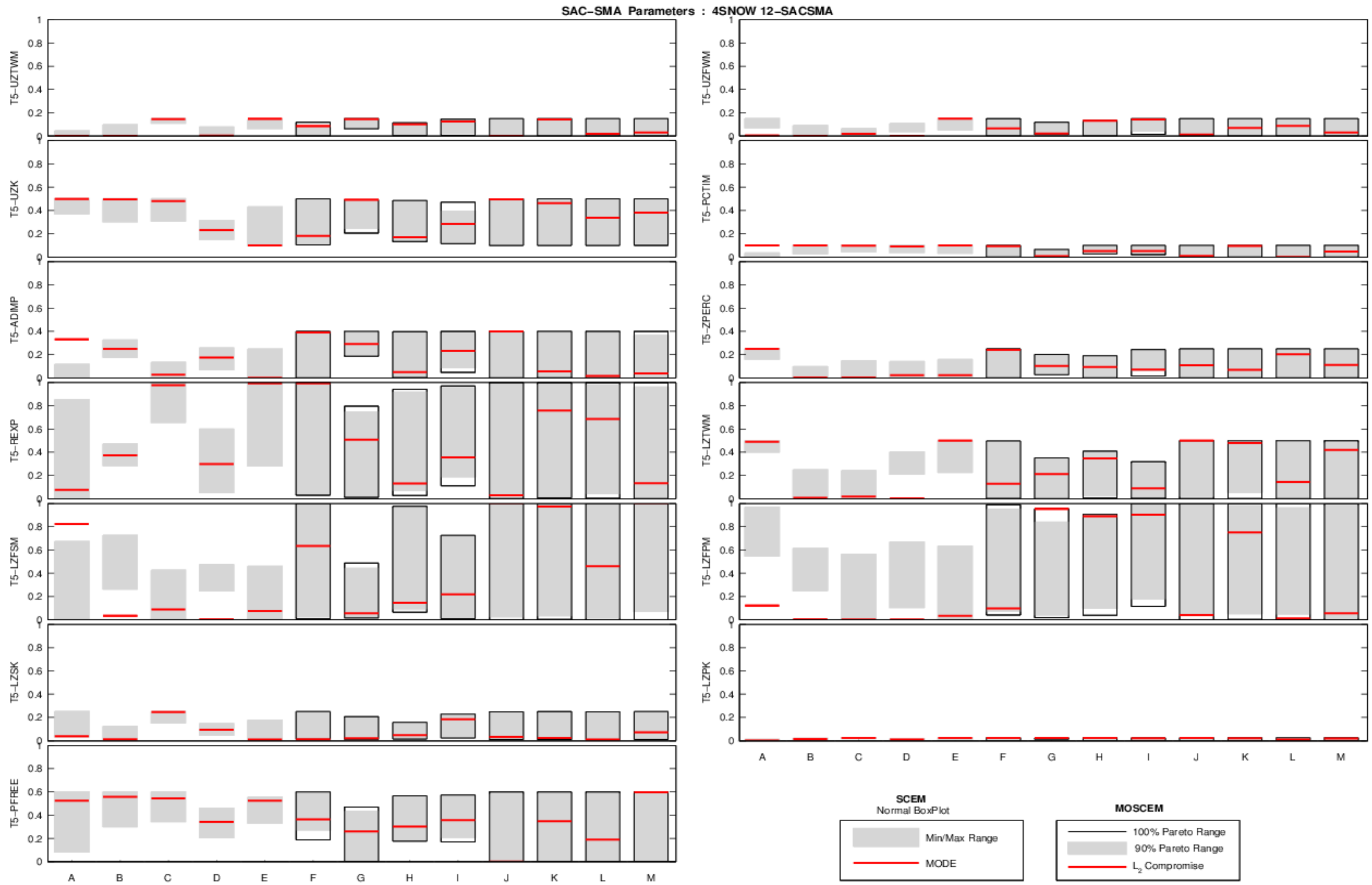

(b) Full-Distributed SAC-SMA parameters – Signature 5.

Figure 6.3 Cont.

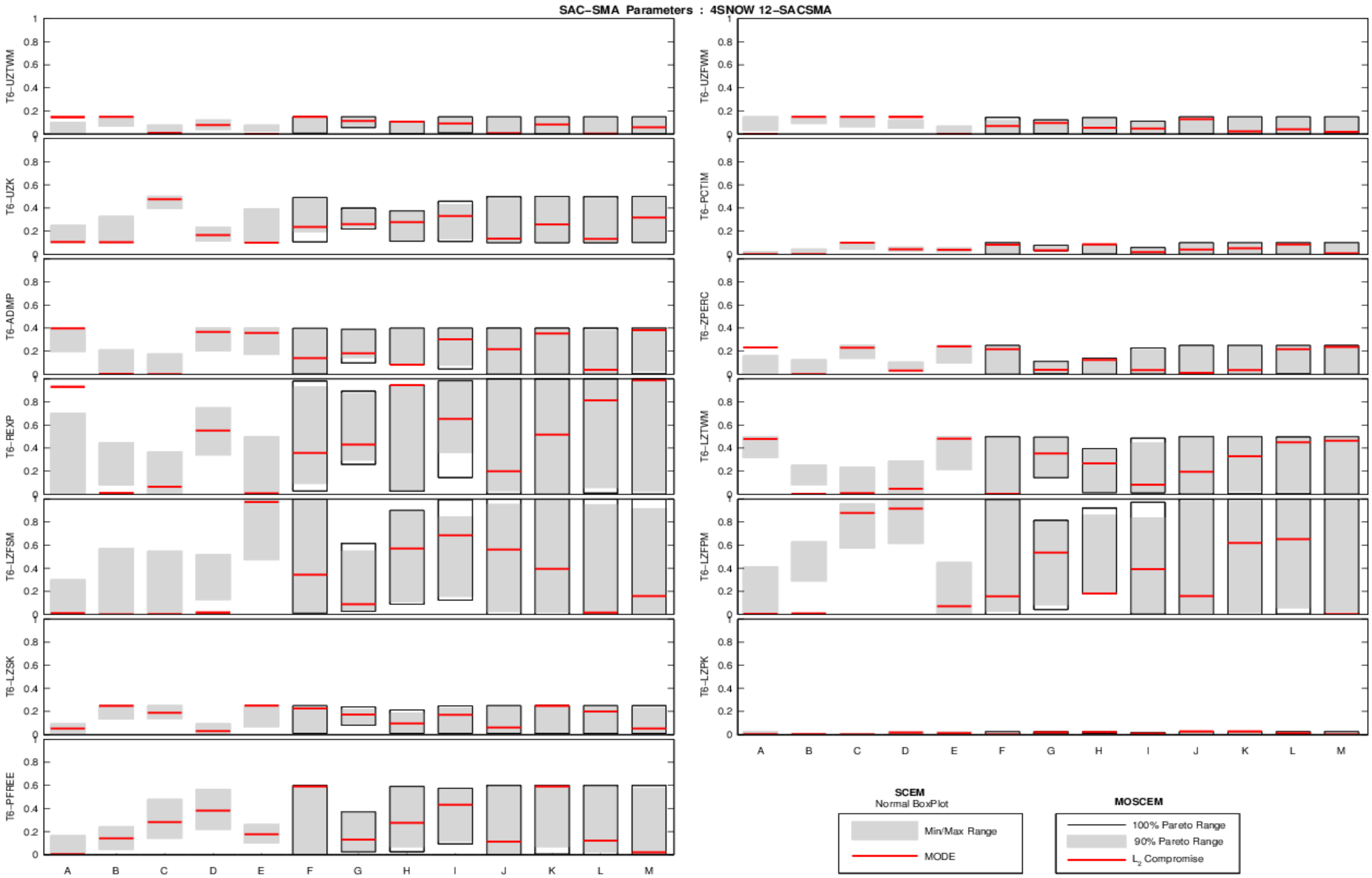

(b) Full-Distributed SAC-SMA parameters – Signature 6.

Figure 6.3 Cont.

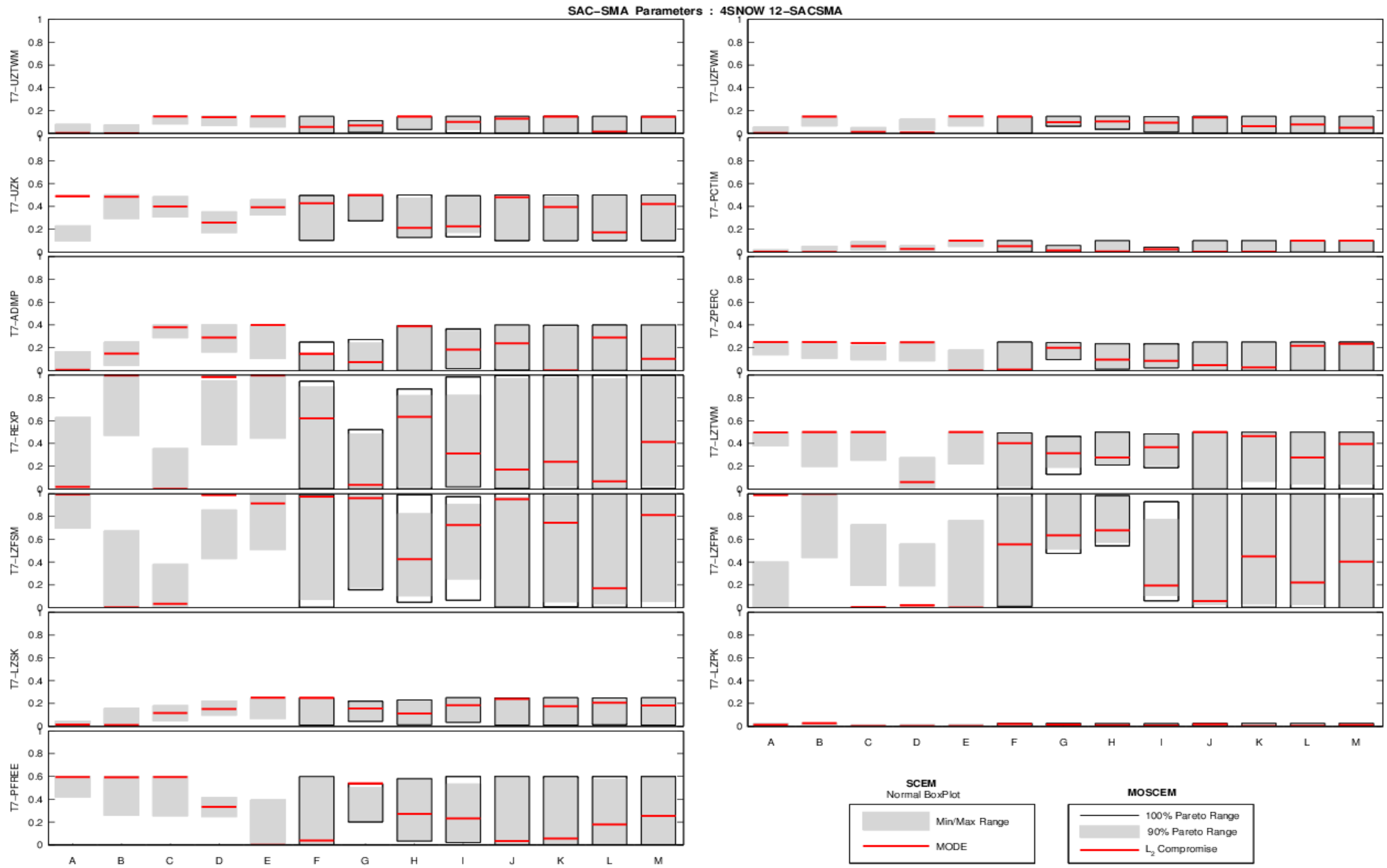

(b) Full-Distributed SAC-SMA parameters – Signature 7.

Figure 6.3 Cont.

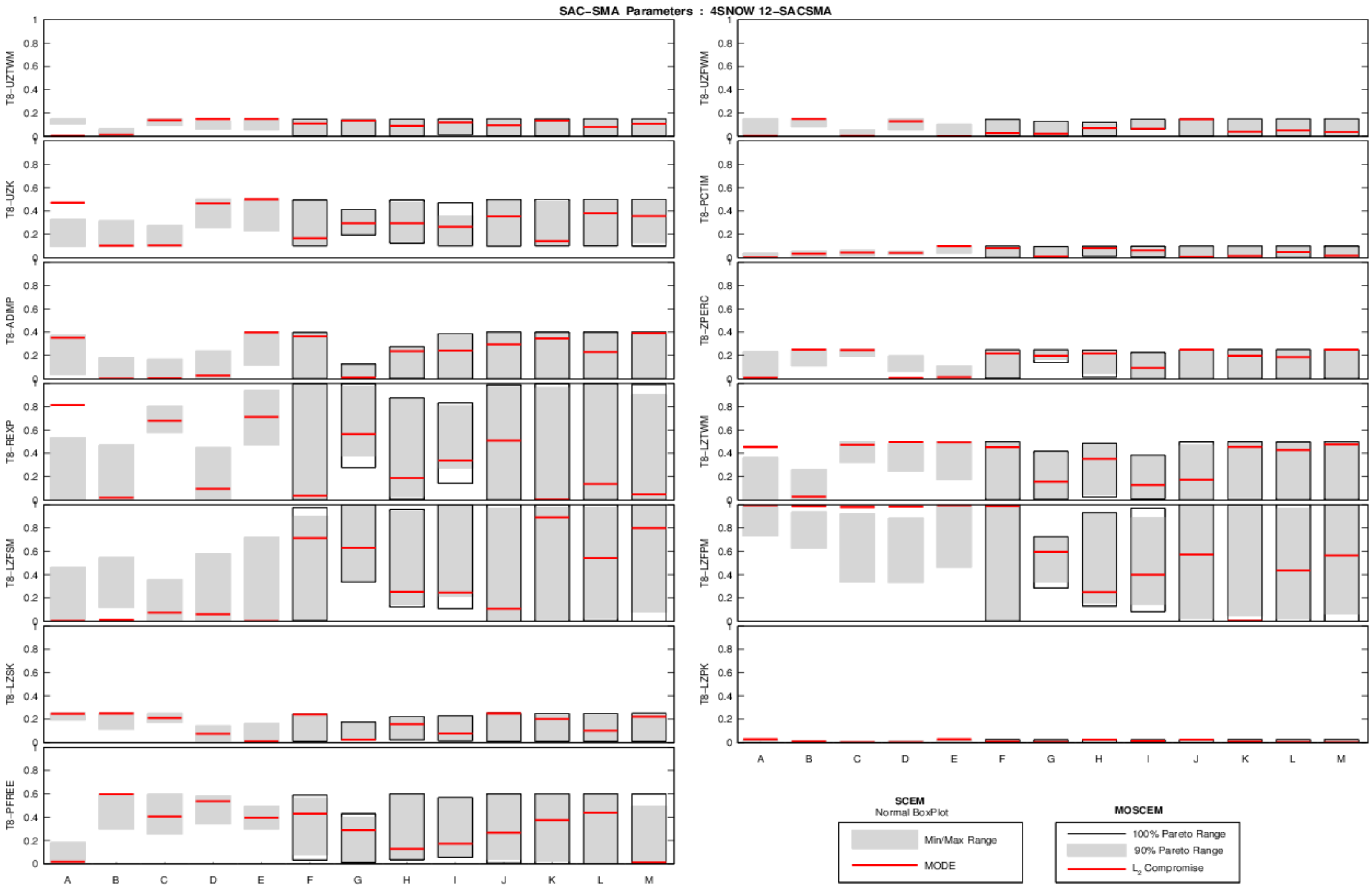

(b) Full-Distributed SAC-SMA parameters – Signature 8.

Figure 6.3 Cont.

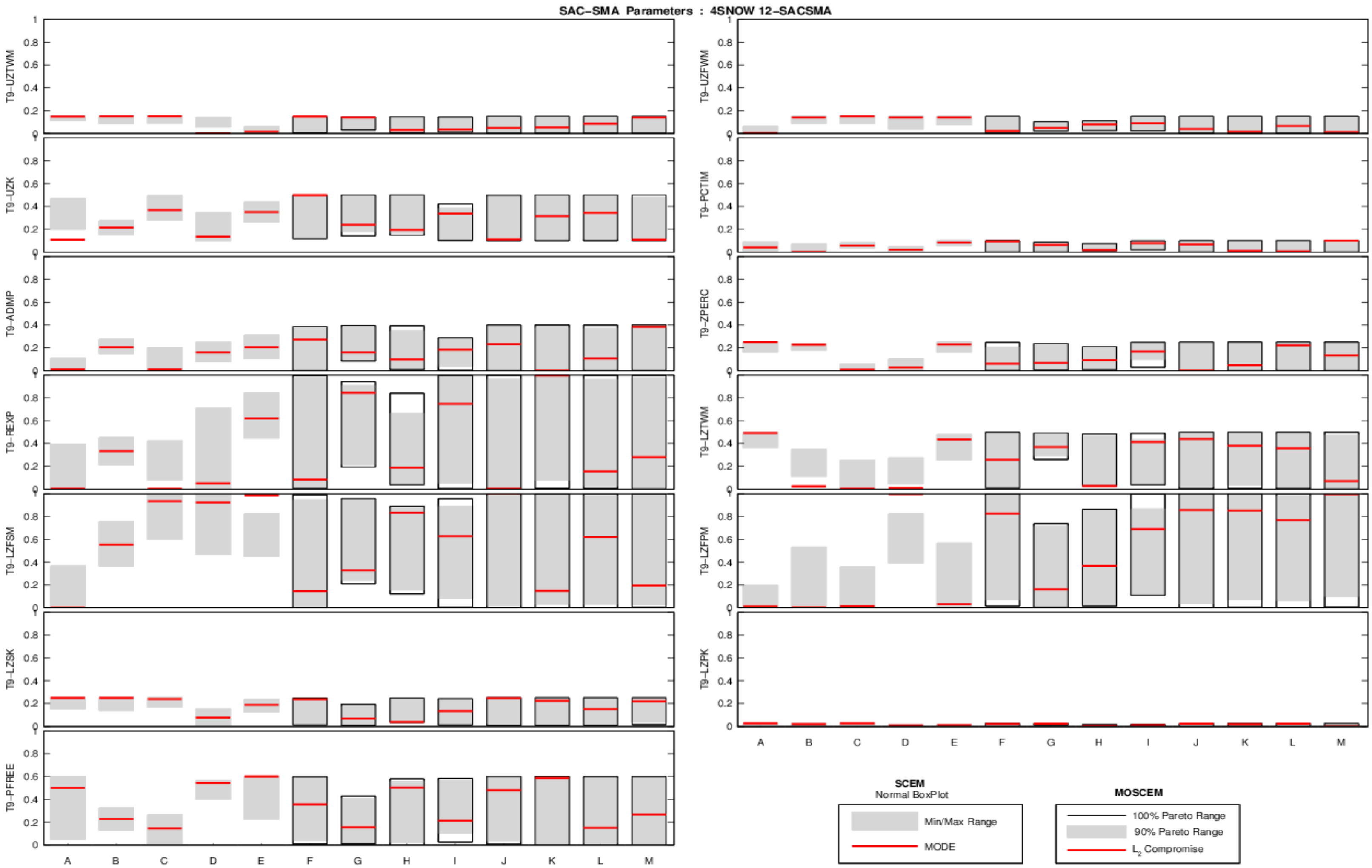

(b) Full-Distributed SAC-SMA parameters – Signature 9.

Figure 6.3 Cont.

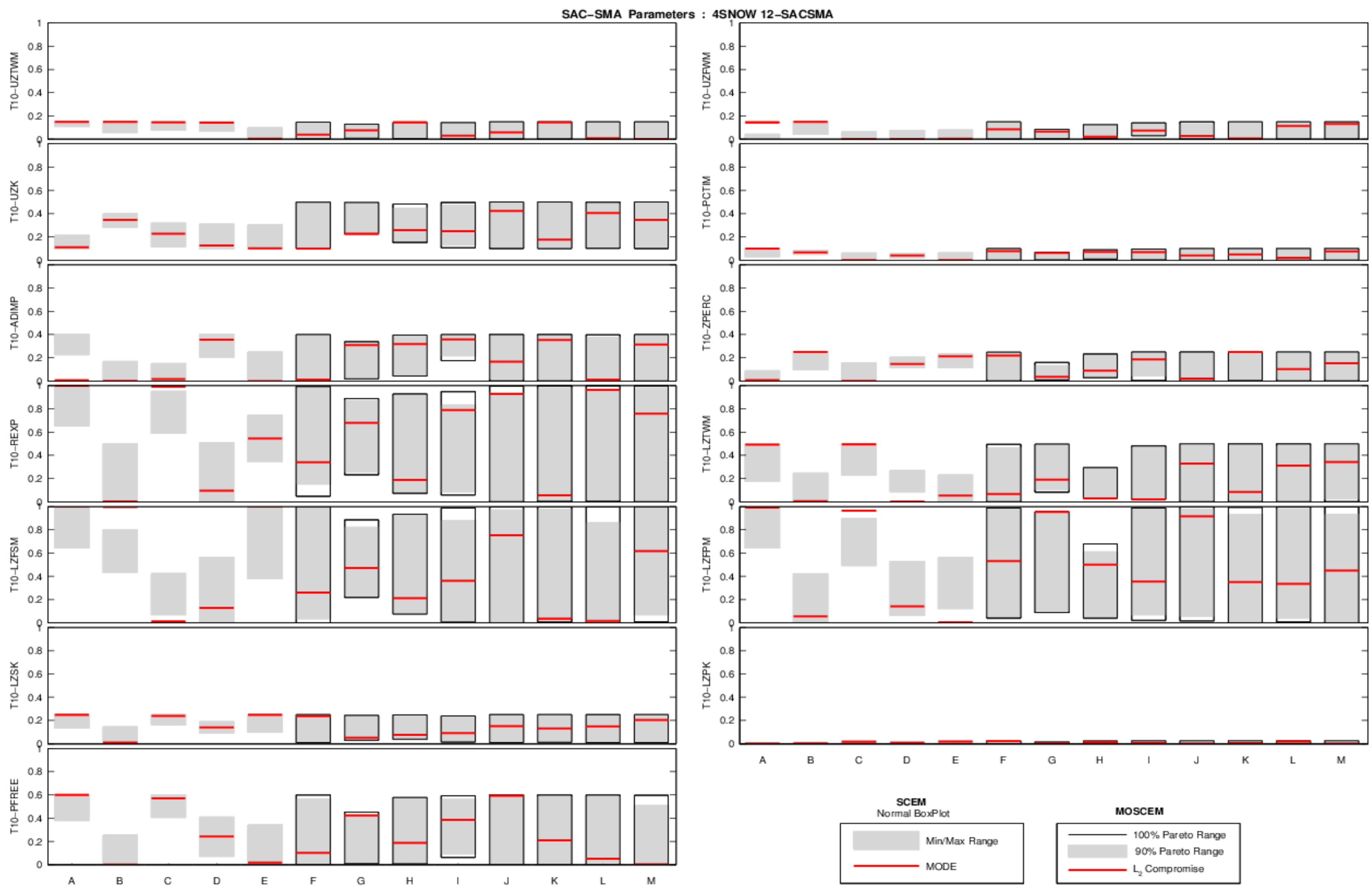

(b) Full-Distributed SAC-SMA parameters – Signature 10.

Figure 6.3 Cont.

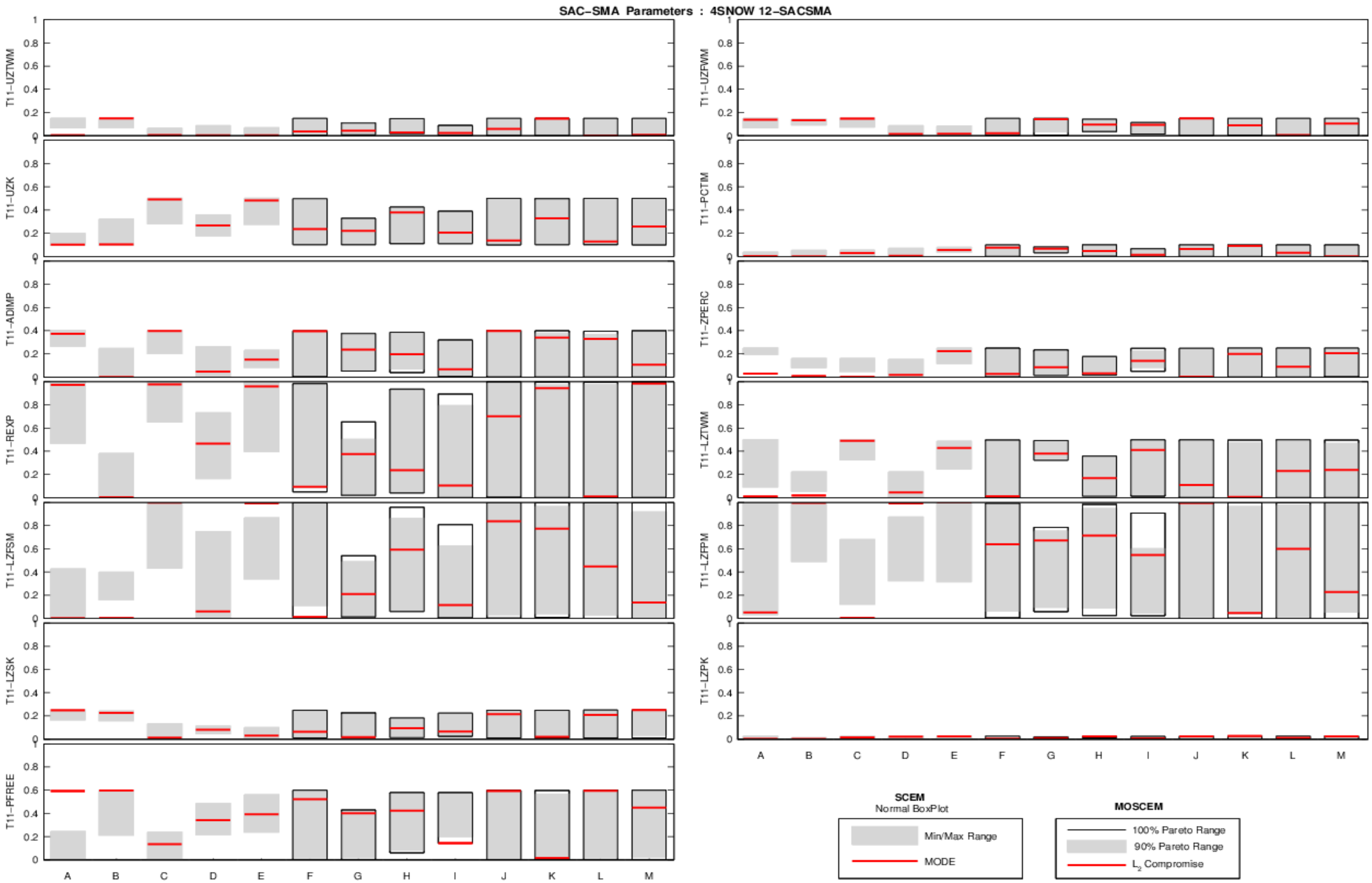

(b) Full-Distributed SAC-SMA parameters – Signature 11.

Figure 6.3 Cont.

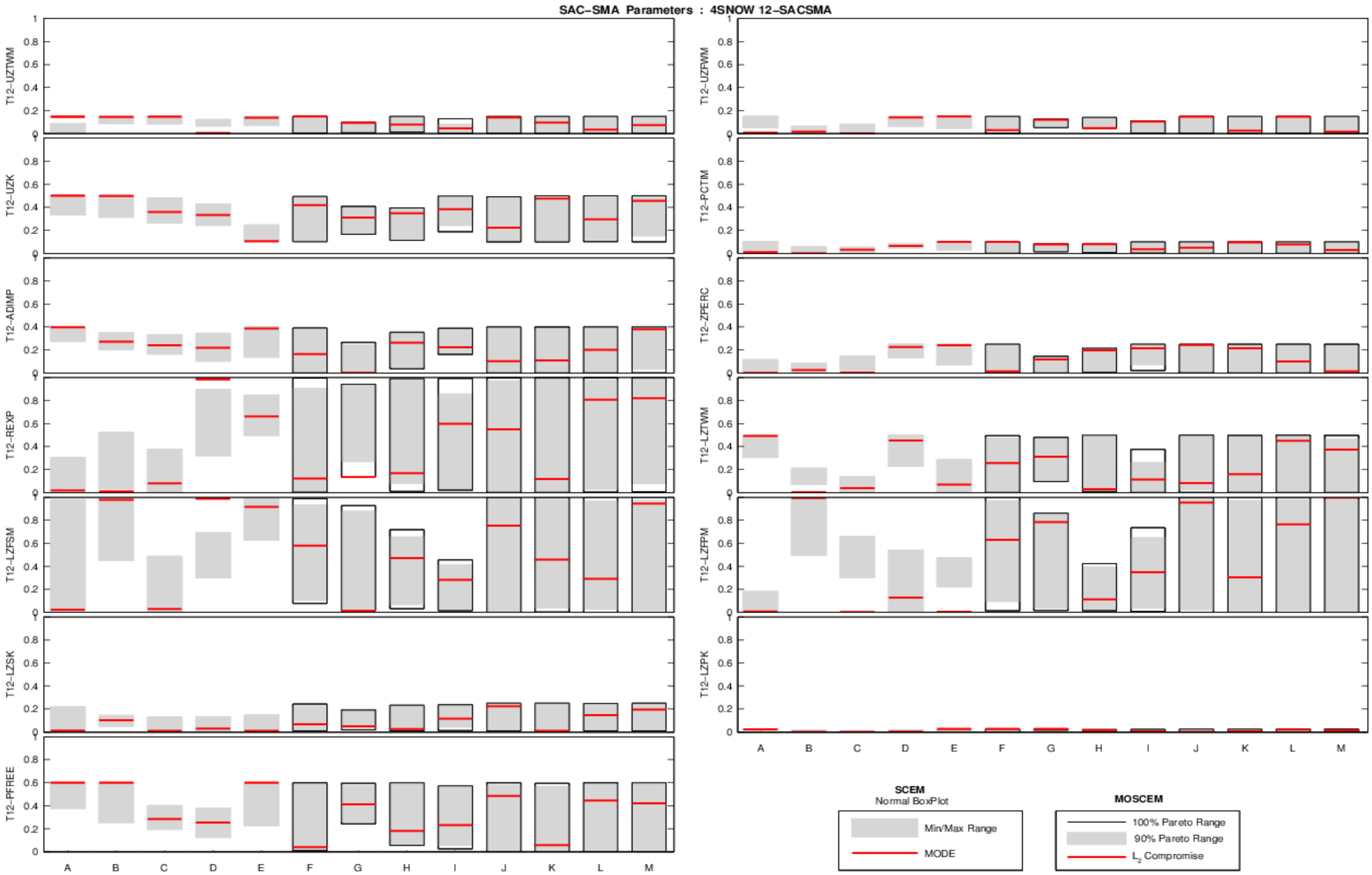

Full-Distributed SAC-SMA parameters – Signature 12.

Figure 6.3 Cont.

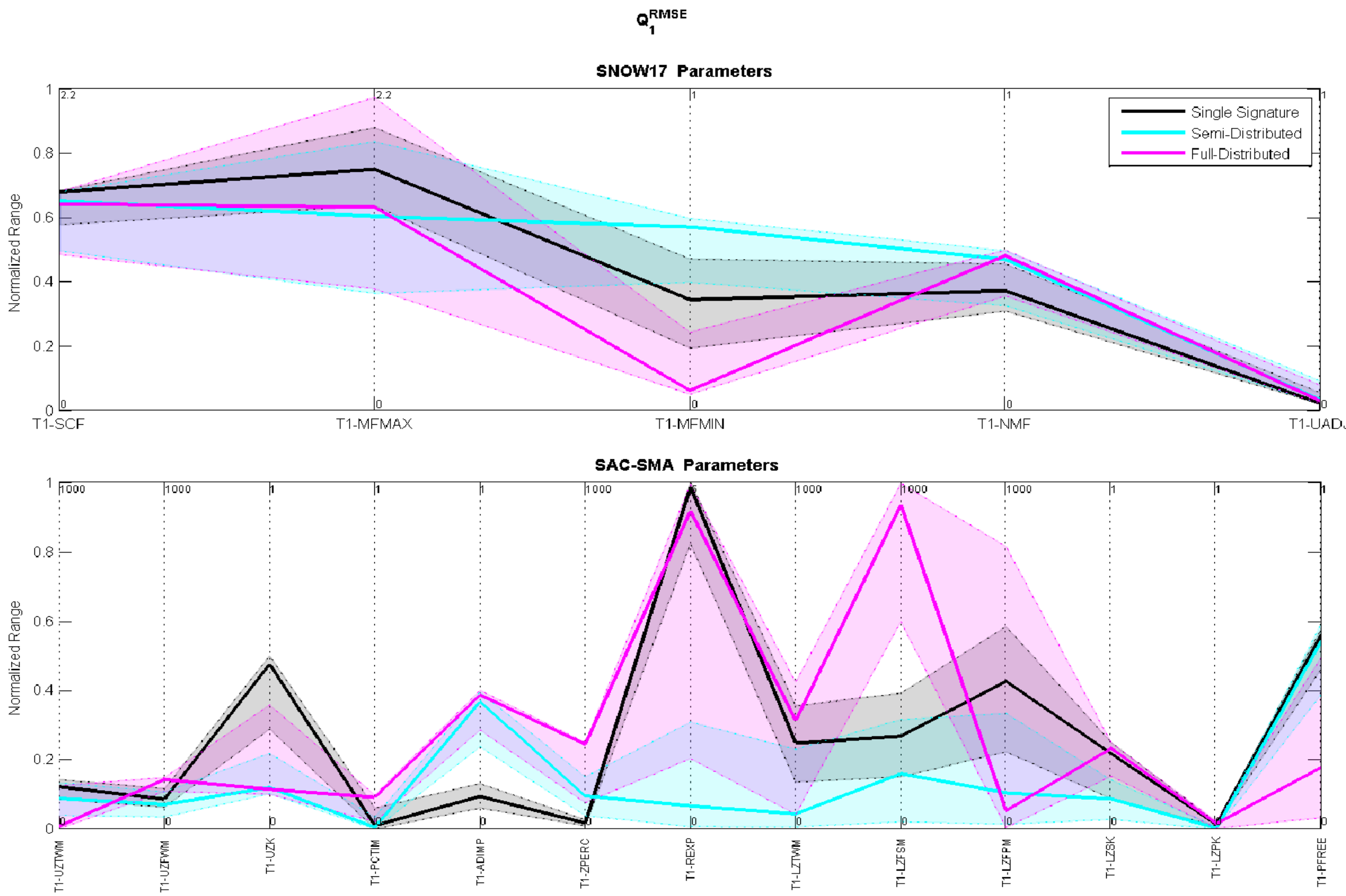

(a) Single-criterion Calibrations - Q_1^{RMSE}

Figure 6.4 The parallel plot for parameters of Signature 1 (Type 1) in HL-RDHM depended on the degree of distributions. The black, blue, and red transparencies are single-signature, semi-, and full-distributed models. The thick lines depict mode values of parameter distributions for (a) Single-criterion calibrations and compromised solutions for (b) multi-criteria calibrations.

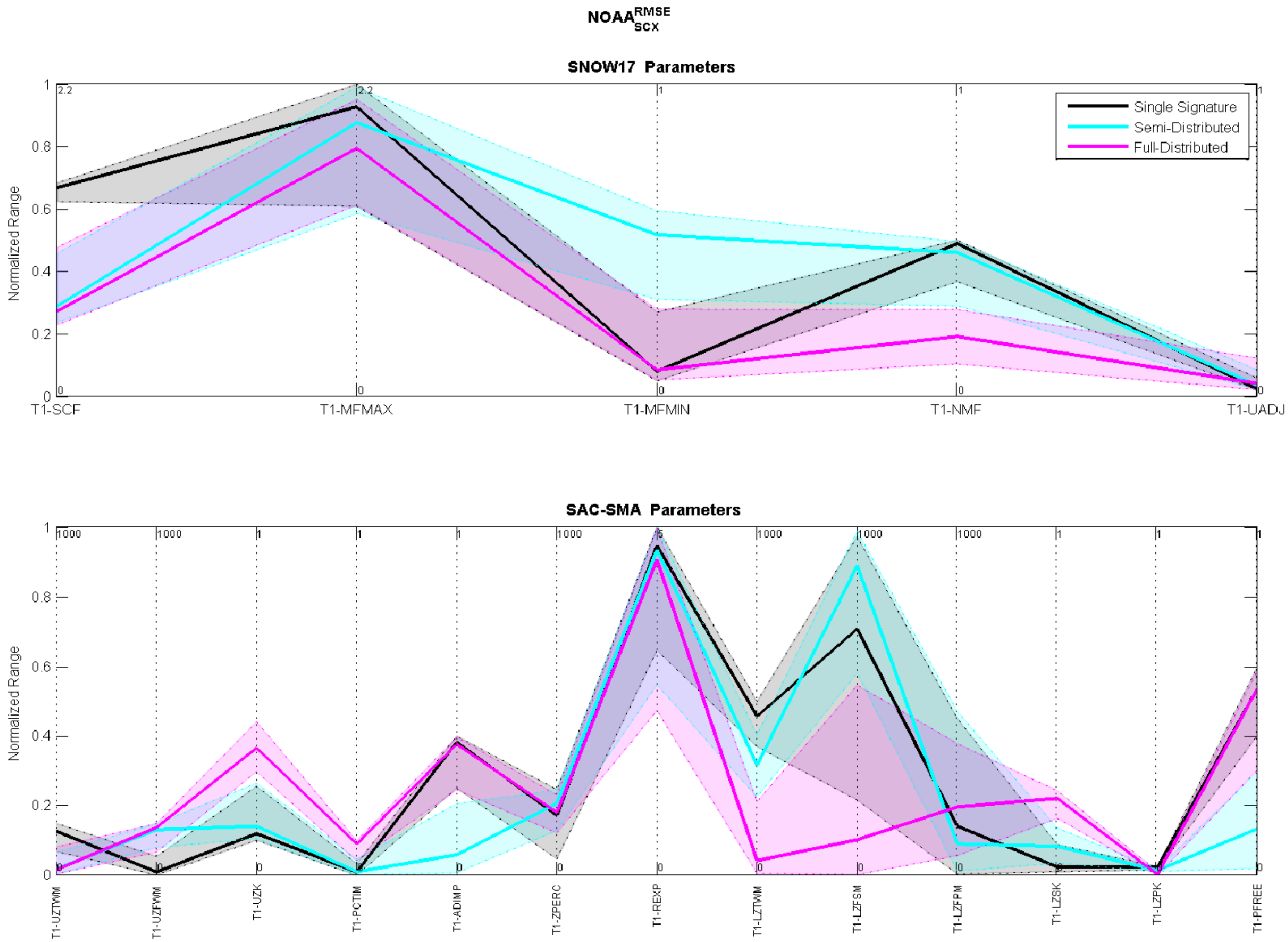

(a) Single-criterion Calibrations - $\mathrm{NOAA}_{\mathrm{SCX}}^{\mathrm{RMSE}}$.

Figure 6.4 Cont.

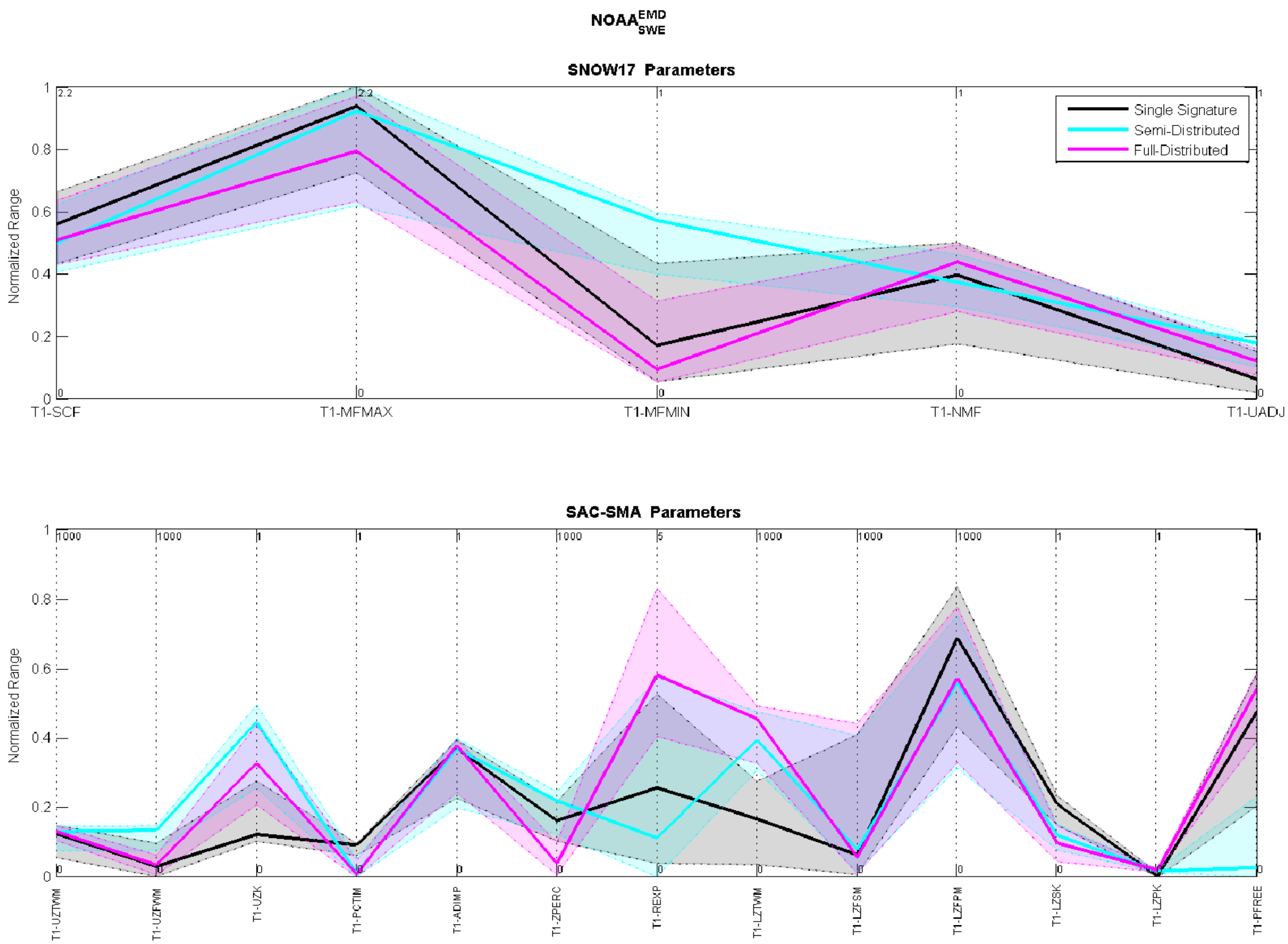

(a) Single-criterion Calibrations - $\mathrm{NOAA}_{\mathrm{SWE}}^{\mathrm{EMD}}$.

Figure 6.4 Cont.

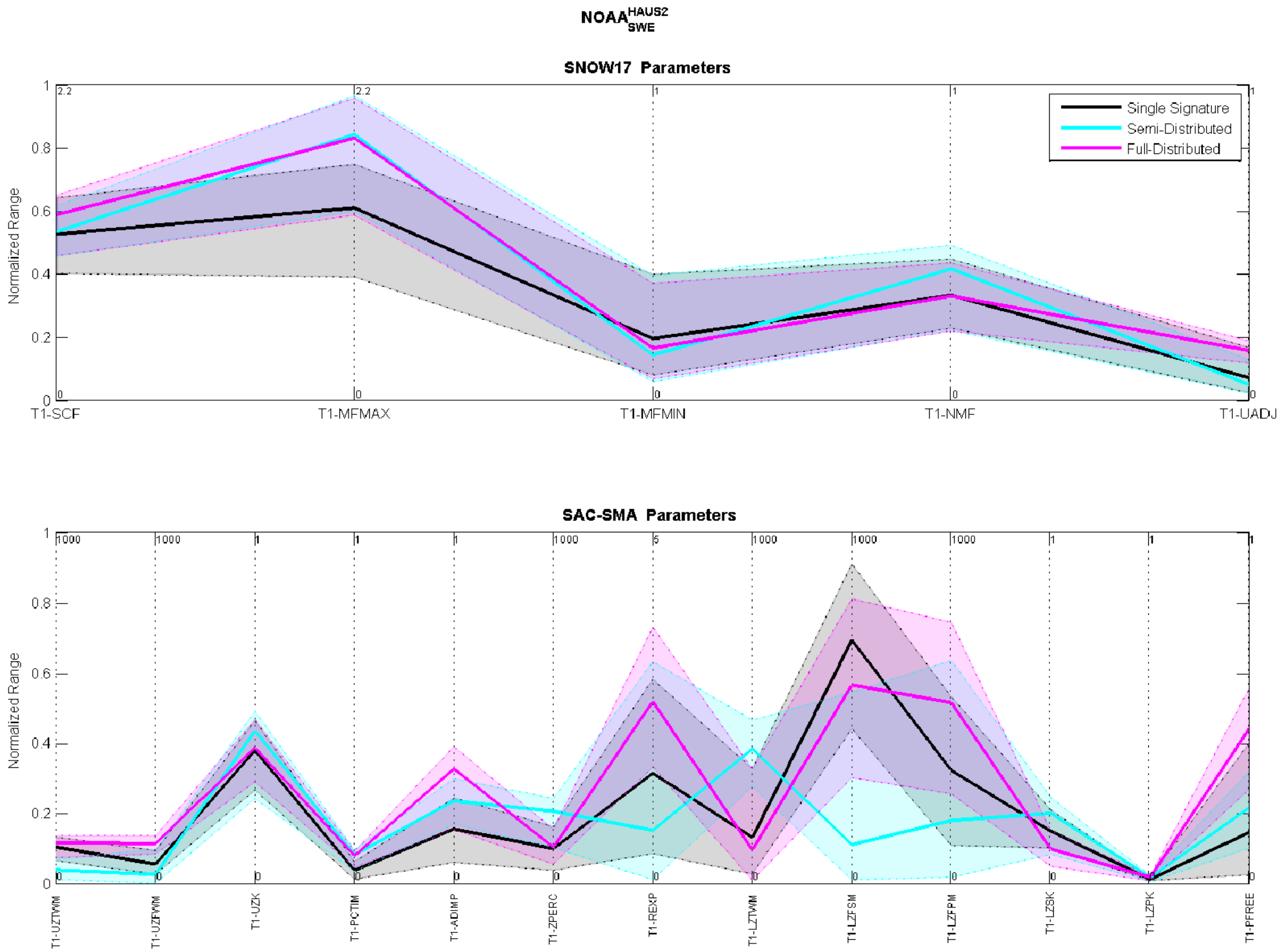

(a) Single- criterion Calibrations - $NOAA^{HAUS2}_{SWE}$.

Figure 6.4 Cont.

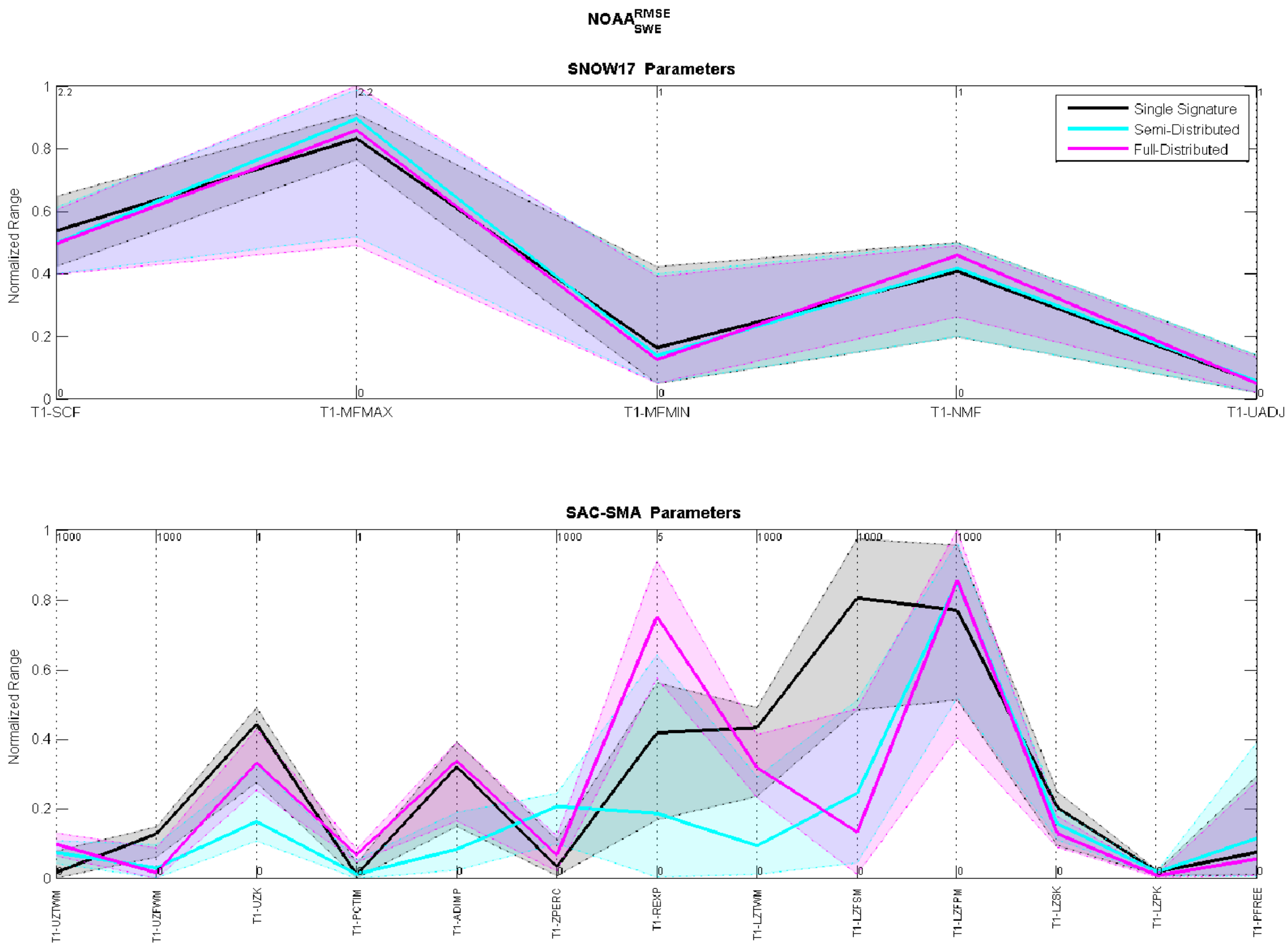

(a) Single- criterion Calibrations - $\mathrm{NOAA}_{\mathrm{SWE}}^{\mathrm{RMSE}}$.

Figure 6.4 Cont.

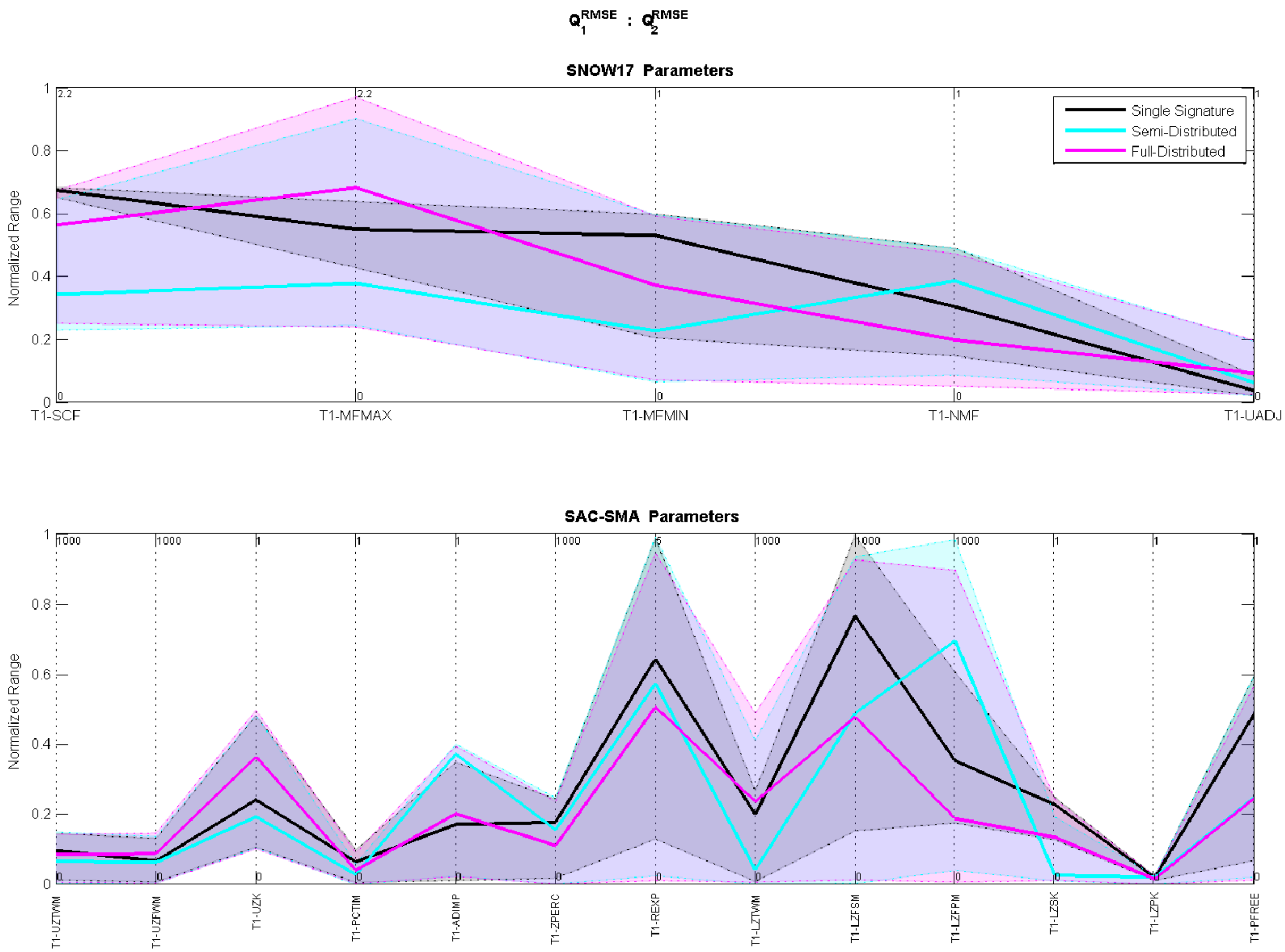

(b) Multi-criteria Calibrations - $Q_1^{RMSE} : Q_2^{RMSE}$.

Figure 6.4 Cont.

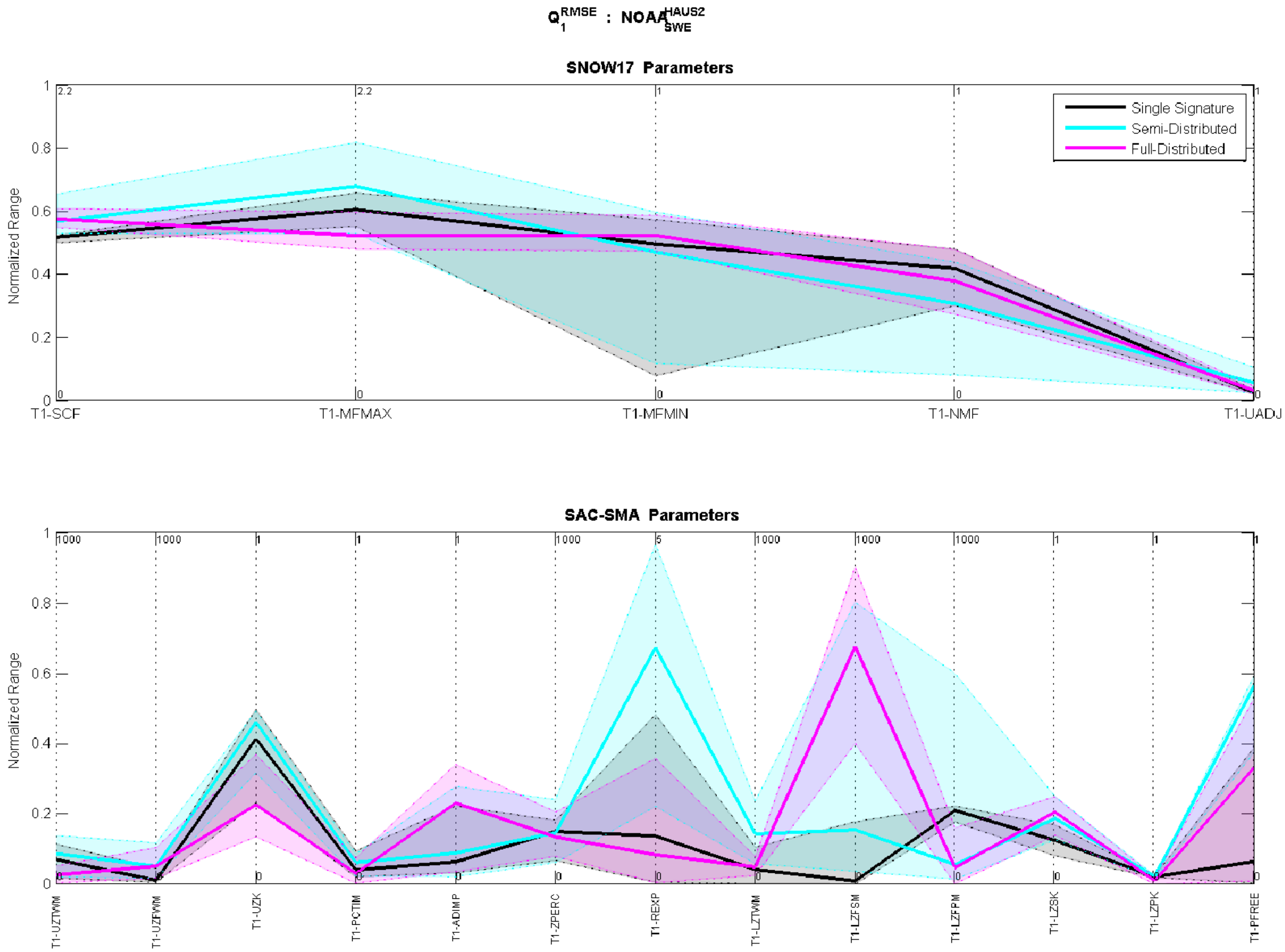

(b) Multi-criteria Calibrations - $Q_1^{RMSE} : NOAA_{SWE}^{HAUS2}$.

Figure 6.4 Cont.

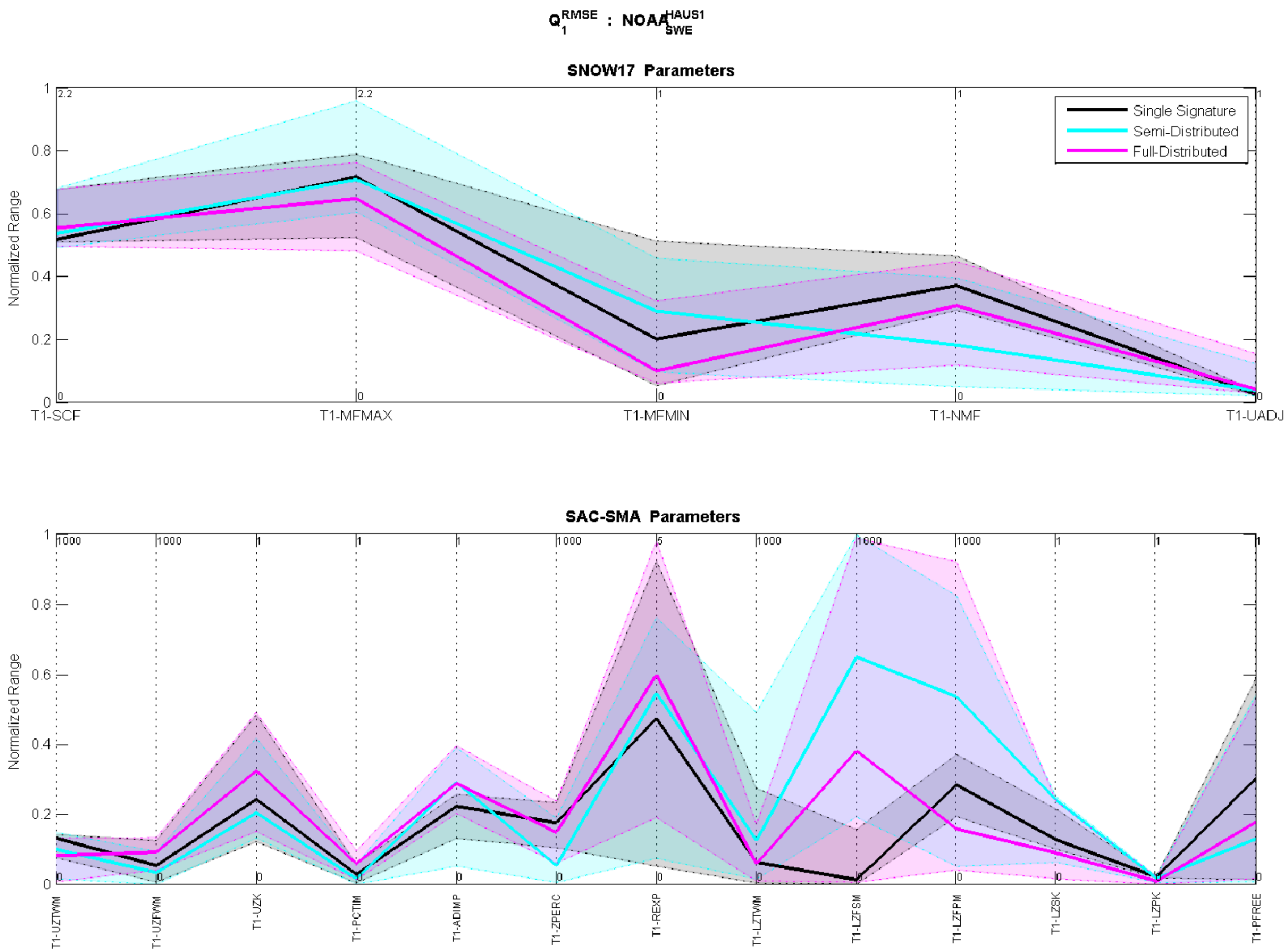

(b) Multi-criteria Calibrations - $Q_1^{RMSE} : NOAA_{SWE}^{HAUS2}$.

Figure 6.4 Cont.

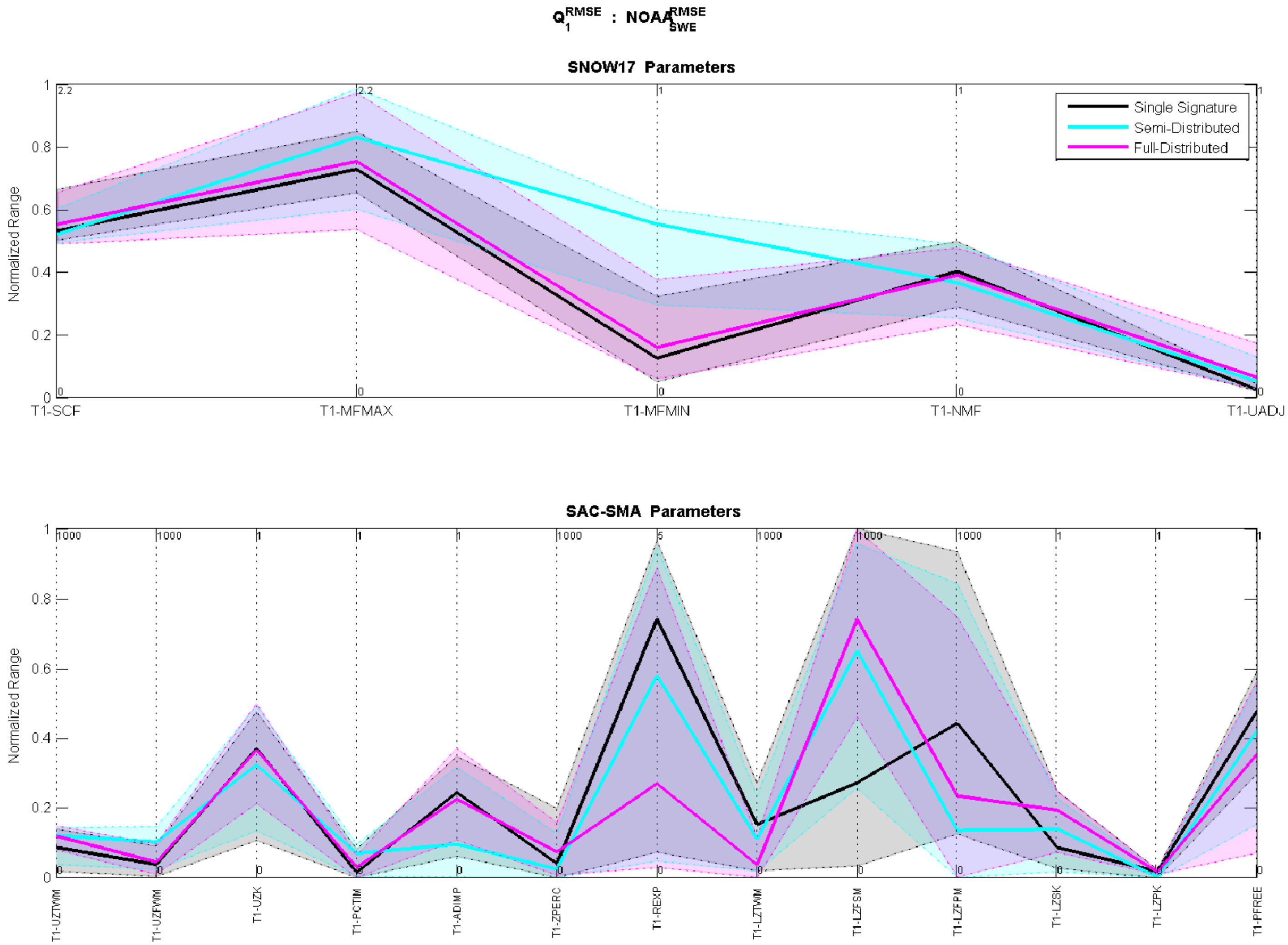

(b) Multi-criteria Calibrations - $Q_1^{RMSE} : NOAA_{SWE}^{RMSE}$.

Figure 6.4 Cont.

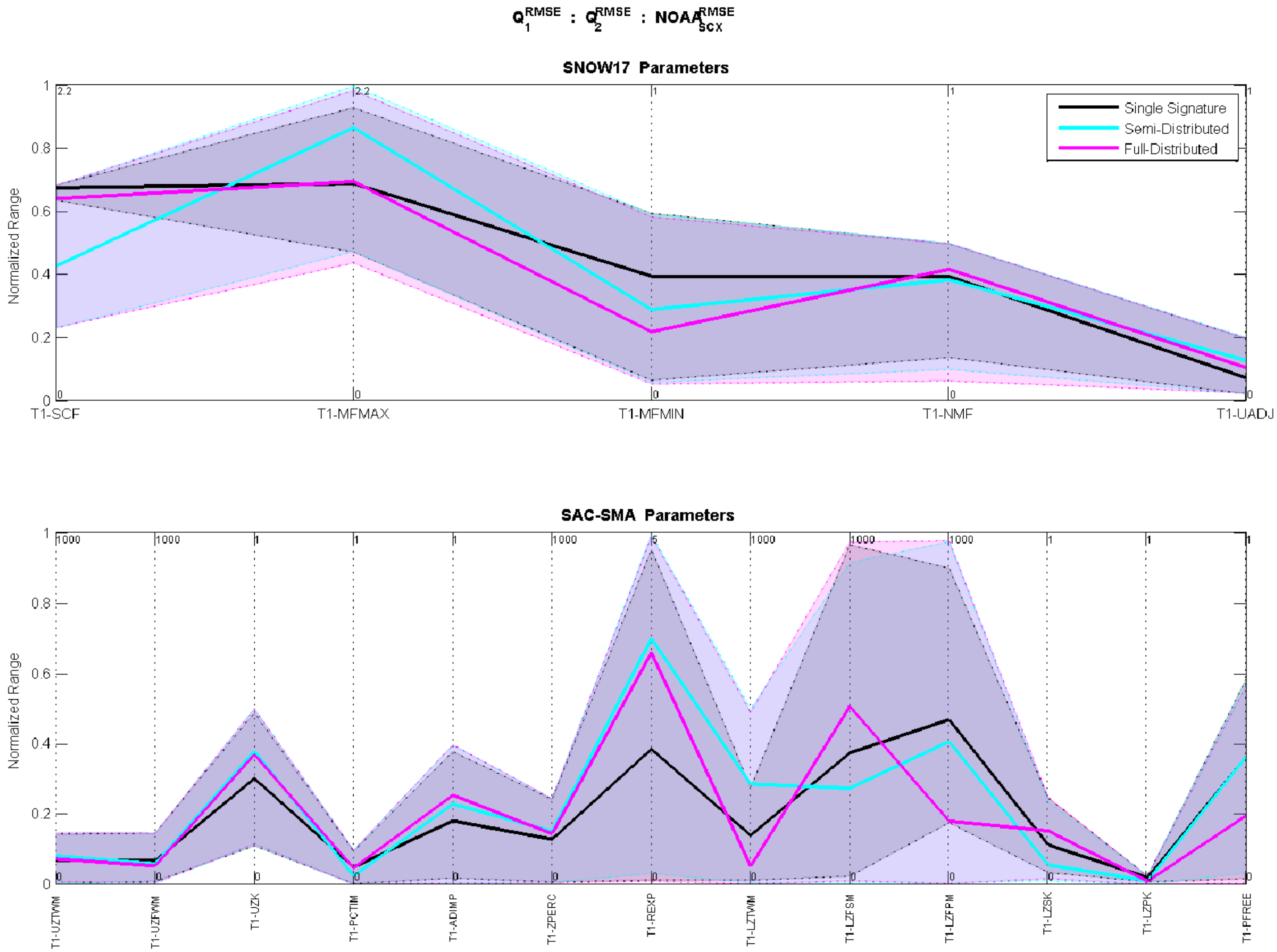

(b) Multi-criteria Calibrations - $Q_1^{RMSE} : Q_2^{RMSE} : NOAA_{SCX}^{RMSE}$.

Figure 6.4 Cont.

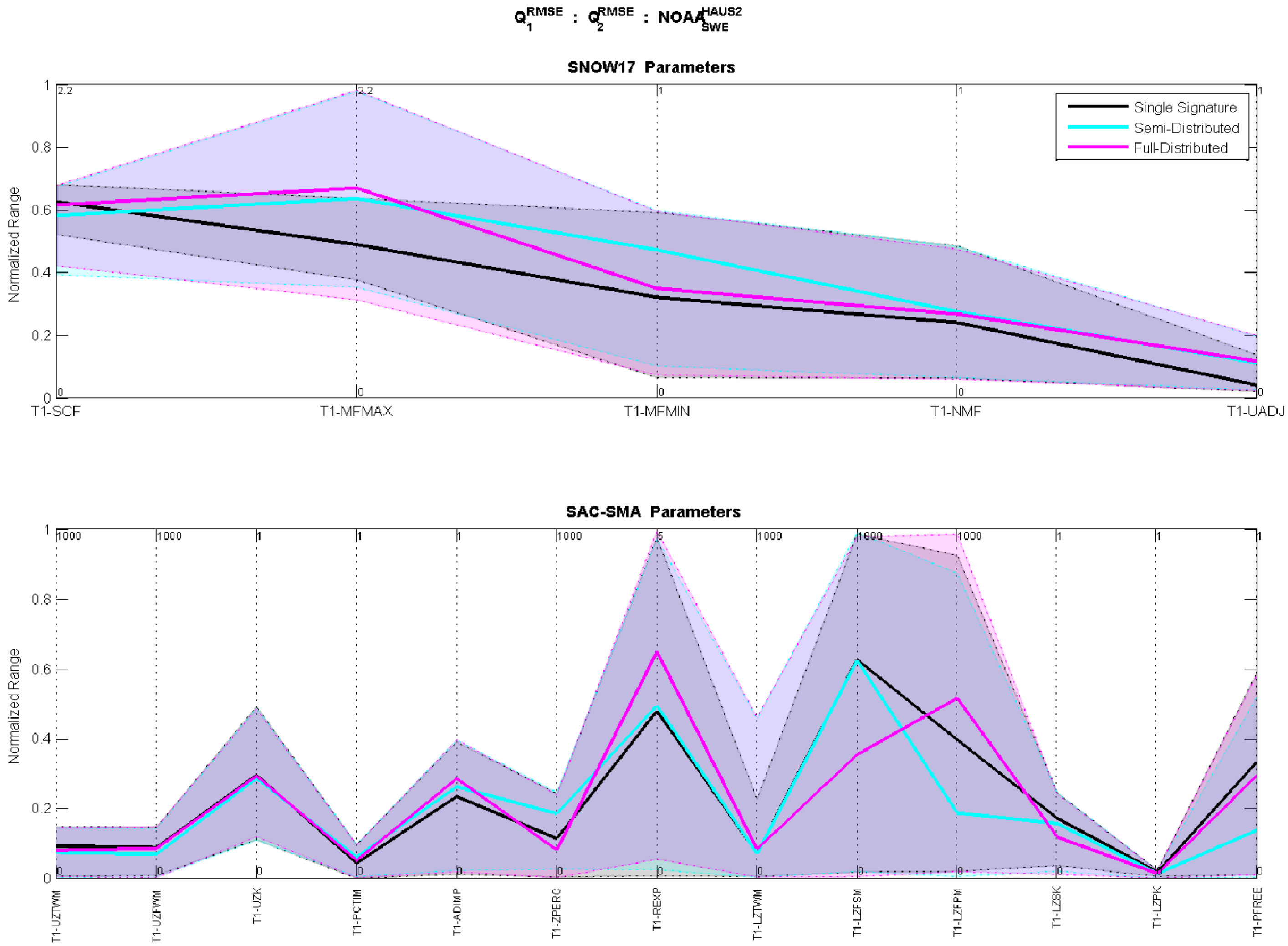

(b) Multi-criteria Calibrations - $Q_1^{RMSE} : Q_2^{RMSE} : NOAA_{SWE}^{HAUS2}$.

Figure 6.4 Cont.

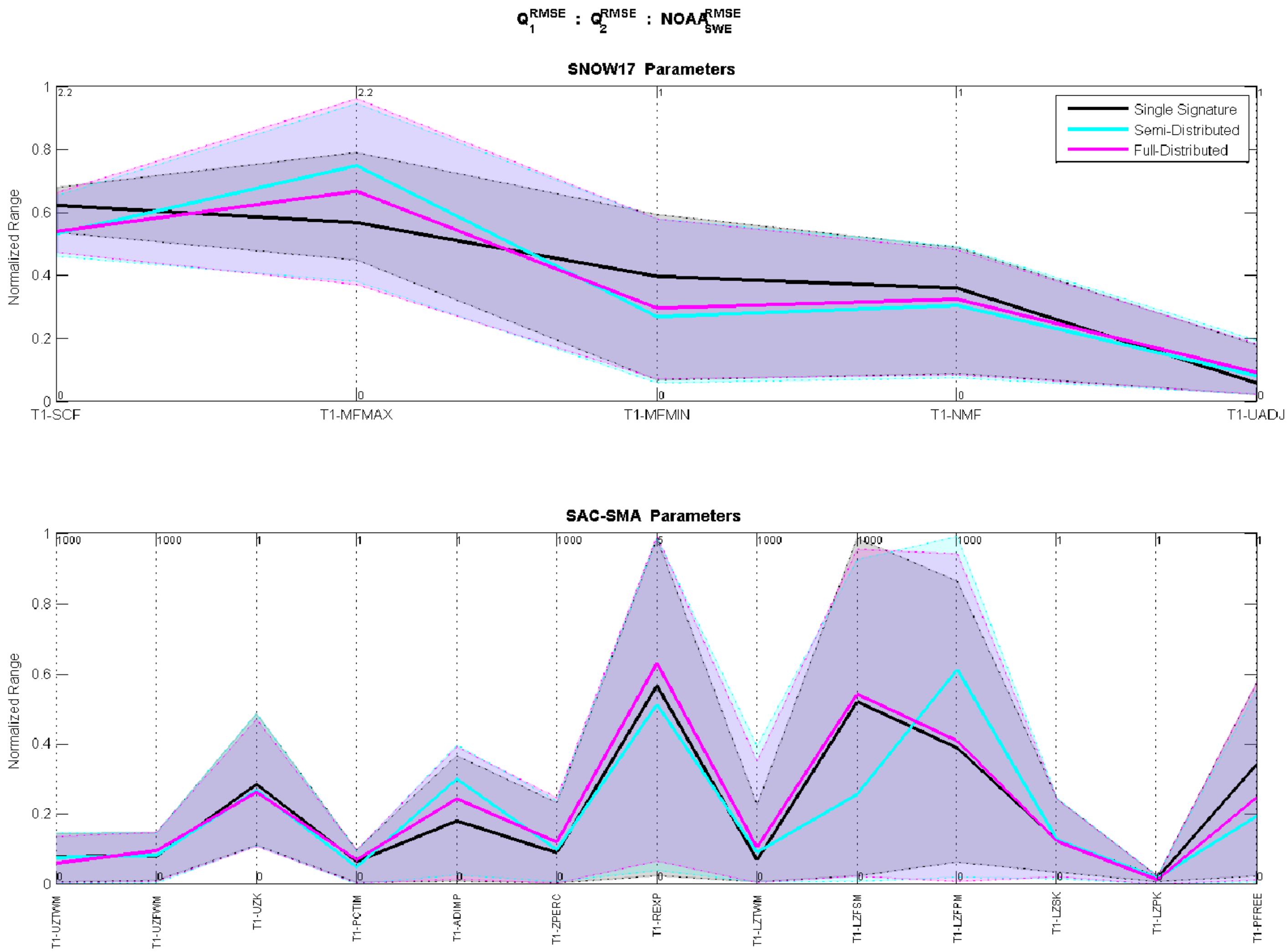

(b) Multi-criteria Calibrations - $Q_1^{RMSE} : Q_2^{RMSE} : NOAA_{SWE}^{RMSE}$.

Figure 6.4 Cont.

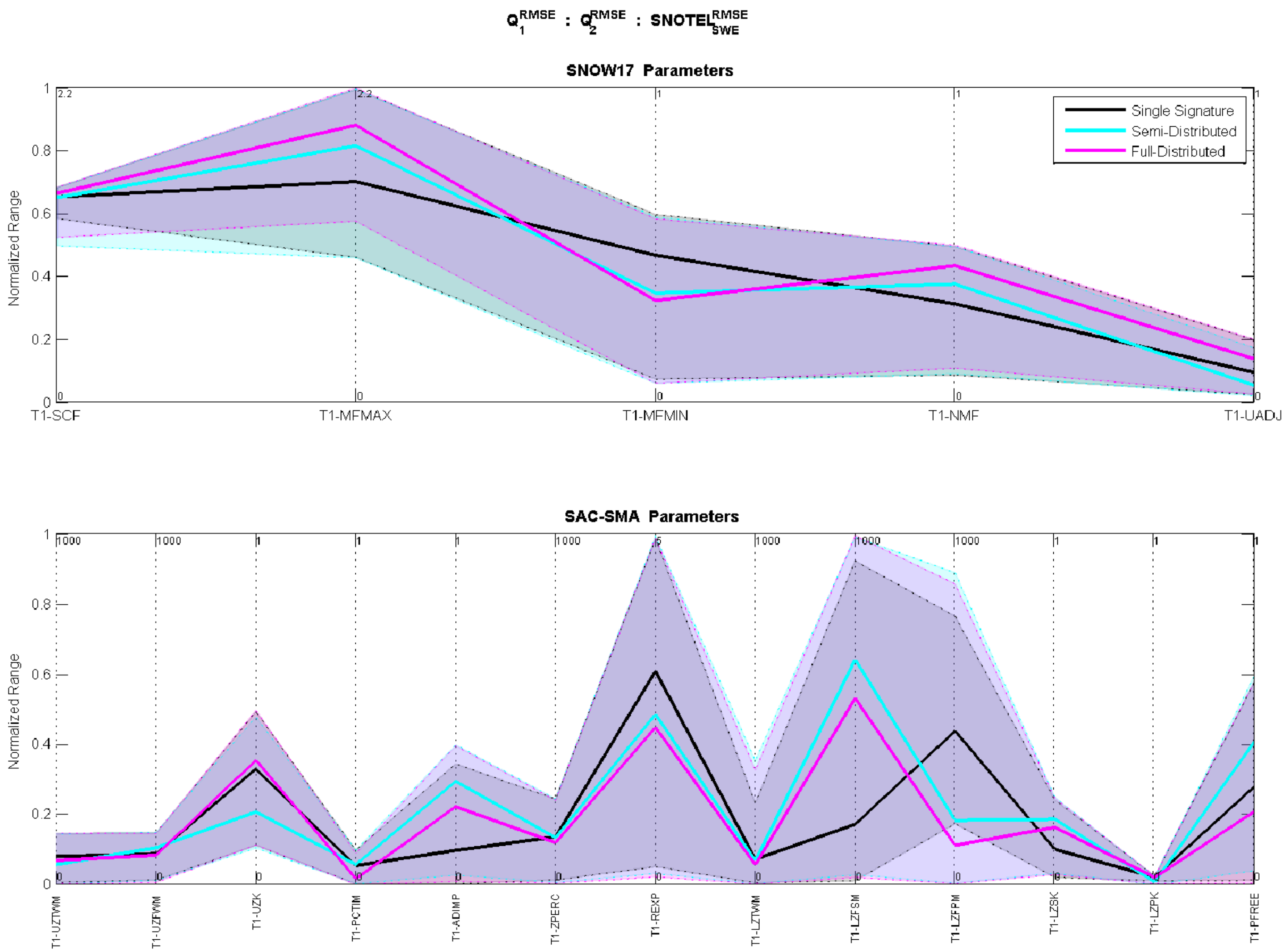

Multi-criteria Calibrations - $Q_1^{RMSE} : Q_2^{RMSE} : SNOTEL_{SWE}^{RMSE}$.

Figure 6.4 Cont.

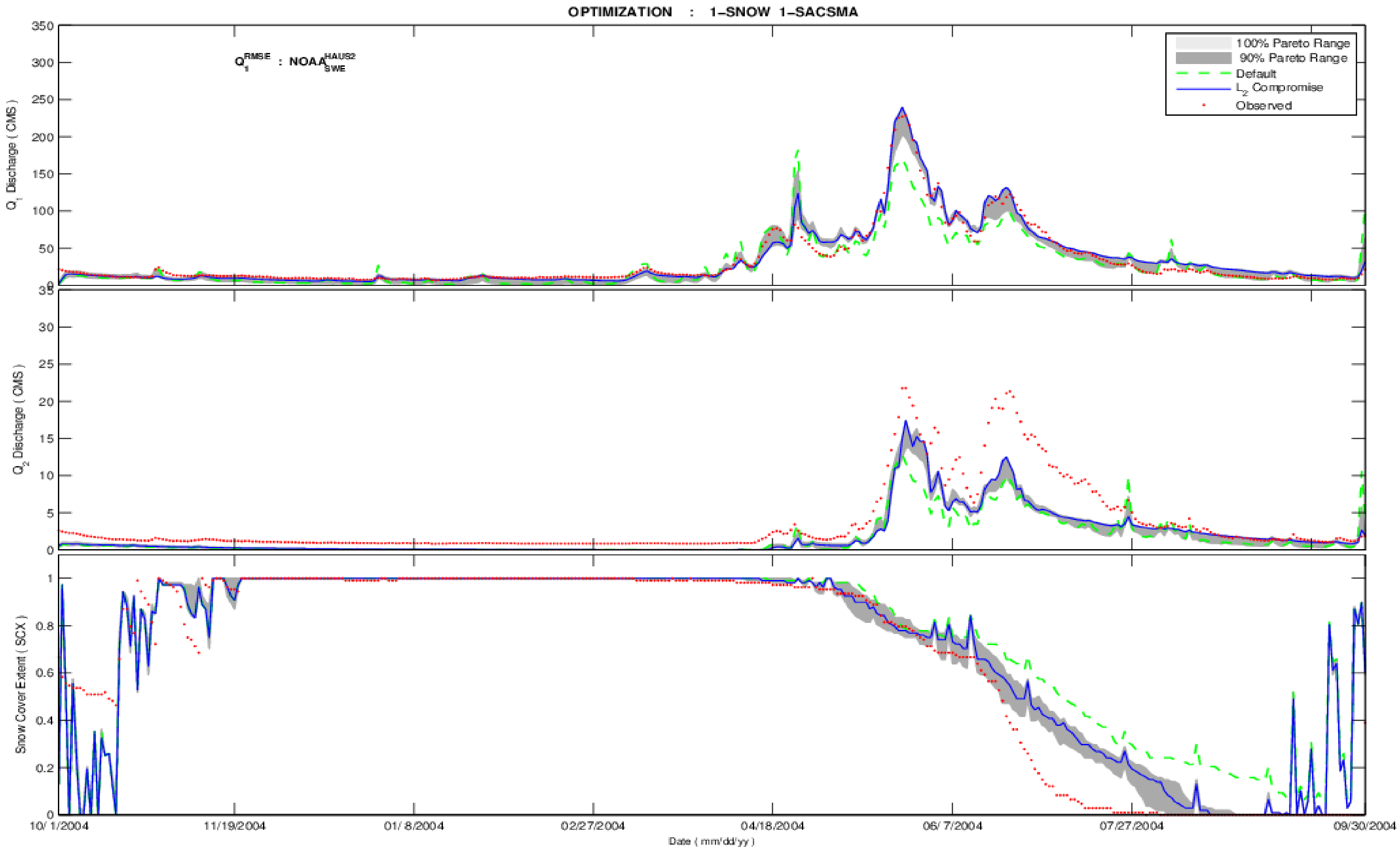

(a) Single-Signature : Best Hausdorff - $Q_1^{RMSE} : NOAA_{SWE}^{HAUS2}$.

Figure 6.5 The model outputs for overall basin and upstream sub-basin runoff and SCX from 90 percentile of optimized parameters. Darker gray ranges are 90 percentile ranges. The green line, blue line, and red dots represent default, compromised solution and observations.

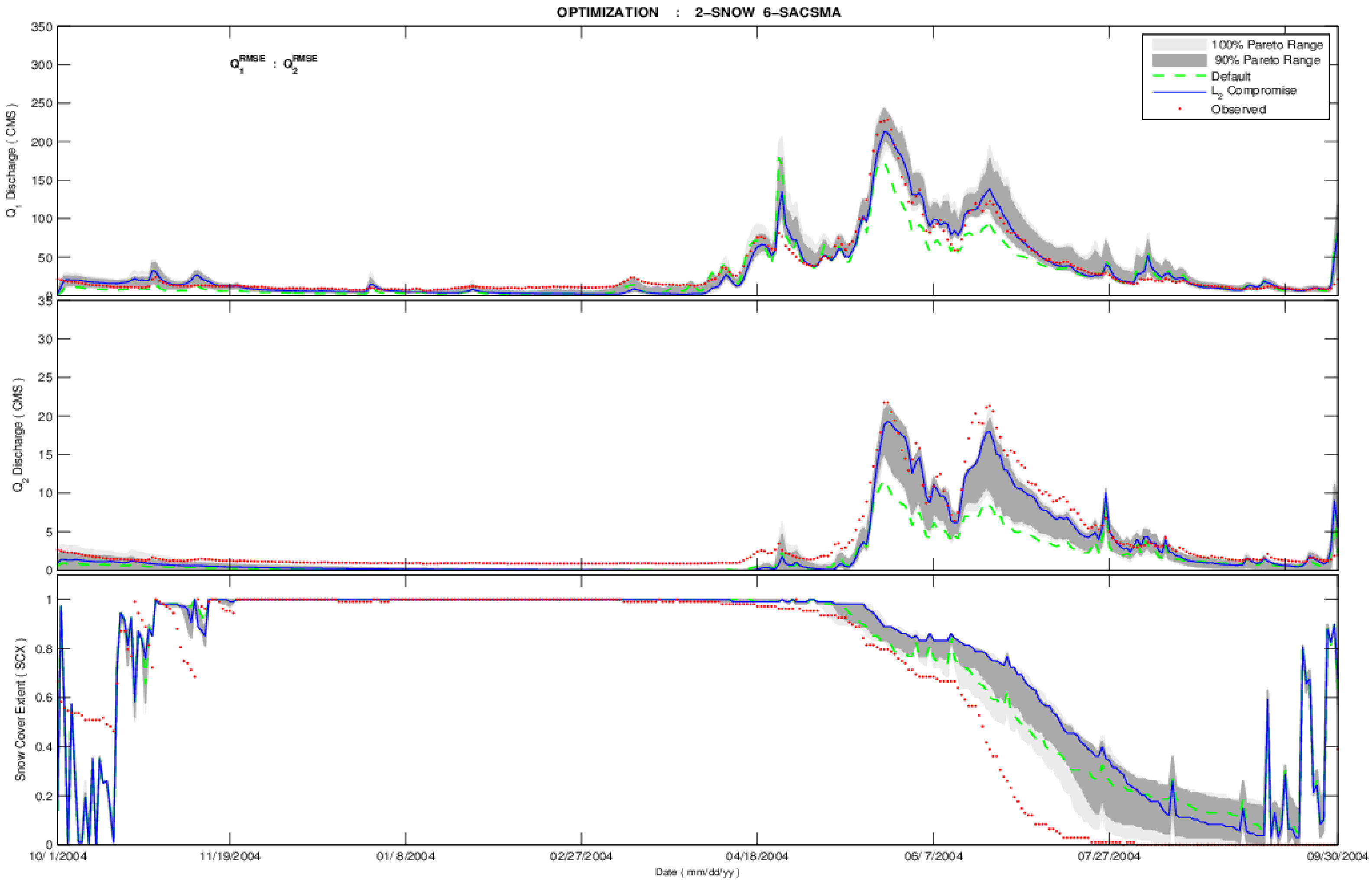

(b) Semi-Distributed : Best Hausdorff - $Q_1^{RMSE} : Q_2^{RMSE}$.

Figure 6.5 Cont.

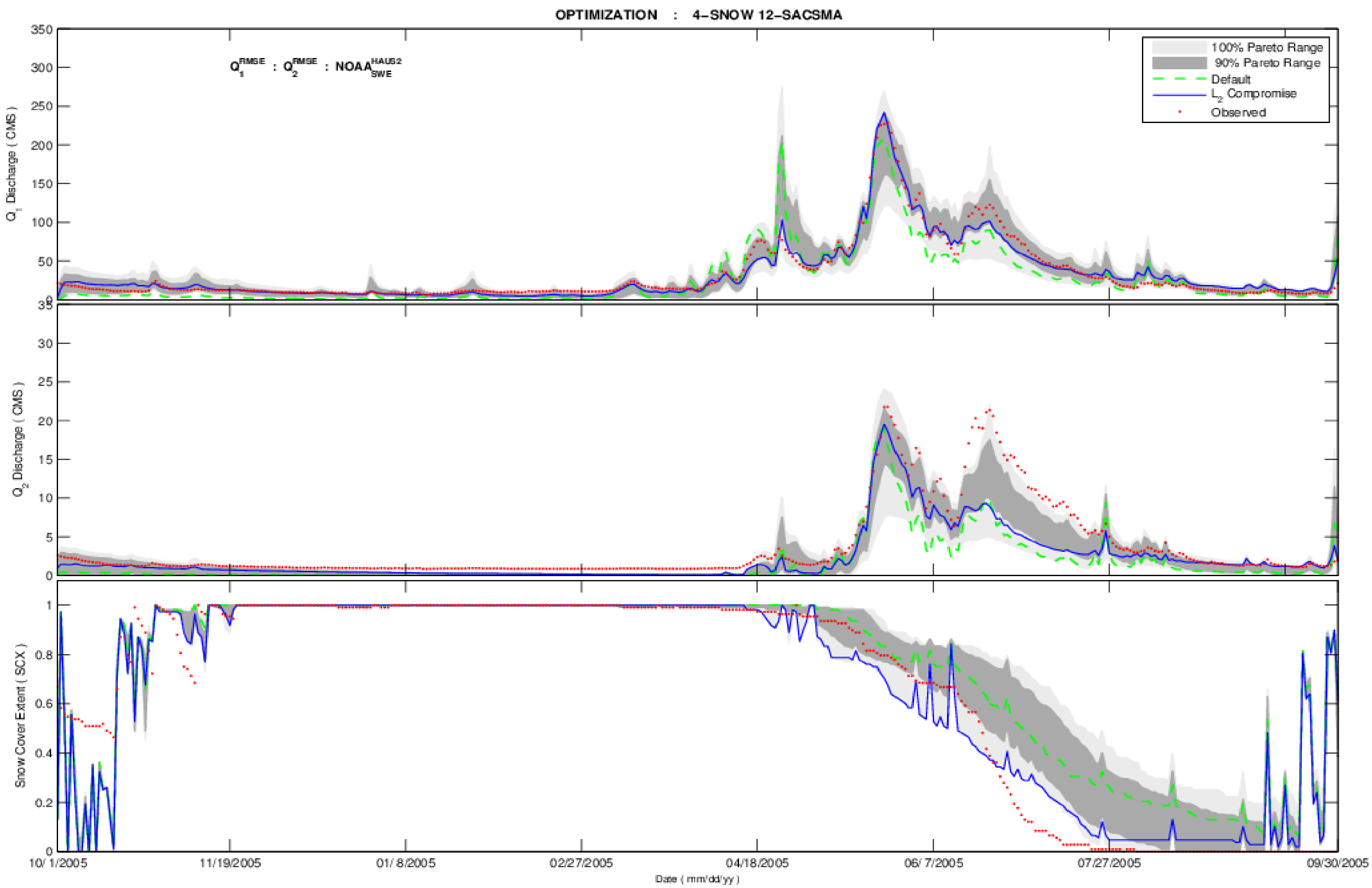

(c) Full-Distributed : Best Hausdorff - $Q_1^{RMSE} : Q_2^{RMSE} : NOAA_{SWE}^{HAUS2}$.

Figure 6.5 Cont.

CHAPTER 7

SUMMARY, CONCLUSION, AND FUTURE RESEARCH

7.1 Summary and Conclusion

In this dissertation, we devise the methods for proper calibration, performance evaluation, and diagnosis of a spatially distributed hydrological model in snow dominated areas. Through the calibrations and using a variety of variables such as overall basin discharge, sub-basin discharge and diverse snow information, the influences and contributions of snow information to the performances of model runoff and snow simulations are quantitatively evaluated. Also, the advantages and disadvantages of using the shape-matching error function are explored in the procedures of calibration and evaluation. The proper degree of model complexity is introduced by comparing model performances based on different model distributions. Lastly, the parameter estimations and distributions are investigated with model performances. The appropriate parameter values are estimated in order to reduce model uncertainty using various informatics of snow and runoff.

As a result, the snow simulations are improved using the calibrations with snow information only and both surface water and snow information for traditional and shape-matching error functions in a spatially distributed hydrological model. In particular, the snow information such as snow water equivalent, snow cover and snow cover extent are useful to calibrate and evaluate a hydrological model. By calibrating the snow water equivalent information, the snow cover and snow cover extent information are improved from the benchmark. However, it is relatively difficult to improve the snow water equivalent information through the calibrations, especially with snow cover extent information, without considering model distributions.

Furthermore, we investigate the effects of snow information calibrations on runoff simulations using single- or multi-criteria calibrations. Four different single-criterion calibrations on snow information only are conducted with each distribution in the study basin. Also, they are compared with the single- or multi-criteria calibrations on runoff information only. However, it is not easy to improve the surface water information using the single-criterion calibrations. On the other hand, the multi-criteria calibrations are more useful in advancing the performances of overall basin and upstream sub-basin runoff simulations. Particularly, the snow water equivalent information is more effective than snow cover extent information to improve overall basin and sub-basin runoff simulations simultaneously. The calibrations using snow water equivalent induce marginal improvements in runoff simulations, while snow present information does not. For the upstream sub-basin runoff simulations, it is possible to improve the sub-basin runoff with the multi-criteria calibrations using snow and overall basin discharge information.

In this dissertation, we explore and investigate the advantages and disadvantages of shape-matching error functions in the procedures of calibration and evaluation of a spatially distributed hydrological model. The shape-matching error functions have various advantages. First, they carry out better calibrations and evaluations with distributed observations of the distributed model. Second, they allow us to use non-commensurate observations and multiple output calibrations of the entire domain simultaneously. Lastly, the shape-matching error functions, especially Hausdorff, work together with spatial information such as location and elevation. By considering the spatial information, the relationship between snow and elevation can be reflected in the procedures of calibration and evaluation for the distributed model. However, despite those advantages, the computational overburden is one of the problems we face in shape-matching error functions. Also, sometimes the Hausdorff could not calculate the proper values with snow present, such as snow cover or snow cover extent, because they have only 1 or 0 as maximum and minimum values.

For the case study, we attempt to determine the appropriate model complexity for a spatially distributed hydrological model. It is difficult to decide which distributions are better, but the distributed model complexity yields better simulations than that of the lumped model, in general. In fact, the semi- or fully-distributed models are closer to observations with traditional or shape-matching error functions and smaller uncertainty. According to the results above, it is clear that the distributed models have better performances than the single-signature model. However, there seems to be a need to consider various case studies in order to decide the proper model complexity for each site.

For the study site, we attempt to analyze the parameters to select the appropriate parameter values and reduce the model uncertainty. The multi-criteria calibrations using diverse snow and runoff discharge information show better performances for mode or compromised solution parameter constraint than those of the single-criterion calibrations. In particular, the shape-matching error functions are very useful to constrain the parameters with distributed models in HL-RDHM.

7.2 Recommendation and Future Research

In this dissertation, we investigate model performances, model parameters, and model uncertainties in a spatially distributed hydrological model using snow and runoff information. For the spatially distributed hydrological model the data sets are still insufficient to cover all grids in the study basin. More exact studies are expected, with plentiful quantitative and qualitative observations. In particular, quantifying spatial and temporal patterns of snow information is very crucial in mountainous regions. We have had some challenges with snow information, quantitatively and qualitatively, in this dissertation. In the study basin, some of SNOTEL sites have too short time-series or insufficient qualities to calibrate or verify the model. Also, the SWE information for distributed models is deficient for model verification. In fact, the remotely sensed SWE information is used to calibrate the HL-RDHM model, but there is no data set of SWE information for the verification period. Therefore, we could not verify the model with SWE information; instead we use the MODIS information for model verification in this dissertation. As a result, it seems to be very important to continuously collect snow information. Because the NSIDC have collected a variety of snow information, both in situ and remotely sensed, more quantitative and qualitative snow information is expected to be collected and attempted.

In this dissertation, we attempt to compare the performances of model calibration and verification with the parameter values for the a priori values as a benchmark. The computations are carried out by the Anderson (2006) method for Snow 17 and Zhang et al. (2011) for SAC-SMA. The a priori parameter set for the water balance component has better conditions in data availability with antecedent soil moisture, hydrologic soil group, type of vegetation, and category of land use for spatially distributed cells in study basin. The Snow 17 is based on an energy balance model; however, the a priori parameters are estimated using only forest type, density, aspect and slope in each grid, without considering energy fluxes such as radiation, sensible and latent heat, and so on, due to limited data availability in the study site. For better performances and comparisons, the a priori parameters for Snow 17 need to be updated with data availability in study site.

REFERENCES

Ajami, N. K., Gupta, H. V., Wagener, T., and Sorooshian, S. (2004). "Calibration of a semi-distributed hydrologic model for streamflow estimation along a river system." *J. Hydrol*., 298, 112-135.

Anderson, E. A. (1973). *National Weather Service River Forecast System – snow accumulation and ablation model*, NOAA Technical Memorandum NWS HYDRO-17, 217.

Anderson, E. A. (2006). "Snow accumulation and ablation model: NWSRFS (National Weather Service River Forecast System) Snow17 Snow Model." <http://www.weather.gov/oh/hrl//nwsrfs/users_manual/part2/_pdf/ 22snow17.pdf>.

Aronica, G., Bates, P. D., and Horritee, M. S. (2002). "Assessing the uncertainty in distributed model predictions using observed binary pattern information within GLUE." *Hydrol. Process.*, 16, 2001-2016.

Assent, I., Wichterich, M., Meisen, T., and Seidl, T. (2008). "Efficient similarity search using the Earth Mover's Distance for large multimedia databases." *IEEE 24th International Conference*, 307-316.

Bandaragoda, C., Tarboton, D. G., and Woods, R. (2004). "Application of TOPNET in the distributed model intercomparison project." *J. Hydrol.*, 298, 178-201.

Barrett, A. P. (2003). *Natoinal Operational Hydrologic Remote Sensing Center SNOw Data Assimilarion System (SNODAS) Products at NSIDC*, NSIDC, special report #11.

Bastidas, L. A. (1998). "Parameter estimation for hydrometeorological models using multi-criteria methods." PhD Dissertation, University of Arizona, Tucson, AZ.

Bastidas, L. A., Gupta, H. V., Sorooshian, S., Shuttleworth, W. J., and Yang, Z. L. (1999). "Sensitivity analysis of a land surface scheme using multi-criteria methods." *J. Geophys. Res.*, 104(D16), doi:10.1029/1999JD900155.

Beauchemin, M., Thomson, K. P. B., and Edwards, G. (1998). "On the Hausdorff distance used for the evaluation of segmentation results." *Canadian J. Remote Sens.*, 24(1), 3-8.

Belogay, E., Cabrelli, C., Molter, U., and Shonkwiler, R. (1997). "Calculating the Hausdorff distance between curves." *Infor. Process. Letters*, 64, 17-22.

Beven, K. (1993). "Prophecy, reality and uncertainty in distributed hydrological modeling." *Adv. Water Resour.*, 16, 41-51.

Beven, K., and Binley, A. (1992). “The future of distributed models: Model calibration and uncertainty prediction.” *Hydro. Process.*, 6, 279-298.

Beven, K., and Freer, J. (2001). “Equifinality, data assimilation, and uncertainty estimation in mechanistic modeling of complex environmental systems using the GLUE methodology.” *J. Hydrol.*, 249, 11-29.

Beven, K., Smith, P., and Freer, J. (2007). “Comment on – Hydrological forecasting uncertainty assessment: Incoherence of the GLUE methodology – by Pietro Mantovan and Ezio Todini.” *J. Hydrol.*, 338, 315-318.

Beven, K. J., Smith, P., and Freer, J. E. (2008). “So just why would a modeler choose to be incoherent?” *J. Hydrol.*, 354, 15-32.

Blasone, R.-S., Madsen, H., and Rosbjerg, D. (2007). “Parameter estimation in distributed hydrological modeling: Comparison of globall and local optimization techniques.” *Nordic Hydrol.*, 38, 451-476.

Blasone, R.-S., Madsen, H., and Rosbjerg, D. (2008a). “Uncertainty assessment of integrated distributed hydrological models using GLUE with Markov chain Monte Carlo sampling.” *J. Hydrol.*, 353, 18-32.

Blasone, R.-S., Vrugt, J. A., Madsen, H., Rosbjerg, D., Robinson, B. A., and Zyvoloski, G. A. (2008b). “Generalized likelihood uncertainty estimation (GLUE) using adaptive Markov Chain Monte Carlo sampling.” *Adv. Water Resour.*, 31, 630-648.

Brath, A., Montanari, A., and Toth, E. (2004). “Analysis of the effects of different scenarios of historical data availability on the calibration of a spatially-distributed hydrological model.” *J. Hydrol.*, 291, 232-253.

Burnash, R. J. C. (1995). “The NWS river forecast system – catchment modeling.” Computer models of watershed hydrology, Singh, ed., Water Resources Publications, Littleton, Colo., 311-366.

Campo, L., Caparrini, F., and Castelli, F. (2006). “Use of multi-platform, multi-temporal remte-sensing data for calibration of a distributed hydrological model: an application in the Arno basin, Italy.” *Hydro. Process.*, 20, 2693-2712.

Cao, W., Bowden, W. B., Davie, T., and Fenemor, A. (2006). “Multi-variable and multi-site calibration and validation of SWAT in a large mountainous catchment with high spatial variability.” *Hydro. Process.*, 20, 1057-1073.

Carrera, M. L., Belair, S., Fortin, V., Bilodeau, B., Charpentier, D., and Dore, I. (2010). “Evaluation of Snowpack Simulations over the Canadian Rockies with an Experimental Hydrometeorological Modeling System.” *J. Hydrometeorol.*, 11, 1123-1140.

Choi, H.-T., and Beven, K. (2007). "Multi-period and multi-criteria model conditioning to reduce prediction uncertainty in an application of TOPMODEL within the GLUE framework." *J. Hydrol.*, 332, 316-336.

Dodov, B., and F.-Georgiou, E. (2005). "Incorporation the spatio-temporal distribution of rainfall and basin geomorphology into nonlinear analyses of streamflow dynamics." *Adv. Water Resour.*, 28, 711-728.

Duan, Q., Gupta, V. K., and Sorooshian, S. (1992). "Effective and efficient global optimization for conceptual rainfall-runoff models." *Water Resour. Res.*, 28, 1015-1031.

Duan, Q., Gupta, V. K., and Sorooshian, S. (1993), "A shuffled complex evolution approach for effective and efficient global minimization." *J. Optim. Theory Appl.*, 76(3), 501-521.

Dunn S. M., and Colohan, R. J. E. (1999). "Developing the snow component of a distributed hydrological model: a step-wise approach based on multi-objective analysis." *J. Hydrol.*, 223, 1-16.

Eckhardt, K., and Arnold, J. G. (2001). "Automatic calibration of a distributed catchment model." *J. Hydrol.*, 251, 103-109.

Frances, F., Velez, J. L., and Velez, J. J. (2007). "Split-parameter structure for the automatic calibration of distributed hydrological models." *J. Hydrol.*, 332, 226-240

Franz, K. J., Butcher, P., and Ajami, N. K. (2010). "Addressing snow model uncertainty for hydrologic prediction." *Adv. Water Resour.*, 33, 820-832.

Franz, K. J., Hogue, T. S., and Sorooshian, S. (2008a). "Snow Model Verification using Ensemble Prediction and Operational Benchmarks." *J. Hydrometeorol.*, 9, 1402-1415.

Franz, K. J., Hogue, T. S., and Sorooshian, S. (2008b). "Operational snow modeling: Addressing the challenges of an energy balance model for National Weather Service forecasts." *J. Hydrol.*, 360, 48-66.

Freer, J. E., McMillan, H., McDonnell, J. J., and Beven, K. J. (2004). "Constraining dynamic TOPMODEL responses for imprecise water table information using fuzzy rule based performance measures." *J. Hydrol.*, 291, 254-277.

Gan, T. Y., Dlamini, E. M., and Biftu, G. F. (1997). "Effects of model complexity and structure, data quality and objective functions on hydrologic modeling." *J. Hydrol.*, 192, 81-103.

Gupta, H. V., Bastidas, L. A, Sorooshian, S., Shuttleworth, W. J., and Yang, Z. L. (1999). "Parameter estimation of a land surface scheme using multi-criteria methods." *J. Geophys. Res.*, 104(D16), 19491-19503.

He, M., Hogue, T. S., Franz, K. J., Margulis, S. A., and Vrugt, J. A. (2011a). "Characterizing parameter sensitivity and uncertainty for a snow model across hydroclimatic regimes." *Adv. Water Resour.*, 34, 114-127.

He, M., Hogue, T. S., Franz, K. J., Margulis, S. A., and Vrugt, J. A. (2011b). "Corruption of parameter behavior and regionalization by model and forcing data errors: A Bayesian example using the SNOW17 model." *Water Resour. Res.*, 47, W07546, doi:10.1029/2010WR009753.

Hogue, T. S., Sorooshian, S., and Gupta, H. V. (2000). "A multistep Automatic Calibration Scheme for River Forecasting Models." *J. Hydrometeorol.*, 1, 524-542.

Huttenlocher, D. P., Klanderman, G. A., and Rucklidge, W. J. (1993). "Comparing images using the Hausdorff distance." *IEEE Transactions on Pattern Analysis and Machine Intelligence*, 15(9), 850-863.

Immerzeel, W. W., and Droogers, P. (2008). "Calibration of a distributed hydrological model based on satellite evapotranspiration." *J. Hydrol.*, 349, 411-424.

Jasper, K., Gurtz, J., and Lang, H. (2002). "Advanced flood forecasting in Alpine watersheds by coupling meteorological observations and forecasts with a distributed hydrological model." *J. Hydrol.*, 267, 40-52.

Kaheil, Y. H., Gill, M. K., McKee, M., and Bastidas, L. (2006). "A new Bayesian recursive technique for parameter estimation." *Water Resour. Res.*, 42, W08423, doi:10.1029/2005WR004529.

Khakbaz, B., Imam, B., and Sorooshian, S. (2012). "From lumped to distributed via semi-distributed: Calibration strategies for semi-distributed hydrologic models." *J. Hydrol.*, 418, 61-77.

Konz, M., Finger, D., Burgi, C., Normand, S., Immerzeel, W. W., Merz, J., Giriraj, A., and Burlando, P. (2010). "Calibration of a distributed hydrological model for simulations of remote glacierized Himalayan catchments using MODIS snow cover data." *Proc., Sixth World FRIEND Conference*, IAHS Publ., Fez, Morocco.

Koren, V., Reed, S., Smith, M., Zhang, Z., and Seo, D-.J. (2004). "Hydrology Laboratory Research Modeling System (HL-RMS) of the US National Weather Service." *J. Hydrol.*, 291, 297-318.

Koren, V., Smith, M., Duan, Q. (2003). "Use of a priori parameter estimates in the derivation of spatially consistent parameter sets of rainfall-runoff models." *Water*

Science and Application, 6, 239–254.

Koren, V. I., Smith, M., Wang, D., and Zhang, Z. (2000). “Use of Soil Property Data in the derivation of Conceptual Rainfall-Runoff Model Parameters.” *Proc., the 15th Conference on Hydrology*, AMS, Long Beach, CA, 103–106.

Li, S. (2006). “Multiple resolution hydrometeorological modeling of semi-arid areas and similarity-based performance evaluation.” PhD Dissertation, Utah State University, Logan, UT.

Liu, Y., and Gupta, H. V. (2007). “Uncertainty in hydrologic modeling: toward an integrated data assimilation framework.” *Water Resour. Res.*, 43, W07401.

Looper, J. P., Vieux B. E., and Moreno M. A. (2012). “Assessing the impacts of precipitation bias on distributed hydrologic model calibration and prediction accuracy.” *J. Hydrol.*, 418-419, 110-122.

Luzio, M. D., and Arnold, J. G. (2004). “Formulation of a hybrid calibration approach for a physically based distributed model with NEXRAD data input.” *J. Hydrol.*, 298, 136-154.

Madsen, H. (2003). “Parameter estimation in distributed hydrological catchment modeling using automatic calibration with multiple objectives.” *Adv. Water Resour.*, 2003, 205-216.

Madsen, H., and Jacobsen, T. (2001). “Automatic calibration of the MIK SHE integrated hydrological modeling system.” *4th DHI software conference*, Helsingor, Denmark.

Marce, R., Ruiz, C. E., and Armengol, J. (2008). “Using spatially distributed parameters and multi-response objective functions to solve parameterization of complex applications of semi-distributed hydrological models.” *Water Resour. Res.*, 44, W02436, doi:10.1029/2006WR005785.

Marks, D., Domingo, J., Susong, D., Link, T., and Garen, D. (1999). “A spatially distributed energy balance snowmelt model for application in mountain basins.” *Hydro. Process.*, 13, 1935-1959.

Marron, J. S., and Tsybakov, A. B. (1995). “Visual error criteria for qualitative smoothing.” *J. Am. Statist. Assoc.*, 90, 430, 499-507.

Martinez, G. F., and Gupta, H. V. (2010). “Toward improved identification of hydrological models: A diagnostic evaluation of the “abcd” monthly water balance model for the conterminous United States.” *Water Resour. Res.*, 46, W08507, doi:10.1029/2009WR008294.

McMichael, C. E., Hope, A. S., and Loaiciga, H. A., (2006). “Distributed hydrological modeling in California semi-arid shrublands: MIKE SHE model calibration and uncertainty estimation." *J. Hydrol.*, 317, 307-324.

Mizukami, N., Perica, S., and Hatch, D. (2011). "Regional approach for mapping climatological snow water equivalent over the mountainous regions of the western United States." *J. Hydrol.*, 400, 72-82.

Molotch, N. P., Painter, T. H., Bales, R. C., and Dozier, J. (2004). "Incorporating remotely-sensed snow albedo into a spatially-distributed snowmelt model." *Geophys. Res. Lett.*, 21, L03501, doi:10.1029/2003GL019063.

Motovilov, Y. G., Gottschalk, L., Engeland, K., and Rodhe, A. (1999). "Validation of a distributed hydrological model against spatial observations." *Agr. Forest Meteorol.*, 98-99, 257-277.

Moussa, R., Chahinian N., and Bocquillon, C. (2007). "Distributed hydrological modeling of a Mediterranean mountainous catchment – Model construction and multi-site validataion." *J. Hydrol.*, 337, 35-51.

Muleta, M., and Nicklow, J. (2005). "Sensitivity and uncertainty analysis coupled with automatic calibration for a distributed watershed model." *J. Hydrol.*, 306, 1-4.

Nan, Z., Wang, S., Liang, X., Adams, T. E., Teng, W., and Liang, Y. (2010). "Analysis of spatial similarities between NEXRAD and NLDAS precipitation data products." *IEEE J. Sel. Topics Appl. Earth Observ.*, 3(3), 1939-1404.

Pokhrel, P., and Gupta, H. V. (2010). "On the use of spatial regularization strategies to improve calibration of distributed watershed models." *Water Resour. Res.*, 46, W01505, doi:10.1029/2009WR008066.

Pokhrel, P., Gupta, H. V., and Wagener, T. (2008). "A spatial regularization approach to parameter estimation for a distributed watershed model." *Water Resour. Res.*, 44, W12419, doi:10.1029/2007WR006615.

Pokhrel, P., Yilmaz, K. K., and Gupta, H. V. (2012). "Multiple-criteria calibration of a distributed watershed model using spatial regularization and response signatures." *J. Hydrol.*, 418-419, 49-60.

Ragettli, S., and Pellicciotti, F. (2012). "Calibration of a physically based, spatially distributed hydrological model in a glacierized basin: On the use of knowledge from glaciometeorlogical processes to constrain model parameters." *Water Resour. Res.*, 48, W03509, doi:10.1029/2011WR010559.

Reed, S., Koren, V., Smith, M., Zhang, Z., Moreda, F., Seo, D.-J., and DMIP Participants. (2004). "Overall distributed model intercomparison project results." *J. Hydrol.*, 298, 27-60.

Reed, S. M., and Maidment, D. R. (1999). "Coordinate transformations for using NEXRAD data in GIS-based hydrologic modeling." *J. Hydrol. Eng.*, 4, 174-183.

Refsgaard, J. C. (1997). "Parameterization, calibration and validation of distributed hydrological models." *J. Hydrol.*, 198, 69-97.

Rubner, Y., Tomasi, C., and Guibas, L. J. (2000). "The Earth Mover's Distance as a Metric for Image Retrieval." *Int. J. Comput. Vision*, 40(2), 99-121.

Safari A., Smedt, F. D., and Moreda, F. (2012). "WetSpa model application in the Distributed Model Intercomprison Project (DMIP2)." *J. Hydrol.*, 418-419, 78-89.

Segui, P. Q., Martin, E., Habets, F., and Noilhan, J. (2009). "Improvement, calibration and validation of a distributed hydrological model over France." *Hydrol. Earth Syst. Sc.*, 13, 163-181.

Sahoo, G. B., Ray, C., and De Carlo, E. H. (2006). "Calibration and validation of a physically distributed hydrological model, MIKE SHE, to predict streamflow at high frequency in a flashy mountainous Hawaii stream." *J. Hydrol.*, 327, 94-109.

Schuol, J., and Abbaspour, K. C. (2006). "Calibration and uncertainty issues of a hydrological model (SWAT) applied to West Africa." *AdG*, 9, 137-143.

Senarath, S. U. S., Ogden F. L., Downer, C. W., and Sharif, H. O. (2000). "On the calibration and verification of two-dimensional, distributed, Hortonian, continuous watershed models." *Water Resour. Res.*, 36, 6, 1495-1510.

Serreze, M. C., Clark, M. P., Armstrong, R. L., McGuiness, D. A., and Pulwarty, R. S. (1999). "Characteristics of the western United States snowpack from snowpack telemetry (SNOTEL) data." *Water Resour. Res.*, 35, 2145-2160.

Shafii M., and Smedt F. D. (2009). "Multi-objective calibration of a distributed hydrological model (WetSpa) using a genetic algorithm." *Hydrol. Earth Syst. Sc.*, 13, 2137-2149.

Smith, M. B., Koren, V., Reed, S. M., Zhang, Z., Zhang, Y., Moreda, F., Cui, Z., Mizukami, N., Anderson, E. A., and Cosgrove, B. A. (2012a). "The distributed model intercomparison project – Phase 2: Motivation and design of the Oklahoma experiments." *J. Hydrol.*, 418-419, 3-16.

Smith, M. B., Koren, V., Zhang, Z., Zhang, Y., Reed, S. M., Cui, Z., Moreda, F., Cosgrove, B. A., Mizukami, N., Anderson, E. A., and DMIP 2 Participants (2012b). "Results of the DMIP 2 Oklahoma experiments." *J. Hydrol.*, 418-419, 17-48.

Smith, M. B., Seo, D.-J., Koren, V. I., Reed, S. M., Zhang, Z., Duan, Q., Moreda, F., and

Cong, S. (2004). “The distributed model intercomparison project (DMIP): Motivation and experiment design.” *J. Hydrol.*, 298, 4-26.

Sorooshian, S., and Dracup, J. A. (1980). “Stochastic parameter estimation procedures for hydrologic rainfall-runoff models: corrolated and heteroscedastic error cases.” *Water Resour. Res.*, 16(2), 430-442.

Sorooshian, S., Gupta, V. K., and Fulton, J. L. (1983). “Evaluation of maximum likelihood parameter estimation techniques for conceptual rainfall-runoff models: influence of calibration data variability and length on model credibility.” *Water Resour. Res.*, 19(1), 251-259.

Thiemann, M., Trosset, M., Gupta, H., and Sorooshian, S., (2001). “Bayesian recursive parameter estimation for hydrologic models.” *Water Resour. Res.*, 37(10), 2521-2535.

Van den Berg, M. J., Vandenberghe, S., Baets, B. D., and Verhoest, N. E. C. (2011). “Copula-based downscaling of spatial rainfall: a proof of concept.” *Hydrol. Earth Syst. Sc.*, 15, 1445-1457.

Venugopal, V., Basu, S., and F.-Georgiou, E. (2005). “A new metric for comparing precipitation patterns with an application to ensemble forecasts.” *J. Geophys. Res.*, 110, D08111, doi:10.1029/2004JD005395.

Vrugt, J. A., Braak, C. J. F., Clark, M. P., Hyman, J., M., and Robinson, B. A. (2008). “Treatment of input uncertainty in hydrologic modeling: Doing hydrology backward with Markov chain Monte Carlo Simulation.” *Water Resour. Res.*, 44, W00B09 doi:10.1029/2007WR006720.

Vrugt, J. A., Gupta, H. V., Bastidas, L., Bouten, W., and Sorooshian, S. (2003a). “Effective and efficient algorithm for multi-objective optimization of hydrologic models.” *Water Resour. Res.*, 39, 1214, doi:10.1029/2002WR001746.

Vrugt, J. A., Gupta, H. V., Bouten, W., and Sorroshian, S. (2003b). “A shuffled complex evolution metropolis algorithm for optimization and uncertainty assessment of hydrologic model parameters.” *Water Resour. Res.*, 39(8), 1201, doi:10.1029/2002WR001642.

Wigmosta, M. S., Vail, L. W., and Lettenmaier, D. P. (1994). “A distributed hydrology-vegetation model for complex terrain, *Water Resour. Res.*, 30(6), 1665-1679.

Wilson, L. L., Tsang, L., Hwang, J.-N., and Chen, C.-T. (1999). “Mapping Snow Water Equivalent by Combining a Spatially Distributed Snow Hydrology Model with Passive Microwave Remote-Sensing Data.” *IEEE Trans. Geosci. Remote Sens.*, 17(2), 690-704.

Xue, Y., Sun, S., Kahan, D., and Jiao, Y. (2003). "Impact of parameterizations in snow physics and interface processes on the simulation of snow cover and runoff at several cold region sites." *J. Geophys. Res.*, 198, D22, 8859, doi:10.1029/2002JD 003174.

Yi, J. H., Bhanu, B., and Li, M. (1996). "Target indexing in SAR images using scattering centers and the Hausdorff distance." *Pattern Recogn. Lett.*, 17(11), 1191-1198.

Yilmaz, K. K., Gupta, H. V., and Wagener, T. (2008). "A process-based diagnostic approach to model evaluation: Application to the NWS distributed hydrologic model." *Water Resour. Res.*, 44, W09417, doi:10.1029/2007WR006716.

Zhang, Y., Zhang, Z., Reed, S., and Koren, V. (2011). "An enhanced and automated approach for deriving a priori SAC-SMA parameters from the soil survey geographic dataset." *Comput. Geosci.*, 37, 219-231.

APPENDIX

Root Mean Square Error (RMSE) on a Distributed Hydrological Model

As a traditional error function, the RMSE is used in this study. This Appendix presents the mathematical process of RMSE used in this paper. The RMSE is calculated with the average of entire cells:

$$RMSE = \frac{\sum_{i=1}^{N} rmse_i}{N} \tag{A-1}$$

Where, i = 1, 2, … , N are the indices of grids over the study basin and *rmse* is the error values for each cell. In each cell, the *rmse* is calculated as the differences between the observation (Q_{obs}) and computation (Q_{com}) with time-series ($j = 1, 2, \ldots, n$):

$$rmse = \sqrt{\frac{\sum_{j=1}^{n} (Q_{obs}^{j} - Q_{com}^{j})^2}{n}} \tag{A-2}$$

CURRICULUM VITAE

JongKwan Kim

Expected Post-doctoral Associate
OHD/Hydrology Laboratory at NOAA-National Weather Service
1325 East West Highway
Silver Spring, MD, 20910
Email : kwanu2000@gmail.com

EDUCATION

Ph.D.	Hydrology, Department of Civil and Environmental Engineering, Utah State University, Logan, Utah.	2012
M.Sc.	Hydrology, Department of Civil and Environmental Engineering, Korea University, Seoul, South Korea.	2003
B.E.	Civil Engineering, Major in Hydrology, Department of Civil and Environmental Engineering, Jeonju University, South Korea.	2001

AREAS OF RESEARCH INTEREST

Hydro-climate modeling, Land surface modeling, Integrated catchment modeling, Watershed modeling, Application of remote sensing in hydrology, Rainfall-runoff modeling, Flood forecasting and control, Model performance evaluation, Spatial hydrology, Multi-objective and global optimization, Evaluation of hydrologic model uncertainty, Hydrologic ensemble prediction, data assimilation

MILITARY SERVICE

Feb. 1997 – Apr. 1999 Served as an army in the Headquarters, the 50th Battalion.

HONORS AND AWARDS

Citation of the 50th Divisional Commander for a diligent and honest member (1997)
Top Student Scholarship, Jeonju University, Jeonju, South Korea (2000)
Excellent Student Scholarship, Korea University, Seoul, South Korea (2002)
Excellent abroad study Student Scholarship, Jeonju University, Jeonju, South Korea (2007-2008)

Excellent Student Scholarship, Joyang cooperation, Jeonju, South Korea (2007-2008)
20 people for UKC 2011, KSEA (2011)

AFFILIATIONS

American Geophysical Union (AGU), Member
American Meteorological Society (AMS), Member
Korean Society of Hazard Mitigation (KSHM), Member
Korea Water Resources Association (KWRA), Member
Korean-American Scientists and Engineering Association (KSEA), Member

PROFESSIONAL EXPERIENCE

Global Reporter (Sep., 2011 – current), Korea Institute of Construction & Transportation Technology Evaluation and Planning in Ministry of Land, Transport and Maritime Affairs, South Korea

Graduate Research Assistant (Jan., 2007 – Dec., 2012), Dept. of Civil and Environmental Eng., Utah Water Research Laboratory, Utah State University, Logan, Utah

Visiting Researcher (Sep., 2010), Dept. of Natural Resources and Environmental Management, University of Hawaii, Manoa, Hawaii

Researcher (Mar., 2003 – Sep., 2005), Water Resources Engineering Lab., Korea University, Seoul, South Korea, Research on "Surface Water Resources Management-The Technology for Sustainable Dam Development" (http://www.water21.re.kr/index.jsp) supported by Ministry of Science and Technology, Seoul, South Korea

An Honorary Inspector (Jul., 2001 – Dec., 2002), Korea Infrastructure Safety and Technology Corporation in Seoul City, Seoul, South Korea

Graduate Research Assistant (Mar., 2001 – Feb., 2003), Dept. of Civil and Environmental Eng., Korea University, Seoul, South Korea

GRADUATE LEVEL COURSEWORK

Deterministic Hydrology, Probabilistic Hydrology, Stochastic Generation, Watershed Modeling, Urban Hydrology, Hydrodynamics, Water Resources System Engineering, Theory of Sedimentation, Water Resource Planning and Management, Remote Sensing of Land Surface, Water Resource Analysis, Groundwater Engineering, Water Resources Engineering, Applied Spatial Statistics, Evolutionary Computation, Applied Multivariate Statistics, Neural Networks, Continuous and Macro-scale Hydrologic Modeling

PRESENTATIONS & POSTER

J.K Kim, C.S Yoo, J.H Kim, A comparative Study of Estimation of Design Flood Using Frequency Analysis and Probability Rainfall, Conference on Korea Society of Civil Engineering, 2001

J.K Kim, C.S Yoo, J.H Kim, Estimation of Changing Point for Hydrologic Time Series, Conference on Korea Society of Civil Engineering, 2002

J.K Kim, Bastidas,L.A, Evaluating the effect of Data Uncertainty on the Uncertainty of Hydrologic Models, Conference on Spring Runoff of Utah Initiative Water, 2008

Tcherednichenko, I.A, Bastidas, L.A, Pande, S., J.K Kim, Effect of data Uncertainty on parameter estimation and model complexity using high-density regions of bootstrapped likelihood and Bayesian measures of complexity and fit, AGU Fall Meeting, San Francisco, California, USA, Dec. 14-18, 2009

J.K Kim, Bastidas,L.A, Performance Evaluation of the Distributed RDHM model in the Rockies, AGU Fall Meeting, San Francisco, California, USA, Dec. 13-17, 2010

J.K Kim, Bastidas,L.A, Uncertainty Evaluation and Appropriate Complexity for the NOAA NWS Distributed Hydrologic Model (RDHM) in a Snow Driven Basin Using a Multiple Criteria Approach, Conference on Spring Runoff of Utah Initiative Water, 2011

J.K Kim, Bastidas,L.A, A Comparative Distributed Evaluation of the NWS-RDHM using Shape-matching and Traditional Measures with In Situ and Remotely Sensed Information, AGU Fall Meeting, San Francisco, California, USA, Dec. 5-9, 2011

PUBLICATIONS

J.K Kim, C.S Yoo, J.H Kim, Change of Hydro-meteorological Environment due to Dam Construction, *Journal of Korea Society of Civil Engineering*, Vol. 23, No. 2B, Mar., 2002, pp. 87-94.

J.K Kim, Bastidas, L.A, Distributed Spatial Calibration and Evaluation of a Hydrological Model Using Single- and Multi-Criteria Automatic Procedures in Snow Dominated Areas, in review

J.K Kim, Bastidas, L.A, Parameter Estimations of a Spatially Distributed Hydrological

Model Using Single- and Multi-Criteria Automatic Calibration Methods, in review

REPORTS

J.K Kim, An Analysis of Hydro-meteorological Environment Changes due to Dam Construction, Master of Thesis, Department of Civil and Environmental Eng., Korea University, Seoul, South Korea, 2003

J.K Kim, The Calibration and Uncertainty Evaluation of Spatially Distributed Hydrological Models, Ph.D. of Dissertation, Department of Civil and Environmental Eng., Utah State University, Logan, UT, 2012

COMPUTER SKILLS

Operating System : Microsoft Window, Unix/Linux
Computer Language : Matlab, Matlab-GUI, C/C++, FORTRAN
Water Resources Engineering Applications : HEC-HMS, HEC-RMS, HEC-ResSim, SWMM
Office Application : MS-Office
Spatial Analysis Application : Arc-GIS
Statistical package : R
Others : NetCDF, HDF